

# Integral Mechanical Attachment for Timber Folded Plate Structures

THÈSE N° 6564 (2015)

PRÉSENTÉE LE 23 FÉVRIER 2015

À LA FACULTÉ DE L'ENVIRONNEMENT NATUREL, ARCHITECTURAL ET CONSTRUIT  
LABORATOIRE DE CONSTRUCTION EN BOIS  
PROGRAMME DOCTORAL EN ARCHITECTURE ET SCIENCES DE LA VILLE

ÉCOLE POLYTECHNIQUE FÉDÉRALE DE LAUSANNE

POUR L'OBTENTION DU GRADE DE DOCTEUR ÈS SCIENCES

PAR

Christopher Werner Matthias ROBELLER

acceptée sur proposition du jury:

Prof. M. Fröhlich, président du jury  
Prof. Y. Weinand, directeur de thèse  
Dr J. Hakkarainen, rapporteur  
Prof. M. Kohler, rapporteur  
Prof. M. Pauly, rapporteur



ÉCOLE POLYTECHNIQUE  
FÉDÉRALE DE LAUSANNE

Suisse  
2015





# Acknowledgements

First of all I would like to express my Gratitude to my supervisor, architect and civil engineer Prof. Yves Weinand, who has given me the opportunity to work on this exciting, interdisciplinary research topic, and supported me throughout the thesis.

I would also like to thank the members of the thesis jury, Prof. Martin Fröhlich, who has accepted the role of the president, and the experts, Jouni Hakkarainen, Prof. Matthias Kohler and Prof. Mark Pauly, for their examination of the work and for their valuable advice and support.

A special thanks to all my colleagues, co-authors and friends at IBOIS and other laboratories, who it was a pleasure to work with, notably Sina Nabaei, Stéphane Roche, Andrea Stitic, and especially Benjamin Hahn. Thank you for many exciting and helpful discussions and for making my time in Lausanne very enjoyable.

Finally I would like to thank my parents Hannelore and Werner for their unconditional support and encouragement.

*Lausanne, February 10, 2015*

C. R.



# Abstract

Timber folded plate Structures combine the advantages of timber as a construction material, such as its carbon-dioxide storage, low energy production and favorable weight-to-strength ratio, with the structural efficiency and elegance of folded surface structures.

The construction of such surface-active structure systems with timber is a relatively new development, driven by an increasing awareness for sustainable building constructions, and enabled by new engineered wood products. However, these constructions require a large amount of edgewise joints between the thin timber plates, which are difficult to address with state-of-the-art connection techniques.

Instead of using mass-produced mechanical fasteners for these connections, this thesis investigates the use of customized *Integral Mechanical Attachment* techniques, which use geometrical features of the parts to establish connections, rather than additional fasteners.

Integral joints were common in traditional woodworking, but their manual crafting became infeasible during the industrialization. However, new computer-controlled fabrication technology, which is already available in the timber prefabrication industry, allows for an efficient, automatic production of integral joints. The advantages of such joints have already been demonstrated in framing constructions, where timber beams are used as the primary structural components. The proliferation of *automatic joinery machines* has repatriated customizable single-degree-of-freedom (1DOF) joints, which allow for the fast and precise assembly of prefabricated components. The objective of this thesis is to transfer these advantages to the construction of timber folded plate structures.

Inspiration is taken from traditional cabinetmaking joints from Europe and Asia, as well as other industry sectors, where mass-produced integral joints are commonly used. The thesis will demonstrate several adaptations which have been made for the application of the joints on cross-laminated wood panels, for their automatic fabrication and for the customized purposes in the jointing timber folded plate structures.

The geometry, fabrication and assembly of these new joints is being implemented and tested through the development of algorithmic tools. This is followed up by a verification of the proposed methods through large- and small scale physical prototypes.

## Abstract

---

In its three peer-reviewed core chapters, the thesis presents investigations ranging from an initial hybrid approach, where integral joints are combined with adhesive bonding, towards a completely integral mechanical attachment solution.

After a first application of the joints on a surface which is folded in one direction, the integral attachment of bidirectionally folded surfaces will be demonstrated. This is achieved through a new technique, which allows for the simultaneous jointing of multiple non-parallel edges, with single-degree-of-freedom joints.

Algorithms will be presented, which allow for the automatic processing and the automatic fabrication of the joints. The automation of these processes will then be used for the construction of a doubly-curved, bidirectionally-folded surface, which obtains its structurally beneficial double-curvature through incremental changes in the geometry of the plates.

Such geometrical variations had already been suggested in previous studies, but both the assembly and the fabrication of doubly-curved folded surface structures, through a large amount of geometrically individual parts, rely on the automatic processing of geometry and fabrication data, which is introduced in this thesis.

**Keywords:** *Integral Mechanical Attachment, Digital Fabrication, Timber Folded Plate Structures, Dovetail Joints, Design for Assembly*

# Zusammenfassung

Holz-Faltwerkskonstruktionen verbinden die Vorteile des Baustoffes Holz, beispielsweise die Kohlendioxid-Speicherung und das niedrige Verhältnis von Gewicht und Festigkeit, mit der konstruktiven Effizienz und Eleganz von gefalteten Flächentragwerken.

Die Konstruktion solcher flächenaktiver Tragwerke mit dem Werkstoff Holz ist eine relativ neue Entwicklung, angetrieben von einem gesteigerten Bewusstsein für nachhaltiges Bauen, und ermöglicht durch neue Holzwerkstoffe. Diese Konstruktionen erfordern jedoch eine grosse Anzahl von unterschiedlichen Verbindungen zwischen den einzelnen Platten, welche mit herkömmlichen Verbindungstechniken schwer zu lösen sind.

Anstelle massengefertigte Verbindungselemente einzusetzen, untersucht diese These den Einsatz von *integralen mechanischen Befestigungstechniken*, welche nicht zusätzliche Verbinder, sondern geometrische Eigenschaften nutzen, um die Verbindung zwischen Teilen herzustellen.

Integrale Verbindungen waren in der traditionellen Holzbearbeitung weit verbreitet, jedoch wurde die Herstellung mit Handwerkzeugen im Zuge der Industrialisierung zunehmend unwirtschaftlich. Neue, computergestützte Fertigungstechnologien, welche im vorgefertigten Holzbau bereits verfügbar sind, erlauben heute wieder eine wirtschaftliche, automatisierte Herstellung von integralen Verbindungen.

Die Vorteile solcher Verbindungen wurden bereits im Holzrahmenbau aufgezeigt, wo stabförmige Holzelemente wie Pfosten und Träger als primäres Tragwerk eingesetzt werden. Die Verbreitung von automatisierten Abbundanlagen hat dort zu einer Rückkehr von integralen Verbindungen geführt, welche eine schnelle, einfache und präzise Fügung vorgefertigter Bauteile ermöglichen. Es ist Ziel dieser These, diese Vorteile auf die Konstruktion von Holz-Faltwerkskonstruktionen zu übertragen.

Die Entwicklungen sind inspiriert durch traditionelle Verbindungstechniken des Tischlerhandwerks in Europa und Asien, als auch durch andere Industriezweige, in denen massengefertigte integrale Verbindungen eingesetzt werden. Die These wird verschiedene Anpassungen dieser Techniken aufzeigen, für den Einsatz der Verbindungen auf querverleimten Holzwerkstoffen, für deren automatisierte Fertigung und für die speziellen Anforderungen

von Holz-Faltwerkskonstruktionen.

Die Geometrie, die Fabrikation und die Fügung dieser neuen Verbindungen werden mit Hilfe von algorithmischen Werkzeugen entwickelt. Darauf folgt eine Überprüfung der Methoden durch klein- und grossmassstäbliche Prototypen.

Die Arbeit präsentiert in drei wissenschaftlich begutachteten Hauptkapiteln verschiedene Untersuchungen, beginnend mit einer hybriden Technik, in der integrale Verbindungen gemeinsam mit Klebstoffen eingesetzt werden, hin zu vollständig integralen Verbindungstechniken.

Nach einer ersten Anwendung der Verbindungen an einer in einer Richtung gefalteten Anordnung von Platten, wird die integrale Verbindung von in zwei Richtungen gefalteten Anordnungen demonstriert. Dies wird durch eine neue Technik ermöglicht, welche die gleichzeitige Fügung mehrerer nicht paralleler Kanten ermöglicht, mit Verbindungen die jeweils nur eine Einschubrichtung zulassen (1DOF).

Es werden Algorithmen präsentiert, die eine automatische Datenverarbeitung und Fabrikation der Verbindungen ermöglichen. Diese automatisierten Prozesse werden dann für die Konstruktion eines doppelt gekrümmten und gleichzeitig in zwei Richtungen gefalteten Flächentragwerks eingesetzt, welches seine konstruktiv vorteilhafte doppelte Krümmung durch inkrementelle Veränderungen in der Form der Platten erhält.

Derartige geometrische Variationen wurden bereits in vorangegangenen Studien vorgeschlagen, jedoch sind deren Fügung, Verbindungen und Fabrikation, durch eine grosse Anzahl von geometrisch unterschiedlichen Bauteilen, nur durch eine automatisierte Verarbeitung möglich, welche in dieser These vorgestellt wird.

**Schlüsselwörter:** *Integrale Mechanische Verbindungen, Digitale Fabrikation, Holz-Faltwerke, Flächenaktive Tragwerke, Schwalbenschwanzzinken*

# Contents

<b>Acknowledgements</b>	<b>iii</b>
<b>Abstract (English/Deutsch)</b>	<b>v</b>
<b>I Introduction and State-of-the-Art</b>	<b>1</b>
<b>1 Introduction</b>	<b>5</b>
<b>2 State-of-the-Art</b>	<b>7</b>
2.1 Integral Mechanical Attachment for Timber Plates . . . . .	7
2.1.1 Origins and Fabrication with Hand-Tool Technology . . . . .	8
2.1.2 Fabrication with Machine-Tool Technology . . . . .	10
2.1.3 Fabrication with Information-Tool Technology . . . . .	12
2.2 Folded Plate Structures . . . . .	22
2.2.1 Origins in Concrete . . . . .	23
2.2.2 Fiber-reinforced Plastics . . . . .	26
2.2.3 Timber Panels . . . . .	28
2.3 Objectives . . . . .	33
2.4 Methodology . . . . .	34
2.4.1 Development of Algorithms . . . . .	34
2.4.2 Development of Prototypes . . . . .	34
2.4.3 Investigations . . . . .	35
2.5 Scope . . . . .	35
References . . . . .	36
<b>II Investigations</b>	<b>41</b>
<b>3 Design and Fabrication of Robot-Manufactured Joints for a Curved-Folded Thin-Shell Structure Made from CLT</b>	<b>43</b>
Foreword . . . . .	44
3.1 Motivation . . . . .	47
3.2 Project Geometry . . . . .	48
3.3 Limitations of State-of-the-Art Connectors . . . . .	48

## Contents

---

3.4	Joint Types and Algorithms . . . . .	49
3.5	Preliminary Structural Analysis . . . . .	52
3.6	Prototype at Scale 1:5 . . . . .	52
3.7	Full-Scale Prototype . . . . .	54
3.8	Conclusions/Towards an Integration of Joints . . . . .	57
	Additions and Remarks . . . . .	64
	References . . . . .	71
<b>4</b>	<b>Interlocking Folded Plate - Integrated Mechanical Attachment for Structural Timber Panels</b>	<b>73</b>
	Foreword . . . . .	74
4.1	Introduction . . . . .	79
4.2	Dovetail Joint Geometry and Mechanical Performance . . . . .	80
4.3	Fabrication Constraints . . . . .	81
4.3.1	Simultaneous Assembly of Multiple Edges . . . . .	83
4.4	Interlocking Arch Prototype . . . . .	84
4.5	Interlocking Shell Prototype . . . . .	86
4.5.1	Automatic Geometry Processing . . . . .	86
4.5.2	Assembly . . . . .	86
4.5.3	Completed Shell Prototype and Load Test . . . . .	87
4.6	Conclusion . . . . .	88
4.7	Acknowledgments . . . . .	89
	Additions and Remarks . . . . .	94
	References . . . . .	112
<b>5</b>	<b>Snap-fit joints - CNC fabricated, Integrated Mechanical Attachment for Structural Timber Panels</b>	<b>115</b>
	Foreword . . . . .	116
5.1	Introduction . . . . .	119
5.2	Concept . . . . .	120
5.2.1	General Joint Design . . . . .	120
5.2.2	Adaptation to Fabrication and Materials in Timber Construction . . . . .	122
5.3	Combination with Tab-and-slot Joints . . . . .	122
5.4	Fabrication and Assembly . . . . .	124
5.5	Mechanical Performance . . . . .	124
5.6	Physical Load Tests . . . . .	125
5.7	Numerical Model . . . . .	125
5.8	Results . . . . .	126
5.9	Optimization of the Snap-fit Connection for the Beam . . . . .	126
5.10	Comparison with Screwed Connections . . . . .	127
5.11	Applications and Features . . . . .	127
5.11.1	Double-layer Structures . . . . .	127
5.12	Conclusions and Outlook . . . . .	129



5.13 Acknowledgements . . . . .	129
Additions and Remarks . . . . .	134
References . . . . .	142
 <b>III Conclusion and Further Work</b>	 <b>145</b>
<b>6 Conclusion</b>	<b>147</b>
<b>7 Further Work</b>	<b>151</b>
 <b>Appendices</b>	 <b>153</b>
<b>A Joint Parameter Interactions</b>	<b>155</b>
<b>B Integral Joints for UHPFRC Formwork</b>	<b>159</b>
<b>List of figures</b>	<b>162</b>
<b>List of tables</b>	<b>166</b>
<b>Curriculum Vitae</b>	<b>169</b>



# **Introduction and State-of-the-Art Part I**



In the past, joining was often an afterthought, even though the need was obvious. Instead of joining being a secondary process, performed as a last, discrete step in the material synthesis common to most manufacturing or construction of the past, it will increasingly become a primary process that occurs at the same time as one or more of these other steps. Joining processes will be automated or will take place automatically.

In the future, integral design features alone may be used to facilitate assembly, accomplish locking, and provide needed sealing of pre-fabricated details produced under controlled, largely automated conditions.

— Robert W. Messler Jr.



# 1 Introduction

Over the past decade, the popularity of timber as a building construction material has increased again in central Europe.<sup>1</sup> This is due to a growing awareness for the sustainability of building constructions, as well as a demand for prefabricated solutions, which allow for the use of automation technology. With its carbon-dioxide storage, low-energy production and favorable weight-to-strength ratio, timber presents an ideal material for prefabrication and transportation.

Modern engineered timber panels such as cross-laminated timber (CLT), or laminated veneer lumber (LVL) add additional benefits: These laminates are available in large sizes; they are dimensionally stable and allow for a more homogeneous, quasi-orthotropic mechanical behavior, providing a high strength even for thin panels.

Recently, the design of form-active surface structures with engineered timber panels has been the subject of several investigations and experimental prototypes in the fields of architectural geometry and civil engineering. While traditional timber-frame structures use timber panels only as a secondary structure for the cladding and cross-bracing of beams, new typologies such as Timber Folded Plates are using plate-assemblies as their primary, load-bearing structure. The folded geometry allows these structures to integrate a combined slab and plate action, resulting in equally efficient and elegant structures.

The construction of self-supporting, surface-active structure systems with timber plates brings new benefits, such as a sustainable material and precise prefabrication technology, but also new challenging details: Folded Plate Structures originate in concrete constructions, which were cast as continuous structures directly on site. Constructions with discrete timber plates however require edgewise joints between the plates.

New challenging details are presented by these typologies: Previous investigations have identified the direct, load-bearing edgewise joints between the thin panels as a key challenge

---

<sup>1</sup>For example, in the period of 1998 to 2010, constructions with timber have increased by 7.8% for non-residential and 3.5% for residential buildings in Germany [DZ12], the largest market for softwood lumber in Europe. For France, the second largest market, see [Hol13].

## Chapter 1. Introduction

---

in such designs<sup>2</sup>. The large amount of joints with variable dihedral angles requires not only a sufficiently rigid and stiff connection, but also a solution that allows for a simple, fast and precise assembly of the prefabricated elements on site.

Inspired by traditional, handcrafted cabinetmaking joints, this thesis investigates if the parts in such structures can be joined through integral features in their form, rather than through additional connectors. Such methods are part of the field of *Integral Mechanical Attachment*, the oldest known method of joining, [Mes06, p.1].

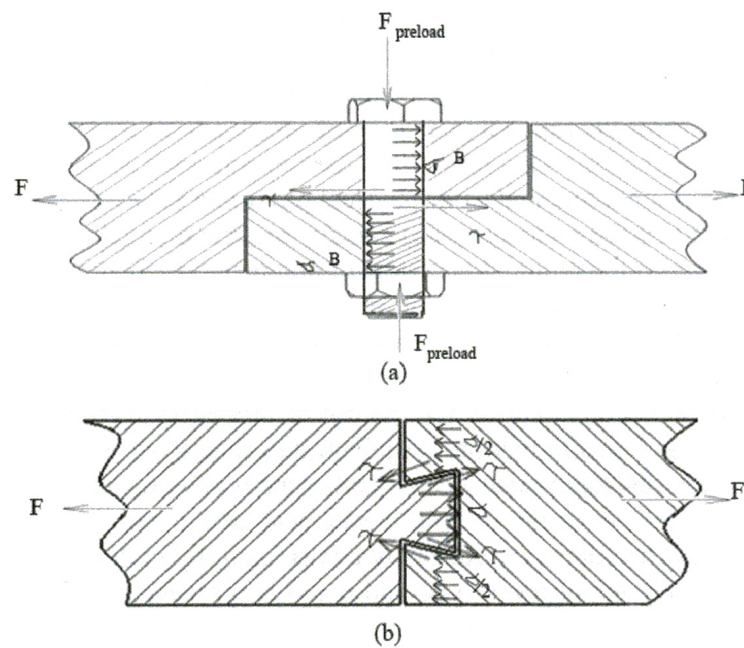


Figure 1.1 – Integral Mechanical Attachment - A mechanical connection between parts is established through integral, geometric features (b), instead of additional fasteners (a). Illustration taken from [Mes06, p.9]

---

<sup>2</sup>see [p.209][Bur10] and [Hah09]



## 2 State-of-the-Art

### 2.1 Integral Mechanical Attachment for Timber Plates

The following three sections present the origins, fabrication techniques and geometry of integral joints for plate-shaped timber elements. The developments over time are presented in chronological order and, following the periodisation model developed by Christoph Schindler [Sch09], divided in three sections related to the distinct advances in technology, which have had great influence on the development of the joints.

Working with timber, joints have always been essential for the assembly of building constructions. While in masonry and steel construction, joints are often established through physical forces, for example the welding of parts, or through chemical forces, such as in adhesive bonding techniques, including cementing and mortaring, timber joints are typically established through mechanical forces<sup>3</sup>. (see table 2.1)

Such mechanical connections may be established through additional connectors, so-called *mechanical fasteners*, through the geometry of the parts themselves, which is called *Integral Mechanical Attachment* [Mes06, p.6], or through combinations of the two methods.

Chemical Forces	Physical Forces	Mechanical Forces	
Adhesive Bonding	Welding	Mech. Fasteners	Integral Mech. Attachment
Cementing	Arc Welding	Screws	Mortise-and-tenons
Mortaring	Spot Welding	Nails	Dovetails
...	...	...	...

Table 2.1 – Taxonomy of joining techniques by the forces used [Mes06]

<sup>3</sup>Load-bearing adhesive joints [Neu94] are also possible, but limited to off-site assemblies [Pur11], because they require constant indoor conditions for the curing. They can be used for the prefabrication of transportable modules, which are later assembled with additional mechanical fasteners.

### 2.1.1 Origins and Fabrication with Hand-Tool Technology

A variety of integral mechanical attachment techniques existed in traditional handcrafted carpentry. Load-bearing joints in building constructions with timber were typically used for the connection of linear elements, such as beams and posts. Examples include Mortise-and-tenons, Lap Joints or Birdsmouth Joints. Plate-shaped elements however, such as timber boards were rather used as overlapping external cladding, flooring, or decking. These elements were typically connected to the structural timber frame with mechanical fasteners. Edgewise connections were not required for these applications. Instead, a variety of integral mechanical attachment solutions for the jointing of plate-shaped elements can be found in traditional cabinetmaking.

In cabinetmaking, edgewise plate joints were required for many objects which were assembled directly from plates, such as boxes, cabinets or drawers. Apart from providing rigid connections between the parts, these joints had to accommodate for the low and non-uniform dimensional stability of wood. For a change in relative humidity of 1%, the dimensional change of spruce wood varies between only 0.01% in the longitudinal direction along the fibres, and up to 0.36% in the tangential direction across the fibres. [WS12, p.83]

A general distinction can be made into two main purposes [Gra86, p.146]: first, the size of timber boards is limited to the cross-section of the trees they are made of, but many applications in cabinetmaking required larger surfaces. So-called *1-plane* joints were required for these applications. Larger surfaces were built through the assembly of multiple wooden boards along their side-grain<sup>4</sup> edges with tongue-and-groove-joints, which allowed for in-plane deformations. Out-of-plane deformations, the so called warping, were prevented through transversal framing elements, or through dovetail-battens, in both of which tongue-and-groove joints served as rails.<sup>5</sup>

The second type of joints was used for the connections of plates at corners, for example on boxes. These *2-plane* joints or corner joints [Gra86, p.152] between the end-grain edges of timber boards are considered both the mechanically strongest and the most challenging-to-craft joints by cabinetmakers. They have to provide for a sufficient rigidity and stiffness both to shear forces and bending moments, allow for dimensional changes such as shrinking and swelling in the side-grain direction along the edge, and prevent the out-of-plane warping of the plates all at the same time.

Such 2-plane connections were typically established through *multiple* dovetail-shaped tab-and-slot joints along the edge<sup>6</sup> (Figure 2.1). The shape of the dovetails blocks all relative movements between the two parts, except for one assembly direction. It can be considered a

---

<sup>4</sup> *Side-grain* edges are parallel to the wood fibres, *end-grain* edges are perpendicular to the wood fibres

<sup>5</sup> for frame-constructions, see [Gra86, p.150], for dovetail battens, see [Gra86, p.155]

<sup>6</sup> in German, a single dovetail joint, for example in carpentry, is called a *Schwalbenschwanz*. Multiple dovetails along one edgewise joints are called a *Schwalbenschanz-Zinkung*. The word *Zinkung* describes multiple tab-and-slot joints, such as finger joints or dovetail joints in cabinetmaking.

## 2.1. Integral Mechanical Attachment for Timber Plates

kinematic pair with a single translational degree-of-freedom (1DOF). This geometry provides multiple benefits: It resists to shear forces parallel to the edge, transfers bending moments around the edge into shear and compression forces<sup>7</sup>, and prevents both of the jointed boards from out-of-plane warping.

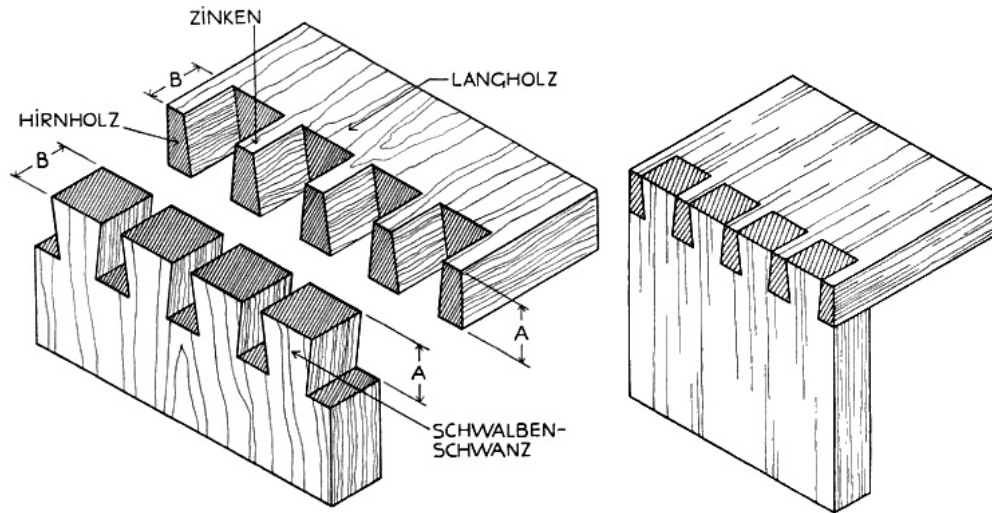


Figure 2.1 – A connection between two timber boards is being established through multiple dovetail connector features. Illustration taken from [Spa54, p. 91]

These techniques date back to the ancient Egypt, where dovetail joints were found on chests and coffins in burial sites<sup>8</sup>. Several geometrical variations of these joints were developed over time, both in Europe and Asia<sup>9</sup>. Figure 2.1 shows a typical European, handcrafted corner joint with multiple dovetail-shaped connectors (1954).

Over time, the parameters of these joints have been optimized for mechanical strength and ease-of-fabrication with handcrafting tools such as chisels and saws. For example, the dovetails (Figure 2.1, lower left) are partially cut diagonal to the wood fibers, resulting in a weak point at their narrow end. Therefore they are crafted twice as wide as the pins on the counterpart (Figure 2.1, upper left), where the diagonal cut is made along the fibers, not across. The angle of the dovetail's diagonal faces was also optimized over time: The earliest known examples in cabinetmaking show a ratio of 1 : 1 (45°), later in the seventeenth and eighteenth century examples with ratios of 1 : 2 and 1 : 3 can be found. A lower 1 : 5 (11°) or (9.5°) 1 : 6 ratio is generally accepted to be the strongest and most widely used version. Examples from the late eighteenth century even show a ratio of 1 : 8 (7°), which demonstrates particular craftsmanship. [Edw10]

Another example is the marking of the joint geometry, which was typically carried out without

<sup>7</sup>for the transformation of forces, see chapter 3, page 65 and chapter 4, page 81

<sup>8</sup>A widely known early example that demonstrates hand-crafted dovetail joints is the 4.000 years-old Cosmetic Box of Kemei, Date: ca. 1814-1805 B.C., from Upper Egypt: Thebes, el-Asasif. Made from Cedar. On display at the Metropolitan Museum of Art, New York

<sup>9</sup>for Japanese dovetail joints in cabinetmaking, see [Tet07] and chapter 4

special tools or jigs, but with procedures much like algorithms, using multiplications of the panel-thickness and the connection of intersection points for the definition of the dovetail's angles. [Spa54, fig. 283/284]

### 2.1.2 Fabrication with Machine-Tool Technology

Throughout the nineteenth century, machine-tool technology was proliferating during the industrialization period and beginning to replace handcrafting techniques. There was also an increasing demand for furniture, accordingly various machines were developed for the production of dovetail joints for furniture. After the invention of sawing machines, joinery machines were amongst the first developments at this time. In the period from 1833 and 1900, there were 106 patent applications for dovetail joining machines in the United States alone.<sup>10</sup>

However the geometry of handcrafted dovetail joints was difficult to automate, especially in the beginnings of the industrialization. Therefore, one of the early and successful joining machines, the *Knapp Dovetailing Machine*, which was developed in 1870 fabricated its own type of integral multiple-tab-and-slot joint. (Figure 2.2, left side). [UR03, p.32] Instead of sharp-cornered dovetails, the machine produced a joint with rounded dowel-like pins, fabricated with a series of hollow-core drill bits. [Gre07, p.124]

Later, more advanced dovetailing machines in the 20th century returned to the geometry of the handcrafted dovetails. For example, figure 2.2 on the right side shows the *Kelly Dovetailing machine*, patented in 1917. Many of these machines were built in a similar way, using an inclined machining tables and vertical saw blades.

In addition to these joinery machines for larger workshops, various versions of jigs and templates for the cutting of dovetails in small workshops were developed and patented in the 20th century. Early versions were made for the guiding of handsaws, until by the end of the 1950s, first versions were developed for the guiding of hand-operated power tools such as milling routers. [Eri56]

Despite all of these efforts for the fabrication of dovetail joints with machine-tool-technology, Integral Mechanical Attachment was slowly replaced by mass-produced mechanical fasteners, such as screws and various types of dowels, as well as increasingly well-developed adhesive bonding techniques. A very important role in this context is taken by the development of new engineered wood products for the production of furniture, most notably *particle boards*, which were originally invented as a replacement for timber and plywood, due to a shortage of wood during the second world war. The industrial production of particle boards started with the opening of a first factory in Switzerland in 1946.

Apart from the ability to produce wood panels from chips, and therefore a more efficient use of lumber, these panels provided a sufficient rigidity for furniture and interior fitting applications,

---

<sup>10</sup>see [Edw10]

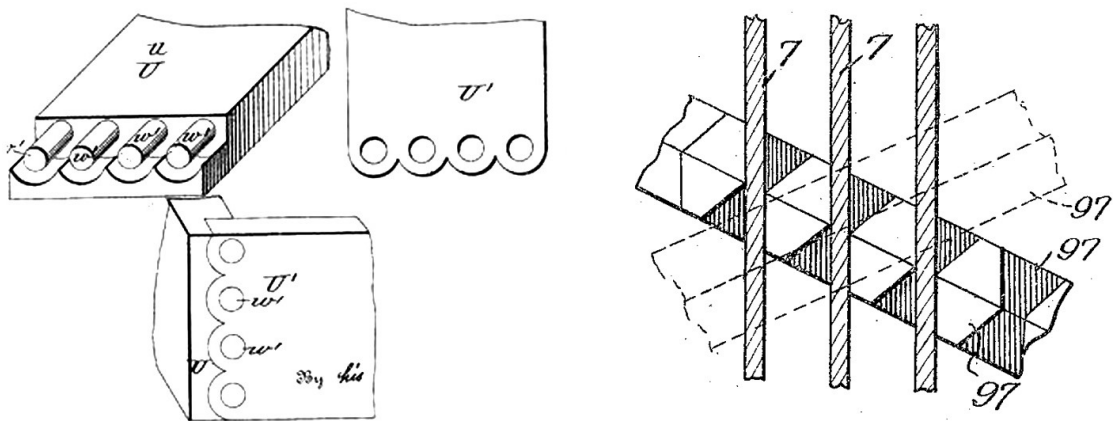


Figure 2.2 – Integral Plate Joints fabricated with Machine-tool-technology - *left side*: Joint fabricated with the Knapp Dovetailing Machine (ca. 1870), [UR03, p.32], *right side*: Kelly Dovetailing Machine (1917) [Kel17]

while being available in large sizes and very dimensionally stable: For a change in relative humidity of 1%, regular spruce boards show a dimensional change of 0.36% in the side grain direction. [WS12, p.83] For particle boards a value of 0.01% is given, which is negligible.<sup>11</sup>

This dimensional stability provided a considerable advantage for furniture applications. In the traditional design of furniture with timber, the swelling and shrinking of components needed to be taken into consideration. Dimensional changes had to be accommodated through complex details, providing specific play and geometrical degrees of freedom in the joints. Dimensionally stable products such as particle boards did not require such details any more and allowed for much simpler, faster and more efficient assemblies.

From a point of view of jointing, particle boards require different joints compared to timber. For once, certain features of dovetail joints are not required on particle boards. For example, the geometry of dovetail joints can prevent the warping of timber boards, which is not necessary for particle boards. Furthermore, the mechanical strength of the particle boards is much lower than the one of timber<sup>12</sup>, and the density in the core of the panels is lower than on the top and bottom surfaces, which is due to the production process. Dovetail Joints can not be used for the connections of such panels.

The jointing of particle boards presented a challenge for cabinetmakers in the 1950s, and demanded for new techniques. A convenient solution, which provided sufficient rigidity and efficient production with machine-tool-technology, was found in dowel-type-fasteners, such

<sup>11</sup> The high dimensional stability of particle panels is due to their in-plane isotropic behaviour [Hol09, p.10]

<sup>12</sup> for example, the bending strength for standardized particle boards for furniture applications (P1,P2) is between 7-13 N/mm<sup>2</sup>, depending on the thickness of the panel (DIN-EN 312). For spruce wood, a value of 68 N/mm<sup>2</sup> is given. (DIN 68364)

as cylindrical beechwood dowels<sup>13</sup> and plate-shaped biscuits<sup>14</sup>.

Finally, so called *cam and bolt connectors*, the most recent development in furniture corner-joints, were introduced in the beginning of the 1970s<sup>15</sup>. While classic dowels were typically made from wood, and typically combined with adhesive bonding, cam-and-bolt connectors are mass-produced steel connectors. Unlike the glued in wood dowels, they provide a *reversible* connection between the parts, and allow for a simple and rapid home-assembly of flat-packed furniture. (Figure 2.3)

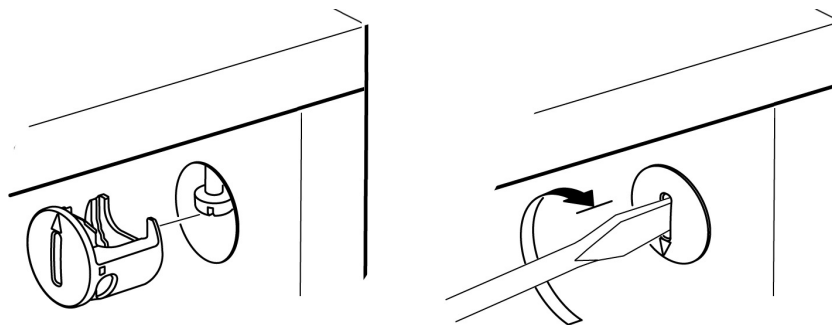


Figure 2.3 – Cam-and-bolt corner-joint for furniture made from particle boards - Modern furniture is typically assembled with mechanical fasteners, rather than Integral Mechanical Attachment (Figure taken from the BILLY cabinet assembly instructions, ©IKEA of Sweden)

### 2.1.3 Fabrication with Information-Tool Technology

The previous sections demonstrate that the disappearance of integral finger- and dovetail joints in the furniture industry was due to new technological developments in the 20th century, such as machine fabrication technology and new engineered wood products.

However, a resurgence of Integral Mechanical Attachment has begun with the digital-geometry-processing and information-tool-technology of the 21st century. While the parametric and detailed geometry of such connections presented a disadvantage in their laborious manual production, these techniques have proven to be ideal for algorithmic processing and digital fabrication. While the production of joints has become very efficient, the simplicity, rapidity and precision of assembly have now gained enormous importance in many industry sectors. This has a particular relevance for prefabricated applications where flat-packed transport is important and the assembly is performed outside of a factory environment.

---

<sup>13</sup>for example Riffeldübel fasteners (DIN 68150)

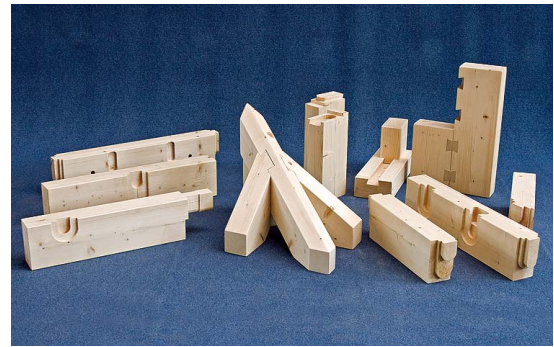
<sup>14</sup>for example the *Lamello* Lamellendübel system, invented by Hermann Steiner in Switzerland, 1955, connected plates at corners through the cutting of multiple short longitudinal grooves (instead of a continuous groove, which weakens the joint) with a milling router. The grooves were then connected with glued-in plate-shaped dowels.

<sup>15</sup>for example the *Minifix-System*, produced by the German manufacturer Haeefe.

## 2.1. Integral Mechanical Attachment for Timber Plates



(a) Hundegger K1 Joinery Machine, 1996



(b) Automatically fabricated integral joints

Figure 2.4 – Numerically Controlled Joinery Machines - A Resurgence of Integral Mechanical Attachment for Timber-frame Constructions. Photo ©Hans Hundegger GmbH

### Origins in Timber Frame Structures

In the building construction industry, the fabrication of integral joints has been repatriated to prefabricated timber-frame constructions with the proliferation of *automatic joinery machines*. These numerically controlled machines can automatically fabricate integral joints for timber beams, similar to the traditional carpentry joints, such as mortise-and-tenons, lap-joints or birdsmouth joints. Such precisely prefabricated beams improved the efficiency and reduced the amount of manual labor both in the production and the assembly of timber-frame constructions, such as roof or balloon frames constructions. However, although automatic joinery machines were already developed in the middle of the 1980s, the technology became feasible only towards the end of the 1990s. A rapidly increasing proliferation could then be observed in the second half of the 2000s.<sup>16</sup>

While information-tool-technology has brought traditional, integral carpentry joints back to constructions with timber beams, similar adaptations for plate-shaped elements, inspired by the traditional cabinetmaking joints are a very recent development, which originates in the experimental development of new form-active timber panel structures, rather than the typical state-of-the-art applications for engineered timber panels.

The industrial production of cross-laminated wood panels such as plywood already began around the end of the 1920s in the United States. In building construction, these structural-grade panels were used for the *Balloon Frame* constructions. While earlier timberframe structures required not only vertical posts and horizontal beams, but also diagonal cross-bracing, the cross-laminated plywood panels provided simultaneous cladding and cross-bracing for timber frame structures. However, these applications do not require load-bearing edgewise joints between the plywood panels.

<sup>16</sup>The Automatic Joinery Machine was first introduced by the company Hundegger in 1985. The 1.000th unit was sold in 2007, the 2.000th unit only two years later, in 2009. In 2014, ca. 4.500 machines are in operation [Hun14]

Direct edgewise connections between wood panels are required by new and increasingly popular construction methods with timber, such as constructions with cross-laminated timber panels (CLT), which was developed only in the beginning of the 1990s, or laminated veneer lumber (LVL). In CLT constructions for example, thick (ca. 50-300mm) prefabricated panels are being used as solid walls and roof elements, much like in concrete or masonry constructions. These CLT panels are used as the primary, load-bearing structure in such constructions. The joints between these panels are typically established through mechanical fastening, for example with screws, metal plate connectors and angle brackets.

### Integral Joints for Form-active Timber Plate Structures

While state-of-the-art connectors such as screws may be an adequate solution for applications with regular, orthogonal geometry such as typical CLT building constructions, new challenges are presented by several experimental structures from the 2000s and 2010s, which propose the use of engineered timber panels such as plywood, CLT or LVL for the construction of geometrically irregular free-form and form-active structures, such as shells, domes and other spatial structures.

The majority of these experimental, form-active constructions with timber panels originates in computer-aided *generative* architectural design, which utilizes computational algorithms for the processing of building information such as geometry, statics or fabrication data. These design methods have a particular relevance for the design of the previously mentioned form-active structures, which often require irregular shapes for their structural concept. Before computer were available, the *computational* design of such structures was laborious, but also possible through physical tools and models.

The use of such computer-aided generative design techniques was made accessible to the architectural community especially with the introduction of *Visual Programming* tools<sup>17</sup> in the mid 2000s, which simplified the development of computational tools through graphical user interfaces, as well as the introduction of *Application Programming Interfaces*<sup>18</sup> (API) in architectural and structural design software (CAD). Similar to the visual programming tools, API's allow for the use of algorithms within a CAD environment, where a library of functions can be used by a simplified scripting language.

A particularly powerful application of these algorithmic design tools was presented in their combination with the readily available information-tool-technology in the building construction industry. In larger timber construction prefabrication companies, computer-controlled 5-axis machines for the formatting of timber panels were already available from the mid-

---

<sup>17</sup>The Visual Programming Add-on *Generative Components* for Bentley's architectural CAD software Microstation was introduced in 2005. 2 years later in 2007, *Grasshopper*, a similar tool was released for Robert McNeel's CAD software Rhinoceros 3D

<sup>18</sup>The architectural CAD software AutoCAD introduced an API in 1986, using its own AutoLISP scripting language. Rhinoceros 3D introduced an API in 2001, using the scripting language Visual Basic Script.



1990s<sup>19</sup>. An open interface between these machines and the algorithmic design tools was also provided by standardized programming languages such as G-Code. [fS09]

The so-called *digital chain* [Lov12] between computer-aided tools for design and fabrication quickly led to new construction methods. While during the industrialization period, machine-tool-technology propagated the efficient construction of buildings with large amounts of mass-produced geometrically identical parts, algorithmic design tools and the digital chain now allowed for the efficient production of batches of geometrically *similar* parts, where certain geometry (or assembly) related parameters were changed incrementally. In other industry sectors, this concept is called *Mass Customization*.

While the fabrication of large amounts of individually shaped elements was not efficient with the earlier hand-tool and machine-tool-technology, these restrictions did not apply any more to more universal, computer-controlled machines, such as CNC gantry routers or industrial robots. [Men06a] This combination of numerical tools for design and fabrication allowed for the simplified construction of large and complex free-form structures, through the assembly of many small and easily transportable, individually shaped components. The exact information about the position and alignment of these components could now simply be embedded into their geometry.

### Single-Tab-and Slot Joints

The material wood plays an important role in this context, because it can be easily cut into irregular, 3-dimensional shapes. These possibilities make the use of integrated joints, both for the ease-of-assembly and for structural purposes, almost self-evident. One of the earliest examples for such timber plate structures with *similar* parts was the *2005 Serpentine Pavilion* in London, designed by Alvaro Siza, Eduardo de Moura and Cecil Balmond in collaboration with the Advanced Geometry Unit of Arup (AGU). The structure was assembled from 427 individually shaped, robot-prefabricated components, which were cut from cross-laminated veneer lumber (LVL) panels. [Men06b, p.77], [SSDMB05] This design was a lattice- rather than plate-type of structure, because it used the plates as vertical truss elements rather than as plates. However it already demonstrated the integration of integral mortise-and-tenon connections (with a single tab-and-slot per edge) into the components, combined with a Zollinger-type shifting and *interlocking* assembly sequence<sup>20</sup> and additional metal fasteners.

Also in 2005, another remarkable example for the integration of CNC-fabricated joints in a form-active plate construction has been presented by the *Swissbau Pavilion 2005* in Basel (Figure 2.5). This structure was assembled from 1.200 geometrically individual elements cut from orientend strand boards (OSB), which were assembled into a spherical array of

---

<sup>19</sup>For example, a 5-axis gantry machine for wood processing was co-developed and used since 1989 by Swiss Manufacturer Blumer Lehmann Holzbau. In 1996, a 7-axis robot router was installed by the German Manufacturer Holzbau Merk.

<sup>20</sup>Due to the mutual interlocking of the parts, the structure could only be erected in a unique assembly sequence

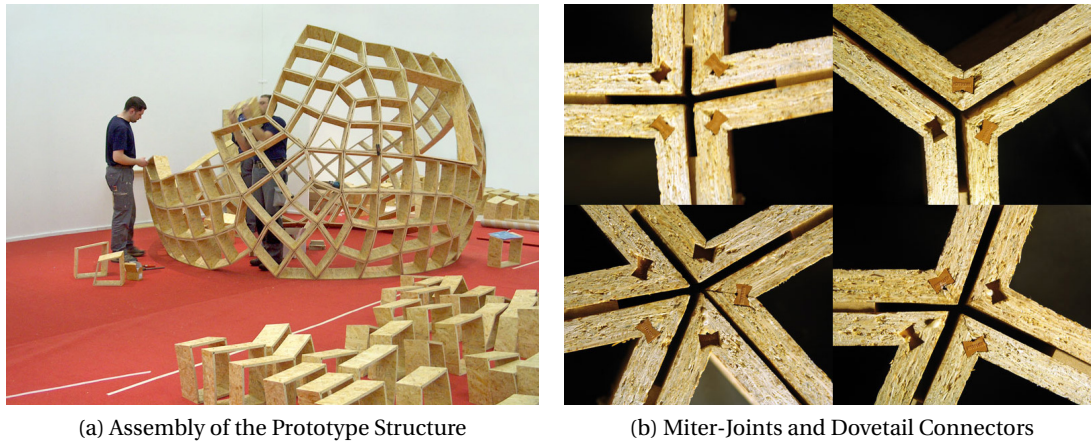


Figure 2.5 – *Swissbau Pavilion*, Experimental Prototype Structure presented at the Swissbau Exhibition in Basel, 2005. [SSB05] ©designtoproduction GmbH, Zürich

miter-jointed cassettes. While the Serpentine Pavilion was only using 3-axis fabrication techniques, this project first demonstrates the integration of 5-axis cutting, which allowed for the fabrication of the miter joints with integral dovetail-shaped longitudinal grooves. On-site, dovetail-shaped Connectors<sup>21</sup> were inserted into the cuts. [SSB05], [Hov09, p.138] From a point of view of integral mechanical attachment, this technique uses both the geometry of the parts and additional connectors to establish the connection. It can therefore be considered a hybrid Integral/ Mechanical Fastening technique.

The use of 5-axis cutting technology in this project is remarkable, because it took particular advantage of an already existing technology, through the use of a new technique: Despite the availability of 5-axis CNC technology, the manual programming of these machines remains time consuming and requires special CAM software, which is not commonly used in the timber construction industry, but rather in industry sectors with mass-produced products. In these sectors, CNC programs are used for the production of large batches of parts, therefore the time spent during the machine programming has a much lower impact on the efficiency of the design process. However in timber construction, CNC programs are typically used only one time, for the production of a custom-sized and custom-shaped part in a particular project.

In the Swissbau Pavilion, this problem was addressed through the use of a *CNC program generator algorithm*. While previous projects had already demonstrated the use of algorithmic tools for the generation of geometrical variations, this project first demonstrates the simultaneous use of an algorithm for the generation of the 5-axis CNC fabrication instructions. The use of this method was necessary due to the geometry of the project, where 300 individually shaped wooden frames had to be assembled with 1.200 miter-joints. A manual fabrication with machine-tool-technology, or the manual programming of a numerically controlled machine, would have both been infeasible for such a design.

<sup>21</sup>Connectors from the *Hoffmann-Schwalbe* System were used in this project

Having an algorithmic tool for the cutting of these inclined miter joints at hand, the additional integration of geometrical joints offered a significant added value to the project, in terms of the rapidity, simplicity and precision of assembly. The same technique was also applied to the 2005 *Futuropolis Sculpture* by Daniel Libeskind in St. Gallen, where 2.164 individual-shaped plate-shaped parts were assembled with integral joints [Hov09, p.130].

### Multiple-Tab-and-Slot Joints

Both the before mentioned Serpentine Gallery Pavilion with its mortise-and-tenon-joints, and the Swissbau Pavilion with its tongue-and-groove-joints demonstrated the use of integral joints with a *single* tab-and-slot per edge. The application of CNC-fabricated *Multiple-tab-and-slot Joints* for cross-laminated wood panels, inspired by the traditional multiple-dovetail joints from cabinetmaking, was investigated by Simek and Sebera in 2010. [SS10b], [SS10a]. This early investigation examines the mechanical behaviour of corner-joints for plywood panels, aiming at potential applications for the production of furniture rather than building constructions. The fabrication of the prototypes with a dihedral angle of 90° was carried out with a 3-axis CNC router.

Apart from pointing out the general relevance of this type of connection in the context of automatic fabrication and its ease-of-assembly, the research of Sebera and Simek illustrates particular advantages of the joints on cross-laminated wood panels. For example, it was demonstrated that multiple-dovetail joints on plywood provide a stiffness superior to those on hardwoods such as oak and ash. [SS10b, p.7]. [SS10a] provides valuable information on the influence of certain variable parameters of such joints.

A first architectural application of integral multiple-tab-and-slot joints on plywood was presented by the *ICD/ITKE Research Pavilion 2010*, an experimental structure built in 2010 at the University of Stuttgart. (Figure 2.6a) <sup>22</sup> This project required about 300 tension-resistant *1-plane* joints<sup>23</sup> for the connection of 80 elastically bent plywood curved plates. Since the panels were used as the primary load-bearing and visible structure, an aesthetic solution was also important for this project. The custom joint that was developed for this specific purpose combined multiple puzzle-jig shaped pins with a half-lap-joint, similar to so-called half-blind dovetail joints in traditional cabinetmaking. The pins allowed for the precise positioning of the parts, and the half-lap joint provided a large contact surface which was used for additional adhesive bonding. The geometry of the joints was generated with an algorithmic tool and fabricated with a 3-axis technique, using CAM software and a robot router.

At the same time, an integral, robot-fabricated *2-plane* finger-joint for non-orthogonal dihedral angles between plates was also developed at the University of Stuttgart (Figure 2.6b). Similar to the Swissbau Pavilion in 2005, these joints utilized the 5-axis capability of the robot router for integral joints between plates at a range of dihedral angles. The angle between the plates is

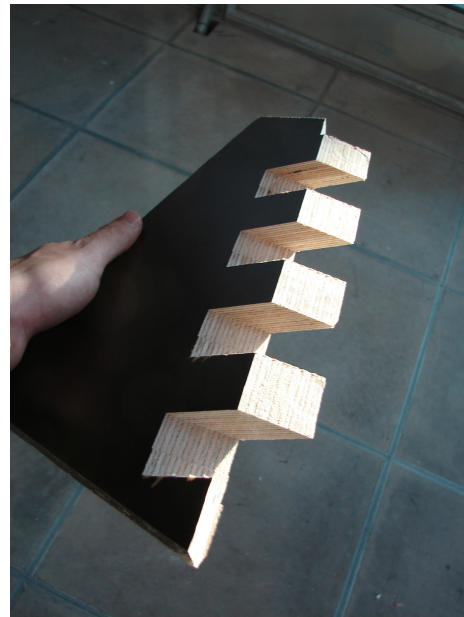
---

<sup>22</sup> see [Kal10, p.559-561]

<sup>23</sup> for a differentiation of 1-plane / 2-plane joints, see page 8



(a) 1-plane Joint Prototype



(b) 2-Plane Fingerjoint Prototype

Figure 2.6 – Integral Multiple-Tab-and-Slot Joint Prototypes. *Left* 1-plane, 1DOF, multiple-tab-and-slot joint [Kal10, p.559-561], *Right* 2-plane, 3DOF multiple-tab-and-slot joint, at a dihedral angle of  $120^\circ$ , 2010. ©ICD, University of Stuttgart

embedded in the geometry of the joints.

A new feature was introduced for the use of such joints in assemblies with multiple edges per vertex, where several joints meet: On traditional multiple-tab-and-slot joints, the intersection between the two plates is attributed to either one of the two jointed plates, in an alternating manner. When multiple such joints meet in one vertex, this becomes complicated and may be unresolvable. A simple solution for this problem was the introduction of miter segments at the first and last segment of the joint, where the intersection between the plates is shared equally. This allows for multiple joints to meet in a vertex without conflicts.

The Fabrication of the joints was carried out with a spot-facing technique [Koc64], where the cutting tool is oriented normal to the finger-joint faces which are parallel to the edge. This new, 5-axis enabled technique allowed for the sharp interior corners of the joint, additional notches were not required for the assembly. The joint geometry was generated with an algorithm, but the CNC code for the prototype was generated manually with a CAM software.

This technique was first applied to a surface structure built from multiple plates, as part of a seminar at the University of Stuttgart in 2010<sup>24</sup> (Figure 2.7a) . The folded surface was assembled from 30 individually shaped components, connected with 37 joints, and demonstrated several challenges in the design, fabrication and assembly of such structures.

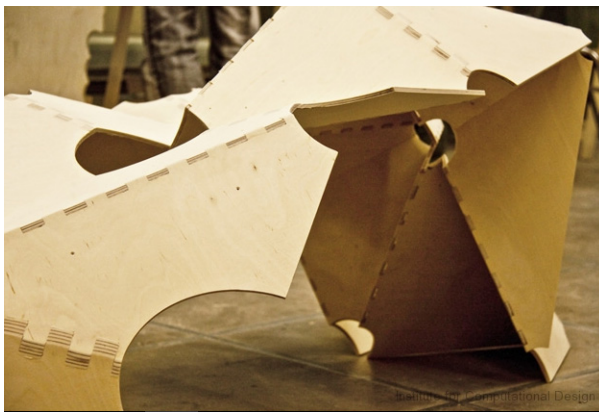
---

<sup>24</sup>see [RM10] and [BK10]

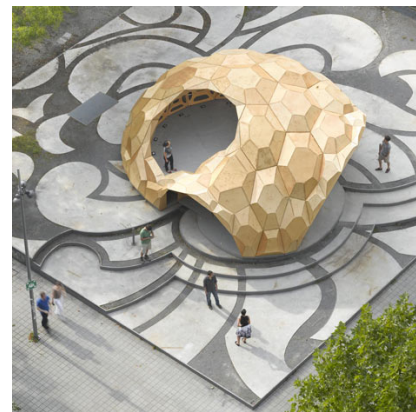
## 2.1. Integral Mechanical Attachment for Timber Plates

One of the novelties in the way the joints were used in this project was the independency from the orientation of the wood fibers: The traditional dovetail joints in cabinetmaking could only be applied to the end-grain edges of wooden plates.<sup>25</sup> This limitation is due to the much lower strength of regular timber panels in the side-grain direction. However the layer-wise cross-lamination in engineered wood panels such as plywood, LVL or CLT allows for the application of finger- or dovetail-joints at any possible edge orientation. In consequence, plate-shaped components can be fabricated with multiple-tab-and-slot joints on multiple non-parallel edges, which has first been demonstrated in this project.

The prototype was designed through the mapping of a regular triangular polygon mesh, which assured the planarity of the plates, onto a doubly-curved parametric surface. A static height was then achieved in the structure through the elevation of vertices normal to the surface, forming hexagonal pyramids. The alternation of the low points in this configuration avoided continuous folding lines that would have created structurally weak points, and spherical cutouts were made at the apex of these pyramids, due to the 6-valence, which was geometrically unresolvable for the joints.



(a) *Adaptive Folded Plate*, ICD Seminar Project, 2010



(b) *ICD/ITKE Research Pavilion*, 2011

Figure 2.7 – First Applications of Integral, 2-plane, 3DOF, Multiple-Tab-and-Slot Joints - *Left* Adaptive Folded Plate, student work developed in the ICD seminar *Robotically Manufactured Material Systems*, 2010. *Right* ICD/ITKE Research Pavilion, 2011. ©ICD/ITKE, University of Stuttgart

The fabrication of the polygonal plates with multiple finger jointed edges showed a disadvantage of the spot facing technique, which requires the cutting tool to be positioned normal to the inclined front faces of the fingers. Using standard flatbed clamping techniques, this becomes problematic when one plate has multiple 2-plane jointed edges, some of which face diagonally up and some diagonally down. After the fabricate the upwards facing joints, the plate must be released, flipped and re-clamped, before fabricating the downwards facing joints

<sup>25</sup>see page 8



Another important observation was made during the assembly of this prototype: The geometry of the joints, which constrains the relative movement of parts to each other, is beneficial for the integration of assembly guides and for the transfer of forces, but it also introduces constraints in the assembly of surfaces from multiple plates.

The 3DOF geometry of the finger joints allows only for translational and rotational movements, on a plane normal to the joints edge. When multiple non-parallel edges have to be jointed simultaneously, a common assembly direction must exist. However, although these constraints were not considered in this first design, the prototype could be assembled due to the elasticity and flexibility of the 6.5mm thin birch plywood plates. Additional adhesive bonding was used to keep the parts in place.

Subsequently, this technique was applied to the *ICD/ITKE Reserach Pavilion 2011* (Figure 2.7b) [lMea13] and published in 2012 [KDR<sup>+</sup>12]. The 2011 Research Pavilion, a segmented plate shell construction, was similarly based on the mapping of a triangulated irregular *Voronoi* pattern, onto a doubly-curved parametric surface. Here, the mid-vertices of the voronoi cells were elevated normal to the surface, forming polyhedral-based pyramids, and truncated at the apex to avoid the high valence at this point.

While the previous 2010 prototype aimed at the assembly of a continuous surface, the 59 pyramidal segments of the 2011 prototype were designed as separate, prefabricated box-components, where the pyramids were offset and connected with additional plates along the sides. These hollow cells were assembled from a total of 850 cross-laminated 6.5mm birch plywood plates.

The joint geometry was identical to the earlier prototypes, however the joint fabrication data was now processed automatically, with a customized CNC program generator. The ISO-CNC code was then converted into Robot code with a separate tool. The fabrication of joints was also improved, through the integration of a turntable positioner for the robot router. As described above, plates with both upwards and downwards facing 2-plane joints must be flipped and re-clamped during the fabrication. This re-clamping will result in a loss of accuracy. The turntable however allowed for a cantilevering positioning of the edges, providing simultaneous access to both from above and below. However, the cantilevering edges make this technique susceptible to vibrations, which generally reduce the quality of the cuts and must be counteracted with lowered feed rates, which slows down the production process.

The most recent application of integral finger joints has been presented by the *Landesgarteschau Exhibition Hall* in Schwäbisch Gmünd, Germany in 2014. (Figure 2.8) This doubly-curved, segmented plate shell has been assembled from 243 planar, polygonal components. The parts were fabricated from 50mm thick structural beechwood panels, which form the single, load-bearing layer of this shell structure. Fabrication was carried out in two steps: First, 3-axis rough cuts were performed with a Hundegger SPM CNC Router, then the joints were fabricated, using a robot router setup with an external turntable, similar to the 2011 prototype. [KSM<sup>+</sup>14]



Figure 2.8 – Landesgartenschau Exhibition Hall 2014 - *Left* Interior view visualisation. *Right* Assembly of the finger-jointed plates on site ©ICD/ITKE, University of Stuttgart

In contrast to the previous projects, the 3DOF finger joints for this shell were fabricated not through spot facing, but with a side-cutting technique. This method requires access to the plates only from above. It allows for the clamping of the workpieces without cantilevering edges, resulting in faster fabrication. Instead of the previously sharp interior corners of the finger joints, the radius of the cutting tool remained as a fillet here.

Furthermore, the connections were not combined with additional adhesive bonding, which is not possible on site. Instead, the finger joints were combined with mechanical fasteners. Due to the three degrees of freedom of the finger joints, the integral connection can only resist in-plane shear forces parallel to the edges in this structure. Other forces are being supported by the additional metal fasteners. However, the three degrees of freedom allow for a relatively simple assembly of the parts. The plates can always be inserted from above, along their surface normal direction. An assembly guide was integrated only for the lateral alignment of the plates.

### 2.2 Folded Plate Structures

All of the prototype structures introduced in the previous section 2.1.3 have been built from timber plate components and belong with the group of *form-active structure systems*, which Engel describes as a “materialized result of the natural force directions”<sup>26</sup>. However, they were based on different structural concepts, which accordingly set different demands and challenges for the connections between the plates.

When working with plate-shaped components such as engineered timber panels, a particularly interesting sub-category within the form-active structures is presented by the so-called *surface-active structures*, which integrate the structural performance of the plates into the elements used for the enclosure and subdivision of spaces. In such structures, the orientation of the surface to the forces is decisive for the structural performance. [Eng77, p.149]

*Folded Plate Structures* present one of the systems in this group. While combined rib-slab structures strengthen a horizontal plate element with additional vertical slab elements, folded-plate structures *integrate* the threefold load-bearing action of a slab, a plate and a truss (Figure 2.9) in one element. Unlike framing structures, where surfaces only cover the structural skeleton of a building, surface-active systems use their surfaces as an envelope for spaces and simultaneously as the main load-bearing components.

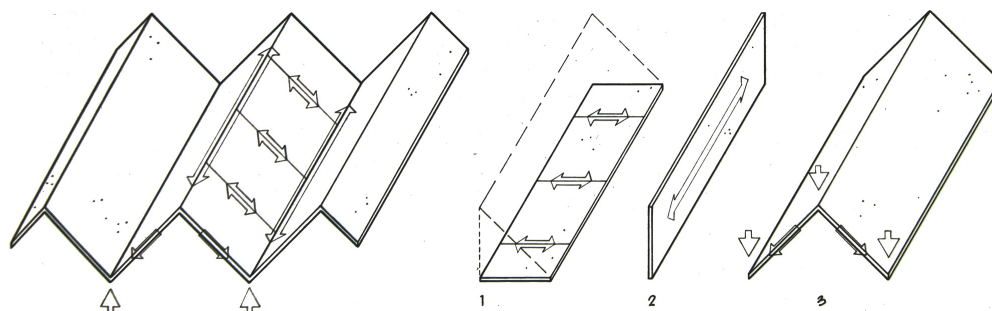


Figure 2.9 – Threefold Load-bearing Action of a Folded Plate - Folded plate structures combine slab-action, plate-action and frame-action. *Left* Simplified flow of stresses in a singly folded plate. *Right* 1. Slab Action, 2. Plate Action, 3. Truss (frame) action. Figure: [Eng77, p.151]

In architecture, folded plate structures are typically used to cover large spans without vertical supports, which allows for mobility beneath. Built examples range from roofs for swimming pools, gymnasiums and storage buildings, to offices or centres. In addition to the column free space beneath a free spanning folded plate, the reduction of pile foundations can be beneficial under certain ground conditions. [Wil97, 1]

This section will elaborate on the origin of the term folded-plate structure, its origins, the purpose of such structures and their development over the past decades. A particular emphasis will be put on the history and relevance of joints in the design of such structures, in relation to

---

<sup>26</sup>see [Eng77]



the different materials that were used, and the impact that the pre-fabrication and jointing methods had on the geometry of Folded Plate Structures.

### 2.2.1 Origins in Concrete

The history of folded plate constructions begins with the discovery of a structural concept in civil engineering, which was first used for the optimization of plate structures built from reinforced concrete. The following proliferation of the folded plates was closely related to the development of methods for their calculation. First analytical studies of folded plate structures have been presented in the 1930s, based on observations and optimizations in the design of concrete coal bunker constructions in the 1920s in Germany. (Figure 2.10a)

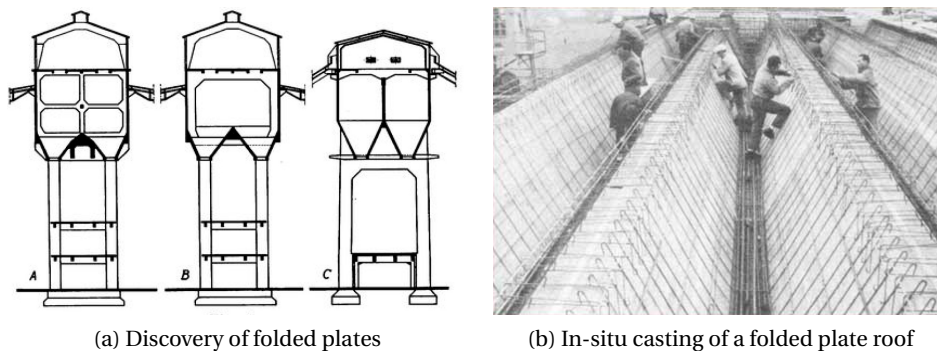


Figure 2.10 – Origins of Folded Plate Structures - Left: Cross-section through coal-bunkers, A. 1915, B. 1921, C. 1925. [Cra29] Right: Folded plate construction through primary forming. In-situ casting and formwork of a roof construction

These coal bunkers had a folded cross-section at their bottom, the form of which was found to perform as a surface-active structure system. While early versions around 1915 were fitted with elaborate additional rib and cross-bracing elements, those were not used any more by 1925. The phenomenon was first investigated and published by Hermann Craemer in 1929<sup>27</sup>, who argued that concrete constructions with conventional modelling, using beam theory, would throw away the advantages of reinforced concrete [KR12, p.1915]. Instead, in the folded plate, “which consists of several in-plane-loaded plates in different planes whose ends are secured against displacement and which are connected seamlessly, the fold completely takes over the role of a down stand beam at that point.” [Cra29, p.270]. Craemer emphasises the importance of “Fugenlosigkeit”, which describes the seamless connections between the plates that can be achieved with in-situ cast steel-reinforced concrete (Figure 2.10b).

Building with steel-reinforced concrete was a popular and already well-developed construction technique at the time. It allowed for large spans and provided resistance to fire, deterioration and corrosion. [Gar06] A first analytical method was published by Ehlers in 1930. [Ehl30] However the early methods were generally considered too complex and arduous in their use.

<sup>27</sup>see [Cra29]

[Wil97, p.1] Simplified calculation methods were developed only in the second half of the 20th century in the United States.<sup>28</sup> Several structures were built in the 1950s and 1960s. At the same time, *curved shells* such as barrel vaults presented a competing geometry, which allowed for equally long spans. In comparison to the folded plates, barrel vaults required a thinner shell thickness and were therefore more material- and form-efficient, but the construction and especially the formwork of folded plates was less complicated than those of curved shells, which required the involvement of specialized firms. [Wil97, 2]. In that regard, the ease-of-manufacture was considered the main advantage of folded plates over curved shell structures.

However, after about a decade of much attention and discussion in research and several built examples, the construction of concrete shell and folded plate structures almost entirely stopped around 1970.<sup>29</sup> A combination of several developments is being discussed as the reason for this sudden loss of interest. For the curved shell structures in particular, the construction methods were very labor-intensive. Many of the notable structures were built in Mexico and other South American countries<sup>30</sup>, where the cost of labor was comparably low.

As mentioned before, the construction and especially the formwork of the folded plates was less elaborate, but it also required in-situ casting. This was facing an increasing competition with the parallel development of precast and pre-stressed concrete elements. The prefabricated components were less labor intensive in their production, because they took advantage of centralized machine technology which replaced manual labor. For the design of folded plate structures however, the use of prefabricated concrete elements presents a problem at the connections between the precast elements. Folded plate structures require a stiff and rigid connection at the folds, which can be achieved relatively easily with in-situ cast reinforced concrete and its continuous reinforcement bars at the folds.

While the folded plate structures originate in in-situ cast concrete, which is a manufacturing process from the group of *primary forming*<sup>31</sup> methods (see Table 2.2), the changes in the labor market and fabrication technology, resulted in an increasing interest in prefabricated structures, which would require additional joining between the precast plates or modules, to provide the *seamlessness* mentioned by Craemer.

---

<sup>28</sup>see H. Simpsons method [Sim58]

<sup>29</sup>see [Ket14]

<sup>30</sup>for examples, see [Fab63]

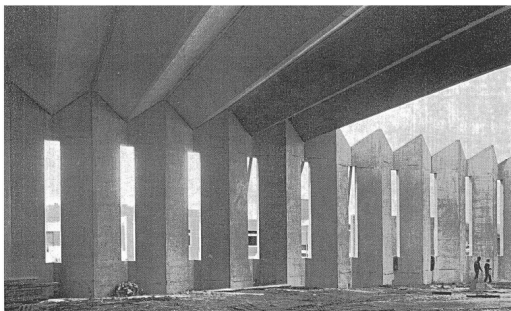
<sup>31</sup>the terms primary forming and secondary forming have been translated from the respective German taxonomy into *Urformen*, where rigid bodies are created from a material without form, and *Umformen*, where one form is transformed into another form, through plastic deformation. This taxonomy was introduced by Otto Kienzle [Kie56] and later adopted by the standard specification [fN74]

Primary Forming	Secondary Forming	Joining
Casting Extruding Sintering ...	Bending Deep Drawing ...	Adhesive Bonding Welding Mech. Fastening Integral Mech. Attachment

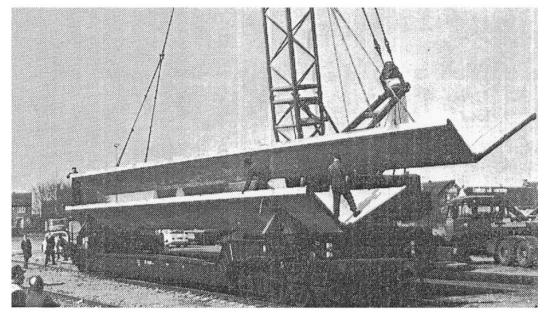
Table 2.2 – Taxonomy of fabrication techniques for folded plates

In such prefabricated designs, transportable components were still produced through casting, but in a factory environment rather than on site. Due to the repetitive form of folded plate structures, the overall construction could be divided into geometrically identical sub-components, which were be fabricated on a single mold.

An early example for such a prefabricated Folded Plate structure was a church in Hoensbroek in the Netherlands, which was built in 1962 (Figure 2.11). The folded-plate walls and roof of this church were constructed from separate, V-shaped concrete elements (Figure 2.11, right side), with a dihedral angle of  $110^\circ$ . These modules were prefabricated and brought to site with a truck to allow for a fast construction period. A disadvantage of this design was that, while the lower folds of this structure, which must predominantly resist tensile forces, were precast with re-bars, the upper folds, which receive predominantly compressive forces, were only resting against each other. This presented a conflict with the general concept of folded plate structures, in which all plates must be connected together in a rigid manner, so they can provide mutual support for each other and transfer forces along their edges.[Mar13] This lack of rigid joints resulted in buckling problems. [Gar06, 1194], [Mei64] and [Bre64]



(a) On-Site Assembly



(b) Transport of the precast elements

Figure 2.11 – Folded Plate Church in Hoensbroek, Netherlands, 1964. Built from precast concrete components, with a span of 25 m. - Buckling problems in this structure resulted from a lack of rigid joints at the upper folds. Images taken from [Mei64]

In the following years the prefabrication of Folded Plate Structures continued and various solutions for the jointing were developed, which should allow for fast on-site assembly, while providing rigid connections between the plates. A particularly successfully technique was developed in Florida in the U.S. by Walter C. Harry: Here, the upper folds of the modules

were precast. Once the prefabricated elements were erected, tensile steel cables were welded to the bottom of the modules as additional *interior supports*. Then, the separate modules were jointed along their valley folds through upwards protruding reinforcement bars (rebars). The geometry of this detail allowed for the elimination of tolerances. Finally the rebars were tied together and jointed through a strip of in-situ cast concrete. [Har63, p.1377]. Another interesting detail of these structures was the cross-section of the precast modules, which consisted of three plates each, with a trapezoidal cross-section, instead of the two-plate modules in the Hoensbroek example, with their triangular cross-section.<sup>32</sup> A considerable number of structures was built with this technique.

A similar technique has been developed in China in the 1980s. [ZAC91] describes how pairs of concrete plates were precast flat on the factory floor, connected only through continuous rebars in between them. These plates were then actually folded about this rebar-hinge for a flat-packed transportation. On site, they were opened again to the correct angles and joints were cast in-situ similar to the previously mentioned technique by Harry. Several building in Honduras have been realized with this technique.

Geometrically, the majority of the concrete folded plate structures built in the 1960s was straight extrusions of corrugated profiles, resulting in only planar quadrilateral faces. (Figure 2.11) This type of Folded Plates was referred to as *through-type*.<sup>33</sup> However, there are also early examples of folded plates with triangular faces. [Eng77] describes such designs as Folded Plates with *counter-running profiles*<sup>34</sup>. Another term for these designs is also sawtooth roofs. In such structures with counter-running profiles, the profiles are shifted by a half fold. The connecting lines between the profiles now run from the top of one fold on the first profile to the bottom of the shifted, counter-running profile. A top-to-top and bottom-to-bottom connection of such counter-running profiles is also possible. Its results not in planar, but in ruled surfaces<sup>35</sup> which are more complex in their design, calculation and construction.

### 2.2.2 Fiber-reinforced Plastics

Around the end of the 1960s and the beginning of the 1970s, when the main period of Folded Plate Constructions with concrete neared its end, fiber-reinforced plastics was researched as an alternative material for Folded Plate Structures. Amongst others, Huybers mentions the translucency of this material as an advantage over concrete, as the integration of rooflights in concrete folded plates always remained problematic. [Huy72]

Another advantage of the plastics was the low weight-to-strength ratio. Designs such as Renzo Piano's sulfur factory [Piz03] and the prototypes designed and built by Zygmunt Makowski's

---

<sup>32</sup>in the trapezoidal configuration, stresses were distributed along two edges instead of only one in the triangular configuration

<sup>33</sup>for examples, see [Wil97, p.7-15]

<sup>34</sup>Examples for counter-running, triangulated folded plates: Entrance to Bradford College, Yorkshire, UK.

<sup>35</sup>The *Miami Marine Stadium* demonstrates a folded plate structure with counter-running profiles which have been connected with ruled surfaces. The structure was realized with reinforced concrete and completed in 1963.

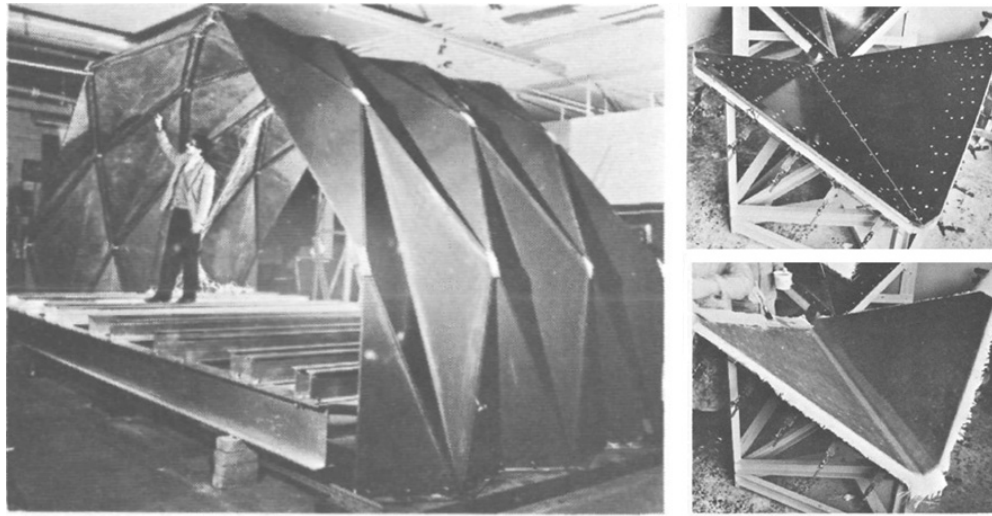


Figure 2.12 – *left side*: Antiprismatic Folded Plate designed by Benjamin [BM65], *right side*, examples for a mold which was used for the fabrication of creased modules. [Huy72]

Research Group<sup>36</sup> and Pieter Huybers took particular advantage of the lightweight property of fiber-reinforced plastics: Large amounts of small, easy-to-handle *modules* were assembled into lightweight and translucent vault structures, some of which were used as temporary and convertible structures.<sup>37</sup>

The Folded-Plate Topologies of these designs were different from those of the concrete Folded Plates. Due to the relatively small faces, a corrugation in two directions was necessary, as well as a certain curvature of the entire assembly. These requirements were accommodated through hybrid Curved-Shell / Folded-Plates designs, which Zygmunt Makowski refers to as *Folded Plate Barrel Vaults*. The production of the individual parts and modules for these structures was carried out manually using molds. The designs were therefore typically assemblies of geometrically identical components, which could all be produced on a single mold.

Like the prefabricated concrete folded plates, the structures built with fiber-reinforced plastics always required some sort of joints. Considering the large amounts of parts that resulted from the small-faceted designs, the feasibility of these connections was important. In his PhD thesis, Pieter Huybers investigated multiple innovative joining solutions, such as lacing, where bundles of glass fibre are laced through pre-drilled holes along the edges and then injected with resin, or hinge-type joints, where straight bars were inserted as connectors. The final prototypes however were joined with standardized steel bolts.<sup>38</sup>

<sup>36</sup>Structural Plastics Research Group, University of Surrey, Guildford, United Kingdom

<sup>37</sup>The sulfur factory designed by Renzo Piano could move along the longitudinal axis of the cylindrical shell, through the disassembly of the lightweight modules (14kg) at one end, and their re-assembly on the other end of the structure.

<sup>38</sup>Huybers states that "As a general rule it can be stated, that curing of resins at the building site should be avoided. Mechanical methods of interconnection, making use of completely cured products, are preferable." [Huy72, p.119]

A particularly interesting topology that was developed in this context are so-called *Antiprismatic Folded Plate Shells*. An early prototype of such a structure had already been built in 1965 by Makowski's research group [BM65]. These structure were assembled from rhombus-shaped quadrilaterals with a diagonal crease between the acute angles. The crease could be created through bending or lamination on a custom mold, and it already replaced one laborious and potentially weak joint per module. These modules were then assembled in a two-dimensional array, where every second module was flipped upside down. This assembly will result in a cylindrical curved shell, where the radius of the shell and the static height in the cross-section of the structure result only from the modules parameters, including the size and angles of the rhombus and its crease angle. Variations and concepts of this topology have been described by [Huy01] and [Fro78].

### 2.2.3 Timber Panels

Similar to the examples with fiber-reinforced plastics, only relatively few *Timber Folded Plates* have been built to date, although timber provides advantages similar to the fiber-reinforced plastics, such as a low-weight-to-strength ratio, plus new and increasingly important advantages related to the sustainability of structures, such as its carbon dioxide storage. Nevertheless, built structures with a short and medium span date back to the end of the 1950s<sup>39</sup>. However, due to a lack of large-size wood panels, many structures were built as timber-frame constructions, using linear timber elements rather than plate-shaped elements.

An early example for the use of industrially produced, cross-laminated panels is presented by a factory building in Jenbach, Austria, which was built in 1996. The main, 44m wide spanning part of this structure was assembled from a total of 33 prefabricated upside-down boat-shaped folded modules. Each of these boat-shaped modules had been assembled from two quadrilateral plates in the middle, forming the main fold at a dihedral angle of 90°, and four triangular plates at the side, which formed the supporting frames.

The plates themselves were built as a timber-frame or sandwich construction, consisting of a middle-layer of parallel timber beams with a height of 200mm, which was then covered and cross-braced by cross-laminated solid wood panels (SWP)<sup>40</sup> with a thickness of 26mm on the top and bottom. At the lower side of these prefabricated modules, additional tensile steel cables were used as stiffeners, similar to the interior supports on the precast-concrete modules developed by Walter (see section 2.2.1) On site, the large-span modules were connected with each other at the lower folds.

Another Timber Folded Plate construction, now built entirely from timber plates was realized in 2004 near Augsburg, Germany. The *Thannhausen Music Rehearsal Hall* (Figure 2.13) [Sch04] was built from glue-laminated wood panels with a thickness of 100 mm. Both the walls and the roof of this building with a span of 10m were built from folded timber panels. The geometry

---

<sup>39</sup>A comprehensive collection of the built structures has been provided by [Lei04]

<sup>40</sup>K1 *Multipan* panels, Mayr-Melnhof Holz, Austria



Figure 2.13 – Gluelam Folded Plate structure for the Music Rehearsal Hall in Thannhausen, 2002 - Copyright and Photos: hiendl\_schineis architekten, Augsburg

of this quadrilateral through-type structure is similar to the concrete examples such as the church in Hoensbroek previously shown in figure 2.11.

However, the geometry of the prefabricated modules is individual, including different widths and dihedral angles between the plates, ranging from angles as large as  $145^\circ$  to smaller ones  $115^\circ$ , at the end segments of the building. Furthermore, at the intersection of the walls and the roof in this building, interior folds merge into interior folds and exterior folds merge into exterior folds. In Hoensbroek the modules were shifted by one segment.

The prefabrication strategy was also similar to the Hoensbroek example. However, in contrast to the Construction in Jenbach, or the modular constructions by Harry, no additional stiffening elements or ties were added to this folded plate structure. [Sch04] emphasises the monolithic appearance of the single, visible material used for the load-bearing structure. The prefabricated modules consisted of two glue-laminated plates each, with glued miter joints at the interior folds, where the plates meet side-grain to side-grain on their edge faces. These prefabricated joints remained visible in the interior space of the building.

On site, the prefabricated modules were jointed along their long edges to form the exterior folds. This was done with a miter joint geometry, screws and additional adhesive bonding<sup>41</sup> (IK-PUR). Finally, the connections between the walls and the roof were not glued, but connected with a horizontal butt joint geometry and mechanical fasteners. This was due to the fact that in these joints, the end-grain faces of the walls must be jointed with the side-grain faces of the roof. This type of connection does not allow for the use of adhesive when using a butt joint geometry<sup>42</sup>.

In 2006, a timber-folded barrel vault (Figure 2.14), similar to the fiber-reinforced-plastics vault prototypes of Makowski and Huybers, was built at the Timber Construction Laboratory at

<sup>41</sup> A special permission was granted for the on-site gluing of this structure

<sup>42</sup> see the discussion in chapter 3, page 64.



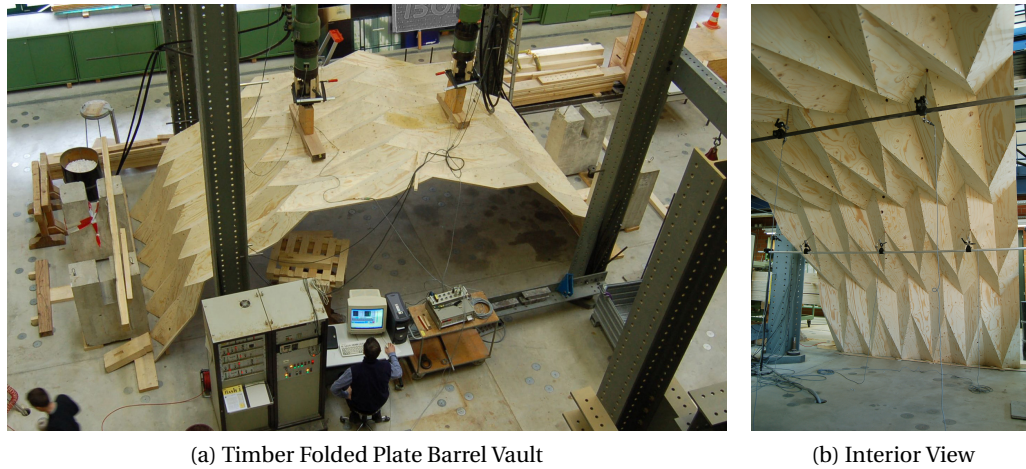


Figure 2.14 – Timber Folded Plate Barrel Vault - built from Plywood Panels at the laboratory for timber construction. [BW06]

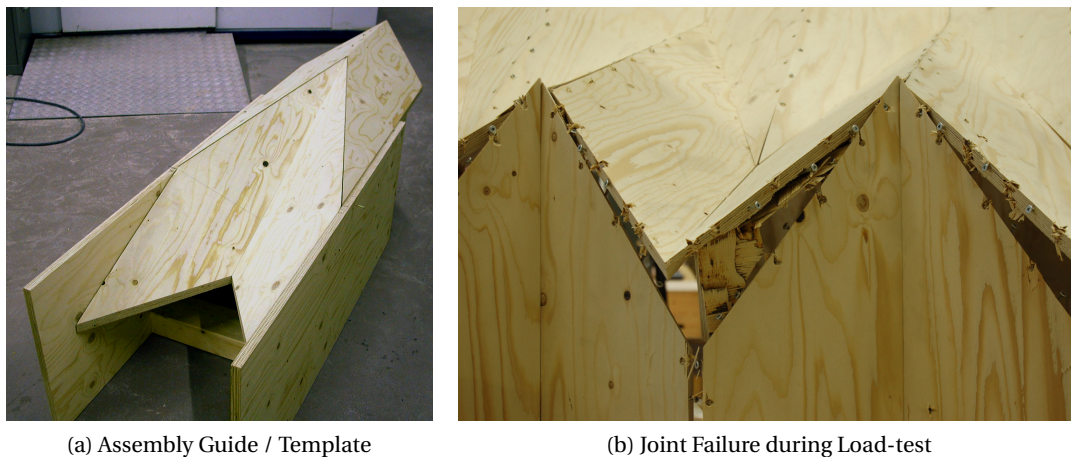


Figure 2.15 – Timber Folded Plate Barrel Vault Details - a. Guide for the assembly of modules at the right angles, b. Miter Joints combined with Self-tapping wood screws: Joint Failure after Flexural Test on a Plywood Folded Plate Prototype - Image taken from [Bur10, p. 208]

the Swiss federal Institute of Technology in Lausanne.[BW06] The topology of this structure however was different from the antiprismatic folded plates of Huybers and Makowski. Instead, the geometry was inspired by the Japanese *Miura-Ori* Origami Paper folds<sup>43</sup>. The prototype structure was built from quadrilateral components with the shape of trapezoids with opposite obtuse angles. 120 geometrically identical plywood plates for the main structure and 24 additional plates for the ground supports. Then, the vault geometry was created through an assembly of these plates in a two-dimensional array of 12x12 plates, where every second component was flipped.

<sup>43</sup>see the comparison of these topologies in chapter 4, page 96



The connection between the plates was established through a miter-joint geometry, which was combined with mechanical fasteners. The angular cuts on the edges of the plates, which were required for the miter joints, were fabricated in a manual procedure using machine-tool-technology. A circular saw was used for the inclined cuts, and a custom guide was built for the assembly of modules (Figure 2.15a). The dihedral angles between the plates were  $120^\circ$  for all transversal joints and  $117^\circ$  for all diagonal joints.

In his Master Thesis [Hah09], Benjamin Hahn investigated the load-bearing behaviour of this prototype, comparing the results of an experimental load test, in which an increasing central vertical line-load was applied to the built prototype until failure (Figure 2.15b), with those of finite-element simulations that assumed rigid joints between the plate components. The analysis demonstrated the generally semi-rigid behaviour of the joints used in this prototype. Both Hahn and Buri [Bur10, p.209] conclude that the overall structural performance of such timber folded plate vaults could be improved through more stiff and rigid connections.

In his PhD Thesis, Buri elaborates on the geometry of Origami-inspired Folded Structures. A variety of *reverse-folded* surface structures can be generated through the definition of two 2-dimensional *corrugation profiles*, which represent the longitudinal and transversal cross-section of a folded structure. The surface geometry is being generated through a projection of the transversal profile along multiple reflection planes, which are located at the vertices of the longitudinal profile, normal to the bisector between the neighboring Polyline segments.

This technique was also applied and demonstrated on a built structure in 2008. The *Temporary Chapel St. Loup*<sup>44</sup> (Figure 2.16a) was constructed in the town of Pompaples, in the Swiss Canton of Vaud. This building was planned as a temporary construction, however it has not been removed as of yet. In addition to the new design method, which allowed for the irregular shape of the design, the structure introduces the use of industrially produced cross-laminated timber panels (CLT) for the construction of a folded plate structure. Due to the surface-active design, a span of 9m could be realized with a plate thickness of only 40mm for the 28 wall elements and 60mm for the 14 roof elements. As a consequence of the irregular shape, the plates are jointed at various different dihedral angles, ranging from  $130^\circ$  to  $104^\circ$  at the end segment towards the entrance of the building.

Figure 2.16b shows the assembly of the CLT elements on site. The connections between the plates were, similar to the previously mentioned barrel vault, established through a miter joint geometry, combined with 2mm thick metal plate connectors (Figure 2.16c), which were custom-made for the individual dihedral angles. These metal plates were then connected to the exterior side of the timber plates with self-tapping wood screws.

---

<sup>44</sup>Design by *localarchitecture* architects in collaboration with *Shel*, Hans-Ulrich Buri and Yves Weinand.



(a) Temporary Chapel St. Loup



(b) Assembly of the plates



(c) Steel-plate Connectors

Figure 2.16 – Chapel St. Loup, Pommaples, 2008 - Folded plate structure with a span of 9 m, built from cross-laminated timber panels. The joints between wall and roof elements were connected with metal-plate connectors. Copyright: localarchitects/IBOIS, Photos: Fred Hatt

## 2.3 Objectives

The first part of the state-of-the-art illustrated the relevance and recent developments of integral *multiple-tab-and-slot* joints for cross-laminated timber plates. Most notably, [SS10b], [SS10a] have demonstrated the mechanical behaviour of multiple-dovetail joints with a dihedral angle of  $90^\circ$  on cross-laminated plywood panels, and the research at the University of Stuttgart demonstrated the advantages of *1-plane* (1DOF) multiple-tab-and-slot joints, for the improved assembly of multiple geometrically different plate elements [FM12]. Further developments showed the design and fabrication of *2-plane* (3DOF) finger-joints [RM10], [KDR<sup>+</sup>12]. The advantages of these joints for the assembly of form-active surface structures built from thin wooden plates have been demonstrated in combination with adhesive bonding [lMea13], [KCC<sup>+</sup>14] and in combination with mechanical fasteners [KSM<sup>+</sup>14].

The second part of the State-of-the-Art showed the development of *Timber Folded Plate Structures*, which combine the efficiency and elegance of folded plate structures with the advantages of timber as a building material. [Sch04] presented a timber folded-plate built from glue-laminated wood plates, which were connected with miter-joints, combined with adhesive bonding and mechanical fasteners. [BW06] demonstrated an experimental timber folded-plate barrel vault, folded in 2-directions. The prototype was built from cross-laminated plywood plates which were connected with miter-joints and mechanical fasteners. Subsequently, [Bur10] presented a method for the simplified design of free-form folded plates, which was also applied to a full-scale building structure built from CLT panels.

The Objective of this Thesis is to develop integral joints for timber folded plate structures, connecting and building upon the previous research in the two domains. The work intends to increase the role of Integral Mechanical Attachment both in the assembly of folded plate structures, through integral locator features, as well as the rigid connection of the plates through integral connector features.

In contrast to the previously developed 2-plane finger-type multiple-tab-and-slot-joints with three-degrees-of-freedom (3DOF) [lMea13], [KCC<sup>+</sup>14], [KSM<sup>+</sup>14], this thesis will focus on the development of new 2-plane *dovetail-type* multiple-tab-and-slot-joints, with only *one degree of freedom* (1DOF). With their 1DOF geometry, these joints shall bring the benefits of 1DOF-joints for beams, such as mortise-and-tenon-joints<sup>45</sup>, to the construction of timber folded plate structures.

Integral locator features are expected to allow for improvements of the assembly process. Position and alignment of parts can be embedded in the joint geometry, allowing for a flat-packed transport, and a simple, fast and precise assembly on site. The integral feature should reduce or replace guides and supports in the construction phase.

Integral Connector features should reduce or replace additional connectors such as mechanical fasteners or adhesives. Instead, the joint geometry will block relative movements between

---

<sup>45</sup>see figure 2.4, on page 13

parts and transfer mechanical forces. Finally the reduction of mechanical fasteners should also improve the aesthetics and allow for visible joints.

## 2.4 Methodology

The interdisciplinary development of the joints requires theoretical research into the architectural history of European and Asian timber joinery and Folded plate structures, but also into the related subjects of digital geometry processing, wood processing, manufacturing systems and robotics, civil and mechanical engineering. Practical research is carried out through the development and subsequent experiments with virtual and physical prototypes.

### 2.4.1 Development of Algorithms

Customized algorithmic tools are required for the development of the physical and virtual prototypes. Prior to all other developments, a tool-kit of basic algorithms for the fabrication of the joints must be developed. While the manual drawing of the joint geometry is sufficient in the first phase, the manual machine code programming of these joint prototypes, which require simultaneous 5-axis machining, is unfeasible. The integration of repetitive custom details requires a CNC program generator. This development requires a direct engagement with the machine(s) used for the production of the joints.

For the application of the joints to folded plates which are folded in 2-directions, built from many geometrically different, small, transportable and prefabricated components, a manual generation of the joint geometry is not feasible. This requires the development of a custom-built tool for the automatic joint geometry generation. A specific framework with techniques and resources for this development is provided by *polygon mesh processing* (see [BKP<sup>+</sup>10]), which allows for the necessary connectivity- and neighborhood requests.

### 2.4.2 Development of Prototypes

While CAD models allow for the development of various geometry- and assembly related joint features and parameters, complementary physical prototypes are required for the empirical study of machining- and material related parameters. These include certain tolerances, defects and imprecisions, as well as productivity-related parameters, such as the rapidity-of-production. A compromise must be established between the machine-specific feasible production speed and the resulting output-quality.

These initial prototypes only deal with the simultaneous jointing of two parts, avoiding complex constraints in the simultaneous assembly of multiple parts. The empirical findings from these prototypes, such as *fabrication constraints* and optimized parameters, can be integrated into the fabrication algorithms.

When using 1DOF joints, a strategy and sequence for the assembly of parts must be developed. This becomes particularly challenging with Folded Plate Structures which are folded in two directions. (for example [BM65], [Huy72] or [BW06]).

### 2.4.3 Investigations

The complexity of the overall objective is being broken down into multiple investigations, which build upon each other. The individual investigations will increase the role of Integral Mechanical Attachment (Table 2.3) and the complexity of assembly (Table 2.4) in incremental steps.

Investigation	Integral Mechanical Attachment	+ Additional Connectors
Chapter 3	Rigid Interlocks (1DOF)	Adhesive Bonding
Chapter 4	Rigid Int. (1DOF) + Group Interlocking	
Chapter 5	Rigid Int. (1DOF) + Group Int. + Elastic Interlocks	

Table 2.3 – Increasing the Role of Integral Mechanical Attachment

Investigation	Folded Plate Type	Layers	Shell Curvature
Chapter 3	Folded in 1 direction	1-layer	2-directions
Chapter 4	Folded in 2 directions	1-layer	
Chapter 5	Folded in 2 directions	2-layers	1-direction

Table 2.4 – Increasing the Complexity of Assembly

## 2.5 Scope

Being located at the intersection between architecture and civil engineering, this thesis primarily discusses questions related to the geometry, materials, fabrication and assembly of individual joints and structures, but it will also integrate the basic mechanical concepts of the proposed systems. However, detailed and conclusive investigations in the field of civil engineering have been initiated within, but are not part of the present work.

### Bibliography

- [BK10] Markus Burger and Oliver Krieg. Zinkungen: Adaptive Faltstrukturen - Parametrisierte Holzverbindungen als Grundlage robotisch gefertigter Materialsysteme, 2010. Seminar project report, ICD University of Stuttgart.
- [BKP<sup>+</sup> 10] M. Botsch, L. Kobbelt, M. Pauly, P. Alliez, and B. Levy. *Polygon Mesh Processing*. Ak Peters Series. Taylor & Francis, 2010.
- [BM65] B.S. Benjamin and Z.S. Makowski. The analysis of folded-plate structures in plastics. In *Proceedings of a conference held in London*, pages 149–163. Pergamon Press, London, 1965.
- [Bre64] L.G.M. Brekelmans. Geprefabriceerde wand elementen en vouwschalen voor een kerk te hoensbroek, 1964.
- [Bur10] Hani Buri. *Origami - Folded Plate Structures*. PhD thesis, EPFL, Lausanne, 2010. EPFL Doctoral Thesis No. 4714.
- [BW06] Hani Buri and Yves Weinand. BSP Visionen - Faltwerkkonstruktionen aus BSP-Elementen. In *Grazer Holzbau-Fachtage*, 2006.
- [Cra29] Hermann Craemer. Scheiben und Betonelemente im Eisenbetonbau. *Zeitschrift Beton und Eisen*, 1929.
- [DZ12] Holzbau Deutschland and Bund Deutscher Zimmermeister. Lagebericht Holzbau, 2012. Source: Statistisches Bundesamt.
- [Edw10] Clive Edwards. Through, lapped or blind: the dovetail joint in furniture history. In *10th International Symposium for Wood & Furniture Conservation, November 2010, Amsterdam*, 2010.
- [Ehl30] G. Ehlers. Ein neues Konstruktionsprinzip / a new construction principle, 1930.
- [Eng77] Heino Engel. *Tragsysteme / Structure Systems*. Deutsche Verlags-Anstalt, 4th edition edition, 1977.
- [Eri56] H. Eric. Dove-tail template, September 25 1956. US Patent 2,764,191.
- [Fab63] C. Faber. *Candela, the shell builder*. Reinhold Pub. Corp., 1963.
- [FM12] Moritz Fleischmann and Achim Menges. ICD/ITKE Research Pavilion: A case study of multi-disciplinary collaborative computational design. In Christoph Gengnagel, Axel Kilian, Norbert Palz, and Fabian Scheurer, editors, *Computational Design Modelling*, pages 239–248. Springer Berlin Heidelberg, 2012.
- [fN74] Deutsches Institut für Normung. Din 8580:1974-06 Manufacturing Processes - Terms and definitions, division, 1974.

- [Fro78] Peter Frostick. Antiprism based form possibilities for folded surface structures. *Architectural Science Review*, 21(3):59–67, 1978.
- [fS09] International Organization for Standardization. Iso 6983-1:2009(en) - automation systems and integration — numerical control of machines, 2009.
- [Gar06] Rafael Garcia. Concrete folded plates in the Netherlands. In *Proceedings of the Second International Congress on Construction History*, volume 2, pages 1189–1208. Queens College, Cambridge University, 2006.
- [Gra86] Wolfram Graubner. *Holzverbindungen, Gegenüberstellung von Holzverbindungen Holz in Holz und mit Metallteilen*. Deutsche Verlags-Anstalt Stuttgart, 1986.
- [Gre07] Harvey Green. *Wood: Craft, Culture, History*. Penguin Books, 2007.
- [Hah09] Benjamin Hahn. Analyse und beschreibung eines räumlichen tragwerks aus massivholzplatten. Master's thesis, EPFL, Lausanne, 2009. Master Thesis.
- [Har63] C. Harry, Walter. Precast folded plates become standard products, 1963.
- [Hol09] Informationsdienst Holz. Span- und Faserplatten, osb, 2009.
- [Hol13] Forum Holzbau. Holzbaunation im Aufwind, 2013.
- [Hov09] Ludger Hovestadt. *Jenseits des Rasters – Architektur und Informationstechnologie / Beyond the Grid – Architecture and Information Technology: Anwendungen einer digitalen Architektonik / Applications of a Digital Architectonic*. Birkhauser Verlag, 2009.
- [Hun14] Hundegger. Hans Hundegger Maschinenbau GmbH, Hawangen, Germany, 2014. <http://www.hundegger.de/en/machine-building/company/our-history.html>.
- [Huy72] Pieter Huybers. *See-through Structuring - A method for large span plastics roofs*. PhD thesis, Technische Hogeschool Delft, 1972.
- [Huy01] P. Huybers. Prism based structural forms. *Engineering Structures*, 23(1):12 – 21, 2001.
- [Kal10] Frank Kaltenbach. Teaching by Doing – A Research Pavilion in Stuttgart. *Detail (English Edition)*, Vol. 2010:559–561, 2010.
- [KCC<sup>+</sup>14] Oliver David Krieg, Zachary Christian, David Correa, Achim Menges, Steffen Reichert, Katja Rinderspacher, and Tobias Schwinn. Hygroskin: Meteorosensitive pavilion. In *Fabricate 2014 Conference Zurich*, pages 272–279, 2014.
- [KDR<sup>+</sup>12] Oliver Krieg, Karola Dierichs, Steffen Reichert, Tobias Schwinn, and Achim Menges. Performative architectural morphology finger-joined plate structures integrating robotic manufacturing, biological principles and location-specific

- requirements. In Christoph Gengnagel, Axel Kilian, Norbert Palz, and Fabian Scheurer, editors, *Computational Design Modelling*, pages 259–266. Springer Berlin Heidelberg, 2012.
- [Kel17] W.D. Kelly. Woodworking-machine., November 6 1917. US Patent 1,245,240.
- [Ket14] Milo Ketchum. What happened to shells?, accessed august 2014, 2014. <http://www.ketchum.org/-milo/what.html>.
- [Kie56] Otto Kienzle. Die grundpfeiler der fertigungstechnik. *VDI Zeitschrift*, 98:1389–1395, 1956.
- [Koc64] Peter Koch. *Wood Machining Processes*. Wood Processing. Carl Hanser Verlag GmbH & Co. KG, 1964.
- [KR12] K.E. Kurrer and E. Ramm. *The History of the Theory of Structures: From Arch Analysis to Computational Mechanics*. Wiley, 2012.
- [KSM<sup>+</sup>14] Oliver Krieg, Tobias Schwinn, Achim Menges, Jian-Min Li, Jan Knippers, Annette Schmitt, and Volker Schwieger. Computational integration of robotic fabrication, architectural geometry and structural design for biomimetic lightweight timber plate shells. In *Advances in Architectural Geometry 2014*. Springer Verlag, 2014.
- [Lei04] Katharina Leitner. *Tragkonstruktionen aus plattenförmigen Holzwerkstoffen mit der Textilen Fuge*. PhD thesis, RWTH Aachen University, 2004. PhD Thesis.
- [lMea13] Riccardo la Magna et al. From nature to fabrication: Biomimetic design principles for the production of complex spatial structures. *International Journal of Spatial Structures*, Vol. 28 No. 1:27–39, 2013.
- [Lov12] Russell Loveridge. *Process Bifurcation and the Digital Chain in Architecture*. PhD thesis, École polytechnique fédérale de Lausanne, 2012.
- [Mar13] Peter Marti. *Theory of Structures: Fundamentals, Framed Structures, Plates and Shells*. Wiley, 2013.
- [Mei64] J.C. Meischke. Geprefabriceerde wandelementen en vouwschalen voor een kerk te hoensbroek, 1964.
- [Men06a] Achim Menges. Instrumental geometry. *Architectural Design*, 76:42–53, 2006.
- [Men06b] Achim Menges. Manufacturing diversity. *Architectural Design*, 76:70–77, 2006.
- [Mes06] Robert W. Messler. *Integral Mechanical Attachment: A Resurgence of the Oldest Method of Joining*. Butterworth Heinemann, 2006.
- [Neu94] Helmuth Neuhaus. *Ingenieurholzbau: Tragende geklebte Verbindungen im Holzbau*. Teubner Verlag, 1994.



- [Piz03] Emilio Pizzi. *Renzo Piano*. Birkhaeuser, Basel, 2003.
- [Pur11] Purbond. *National Technical Approval Z-9.1-711 / Single-component polyurethane adhesive for the manufacture of engineered wood products*. Deutsches Institut für Bautechnik, 2011.
- [RM10] Christopher Robeller and Achim Menges. Seminar Robotically Manufactured Material Systems, Institute for Computational Design ICD, University of Stuttgart, 2010. <http://icd.uni-stuttgart.de/?p=3643>.
- [Sch04] Regina Schineis. Gefalteter Klangkörper Musikprobensaal Thannhausen / Thannhausen Rehearsal Room. In *10. Internationales Holzbau Forum (IHF), Garmisch-Partenkirchen*, 2004.
- [Sch09] Christoph Schindler. *Ein architektonisches Periodisierungsmodell anhand fertigungstechnischer Kriterien, dargestellt am Beispiel des Holzbaus*. PhD thesis, ETH Zurich, 2009. DISS. ETH Nr. 1860.
- [Sim58] H. Simpson. Reinforced concrete plate construction, 1958.
- [Spa54] Fritz Spannagel. *Der Möbelbau. Ein Fachbuch für Tischler, Architekten und Lehrer*. Schäfer Verlag, 1954.
- [SS10a] Vaclav Sebera and Milan Simek. Finite element analysis of dovetail joint made with the use of cnc technology. *Acta Universitatis Agriculturae Et Silviculturae Mendeliana Brunensis*, Volume LVIII:321–328, 2010.
- [SS10b] Milan Simek and Vaclav Sebera. Traditional furniture joinery from the point of view of advanced technologies. In *Proceedings of the International Convention of Society of Wood Science and Technology and United Nations Economic Commission for Europe, Geneva, Switzerland*, 2010.
- [SSB05] Fabian Scheurer, Christoph Schindler, and Markus Braach. From design to production: Three complex structures materialised in wood. In *6th International Conference Generative Art*, 2005.
- [SSDMB05] Alvaro Siza, Eduardo Souto De Moura, and Cecil Balmond. Serpentine gallery pavilion 2005, 2005.
- [Tet07] Kōndo Tetsuya. *Dento kanehozo kumitsugi : Sekkei to seisaku no jissai*. LLP Gijutsushi Shuppankai, Tokyo : Seiunsha, 2007.
- [UR03] Nich Umney and Shayne Rivers. *Conservation of Furniture*. Butterworth-Heinemann, 2003.
- [Wil97] C. Wilby. *Concrete Folded Plate Roofs*. CRC Press, 1997.

- [WS12] A. Wagenführ and F. Scholz. *Taschenbuch der Holztechnik*. Carl Hanser Verlag GmbH & Company KG, 2012.
- [ZAC91] Li Zhenqiang and Xavier Arguello-Carazo. Construction of precast prestressed folded plate structures in honduras. *Journal of the Precast/Prestressed Concrete Institute*, 28:46–61, 1991.

# Investigations **Part II**



### 3 Design and Fabrication of Robot-Manufactured Joints for a Curved-Folded Thin-Shell Structure Made from CLT

Christopher Robeller, Seyed Sina Nabaei and Yves Weinand

Peer-reviewed and published as a chapter in: W. McGee and M. Ponce de Leon (eds.), *Robotic Fabrication in Architecture, Art and Design 2014*, DOI: 10.1007/978-3-319-04663-1\_5, Springer International Publishing Switzerland 2014

**Abstract** The prototype presented in this chapter utilizes the technique of curved folding for the design of a thin-shell structure built from curved cross-laminated timber panels (CLT). The curved-folded geometry allows for a span of 13.5 m, at a shell thickness of only 77 mm. The construction requires curved line CLT joints, which are difficult to address with state-of-the-art jointing techniques for CLT. Inspired by traditional woodworking joinery, we have designed connections for the integrated attachment of curved CLT panels, utilizing digital geometry processing tools to combine the advantages of traditional joinery techniques with those of modern automation technology.

**Keywords** Curved folded plate structures, Robot fabrication, Cross-laminated timber, Mono-material

## Foreword<sup>46</sup>

### Realization of an Origami-inspired Design

The first prototypes and investigations on timber folded plate structures were focused on the use of planar plate elements. However, the use of timber presents the possibility to work with curved plate elements, taking advantage of the materials elasticity property. The use and certain benefits of curved-folded surface structures are known from applications with concrete, where curved shapes require custom built curved shuttering.

The geometry of the Folded Surface Structure, which is presented in the following chapter, is based on an origami-inspired design by Hans-Ulrich Buri. (Figure 3.1) The use of curved-folded shapes for timber folded surface structures was already proposed in a previous publication. [BSW11] The shape of the original design was obtained through a paper-folded model, the geometry of which is explained in more detail in the chapter.

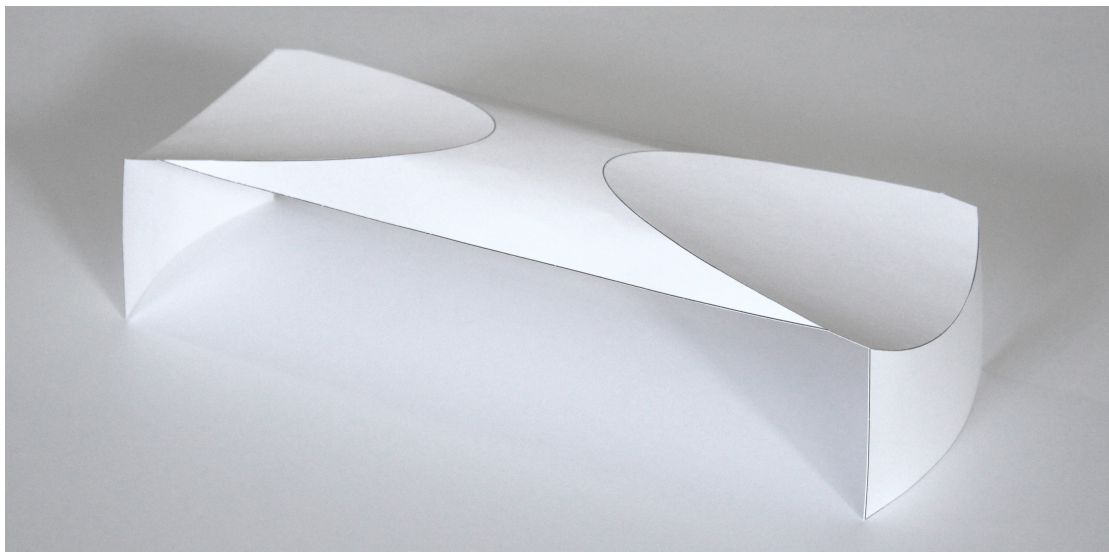


Figure 3.1 – Curved-folded Paper Model - Design proposal for a thin-shell structure built from curved timber panels. This design presented the possibility to demonstrate the potential of integral joints for applications with irregular geometry, such as curved folded plates.

With its thin-shell concept, and additionally curved plate elements, the implementation of this design required particularly challenging details. This presented an opportunity to develop an integral jointing solution that demonstrates the advantages of such solutions. The project underlines the particular relevance and potential of integral solutions for irregular geometries, such as a curved-folded assembly.

---

<sup>46</sup>This additional section was not included in the original publication.

---

## Curved Timber Panels

The design was originally planned as a single or double-layer construction with *elastically bent* panels, which could not be realized at the time. This was due to the particular geometry of the shell<sup>47</sup>, which does not permit the use of a single-layer elastically bent solution, as well as a lack of sufficient details that would allow for a double-layer composite construction. However, while one possible solution is presented in this chapter, these challenges were kept in mind and will be addressed in the subsequent chapters.

Avoiding the use of elastically bent panels at this point, the project presented the alternative possibility to work with *curved cross-laminated timber* panels. These panels are laminated from linear timber elements, like regular cross-laminated timber (CLT), but on top of custom built curved molds instead of flat ones. All timber elements in the cross-laminated layers, which are transversal to the curvature of the mold, will be bent elastically. A residual force  $\sigma$ , which is induced through this bending, will remain in the composite after its lamination. 3.2 It is counteracted by the adhesive bonding between the layers, which prevents the elements from bending back into their original shape. However, this is limited to a certain range of parameters: While  $\sigma$  will increase with an increasing curvature of the laminate, it can be reduced by a reduction of the thickness of the transversal layers of the composite.

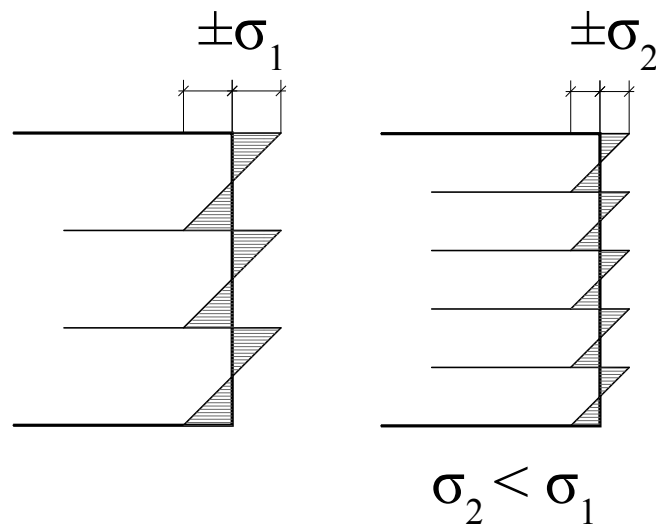


Figure 3.2 – Residual Stresses  $\sigma$  in the cross-section of an elastically bent multi-layered plywood panel. The residual stress in the bent panel decreases with an increasing amount of layers. (right side)

Disadvantages of the curved cross-laminated timber panels include high production cost, due to a partially manual production process and the need for an additional, solid mold for the lamination process, as well as a less convenient transportation of pre-curved parts.

---

<sup>47</sup>In the configuration shown in figure 3.1, elastically bent panels would be clamped and supported along the joints, where inversely curved segments are connected with each other, however they would bend back along the long, unsupported edges on the side of the structure (see Figure 3.9)

### **Chapter 3. Design and Fabrication of Robot-Manufactured Joints for a Curved-Folded Thin-Shell Structure Made from CLT**

---

Advantages however include that curved-cross-laminated timber panels are a certified, well developed and realistic approach to the realization of form-active structures with timber panels.<sup>48</sup> Relatively small radii can be realized, similar to elastically bent plywood or laminated veneer lumber (LVL) panel<sup>49</sup>. The composition of layers can be custom-designed for a specific application and the individual, thin layers can be bent incrementally during the lamination.

#### **Contributions**

The integral joints presented in this chapter were developed specifically for the proposed Folded Plate structure, its geometry and materials. The development required a structural analysis of the shell, which was carried out by the co-author and civil engineer Sina Nabaei. This analysis is shown in the figures 3.9, 3.12 and 3.13.

---

<sup>48</sup>A well known and recent example for the application has been demonstrated in the Zurich Elephant House. (Design: Markus Schietsch Architekten) The doubly-curved dome has been built from patches of singly-curved elements of curved cross-laminated timber.

<sup>49</sup>for CLT and LVL, radii of up to 3 meters are possible. For CLT, see [fB13, p.5], for LVL, see [fB11, p.6]





Figure 3.3 – Full-scale, mono-material prototype structure, spanning 13.5 m at a shell thickness of 77 mm, exhibited at the academy of architecture in Mendrisio, Switzerland

### 3.1 Motivation

Recent studies about folded plate structures such as the Chapel St. Loup [BW10] and the ICD/ITKE Research Pavilion 2011 [lMea13], have demonstrated architectural and structural applications of folded-plate structures built from plywood and cross-laminated timber panels (CLT). Architectural applications of curved-folded geometry have previously been studied for benefits such as the panelization of complex shapes [KFC<sup>+</sup>08].

The curved-folded thin-shell structure presented in the present chapter builds up on this research and demonstrates a structural application of curved CLT, a relatively new but increasingly popular product offered by European CLT manufacturers. Our prototype (Figure 3.3) utilizes the curved shape of the panels to increase the inertia of the structure in its main load-bearing direction, acting very much the same way as a bi-cantilever frame. Our interpretation of the traditional simple frame is meanwhile innovative using curved thin-shell panels instead of beams, which are transmitting structural efforts in a curved line of action through robot fabricated wood working joints.

Moreover, connecting two reversely curved panels through a curved fold would propagate the curvature from one into another when one of them is bent. This interaction helps resisting lateral forces which tend to flatten their curvature. These lateral forces are transformed into out of plane forces due to the shell behavior of panels, at the interface and transmitted through the curved panels until the clamped edge.

Alternatively, such deformations are supported in practice by tensile steel cables along the

### Chapter 3. Design and Fabrication of Robot-Manufactured Joints for a Curved-Folded Thin-Shell Structure Made from CLT

chord of the curved CLT elements, as demonstrated in the recent wide-span roof construction of a factory building in Ainet, Austria [HU13]. Instead of tensile cables, our prototype supports these forces by taking advantage of the curved folding technique. Unlike origami paper folded forms, wood panels cannot actually be “folded”. Instead, the performance of such structures depends on linear edge-to-edge connections between the panels, making these joints a key component in the design of wooden folded-plate structures.

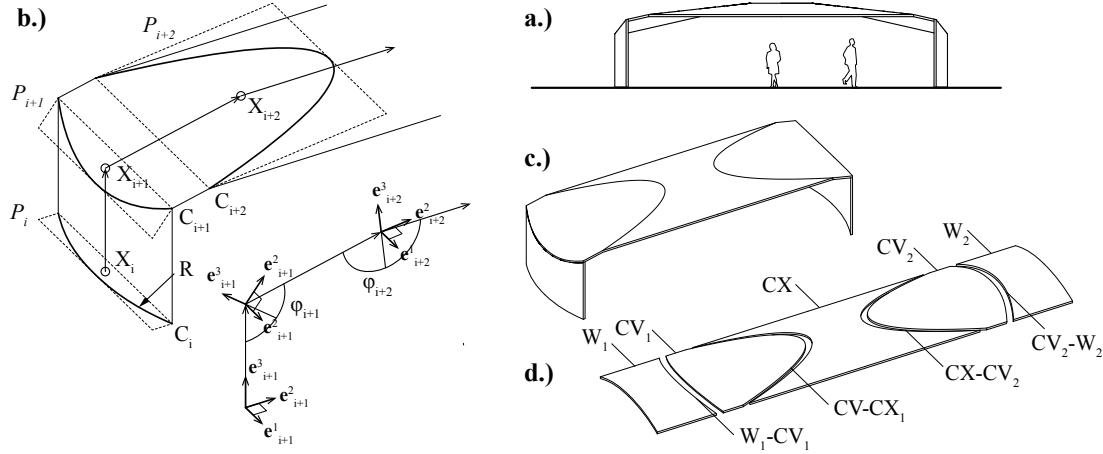


Figure 3.4 – a Full-scale prototype side view schematic. b Curved-folding technique. c Curved-folded thin-shell geometry. d Unfolded CLT parts/fabrication layout

## 3.2 Project Geometry

As illustrated in Figure 3.4b, the curved-folded geometry is generated through a circular arc  $C_i$  (Radius  $R = 5.9m$ ) and its reflection about a set of planes  $P_i$ . These reflection planes are located at the nodes  $X_i$  of a polyline, which lies on a vertical plane normal to the chord of  $C_i$ . Each Reflection Plane  $P_i$  is normal to the bisector of the two neighbor segments of the polyline. The fold angles  $\phi_i$  are determined by the interior angles between the polyline segments. We used this polyline as a variable control polygon in a parametric design model. The unfoldable geometry (Figure 3.4d) allows for an efficient fabrication without offcuts. Depending on the length of the panel manufacturer’s production line, all parts can be produced from a single, 17 m long curved CLT panel.

## 3.3 Limitations of State-of-the-Art Connectors

Figure 3.4d illustrates the four connections  $W_1 - CV_1$ ,  $CV_1 - CX$ ,  $CX - CV_2$  and  $CV_2 - W_2$  that are required for the assembly of the curved-folded CLT thin-shell. The curved panels must be jointed at precise, non-orthogonal angles, which are difficult to address with state of the art CLT jointing techniques: Glued-in metal connectors, which are common in glulam and LVL constructions, cannot be applied to CLT because of its internal stress cuts, into which the

adhesive could discharge.

Alternatively, external metal plate connectors could be applied visibly on top of the panels with wood screws. A large amount of such connectors would be required in order to achieve a sufficiently rigid and stiff joint. In general, the before mentioned connectors reduce the stiffness of a folded-plate, while modern wood adhesives, such as 1K-PUR, allow for a lossless, fully stiff joint.

However, the gluing procedure requires a fast and precise alignment and clamping of the parts, within the open time of the adhesive. For joints on orthogonal edges and flat panels, standard tools can be used for the alignment and clamping. However, non-orthogonal edges and bent or curved panels will require custom made guides or supports.

### 3.4 Joint Types and Algorithms

Inspiration for an integrated solution for alignment and attachment can be found in traditional wood joinery techniques such as dovetail joints, on which the prismatic edge geometry results in a single-degree-of-freedom (1DOF) joint, which predetermines the alignment and orientation of the two connected parts. Due to their involving manual fabrication, these traditional joints have lost importance during the industrialization. Later on, early mass-production technology was incapable of fabricating such connections.

Modern robot- and CNC fabrication technology however allows for the reconsideration of these techniques. An application on plywood panels has been demonstrated recently [SS10] as well as a spotfacing technique for the robot fabrication of finger joints on plywood (Magna et al. 2013). On our curved-folded prototype structure, we have to address two different types of folds. For the joints  $W_1 - CV_1$  and  $CV_2 - W_2$  each with a fold angle  $\varphi$  of  $102.7^\circ$ , we have chosen a 1DOF dovetail-type joint geometry (Figure 3.5).

The geometry is generated by an algorithm, which divides the joint edge into an odd number of segments, returning a set of points  $X_i$ . A local frame  $u_i^1; u_i^2; u_i^3$  is added to these points, where  $u_i^2$  is parallel to the  $e_2$  and  $u_i^1$  is the direction of insertion for the joint. These frames are rotated about  $u_i^1$  at an alternating angle  $\pm h$ . For each frame, a plane  $PX_i$ , normal to  $u_i^3$  is intersected with the curves  $L1, L2, L3, L4$ , which gives us the curve and line segments for the dovetail joint geometry (Figure 3.5b).

For the fabrication of these joints, we have chosen a side-cutting technique, using a shank type cutter (Koch 1964). The cutting requires simultaneous 5x machining, for which we provide a set of tool center points  $TCP_i$ , each with a direction  $m_{orientation}$  (Figure 3.7). We have obtained these points and vectors through an algorithmic evaluation of a set of parametric surfaces  $S_i$ . The algorithm detects inside corners automatically and adds notches (Figure 3.7), which allow for the insertion of the joint's counterpart and reduce the notch stress [SS10] [EN104]. The transition of the cutter between joint faces with different orientations is solved

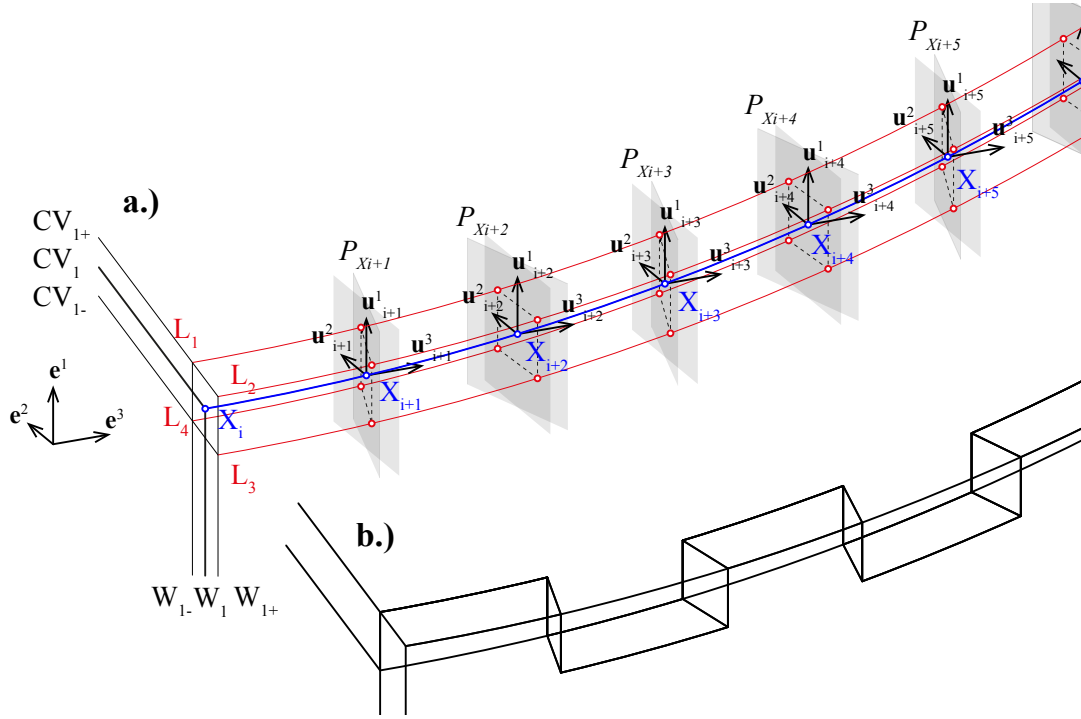


Figure 3.5 – Generation of the dovetail-type joint SDOF geometry through intersection of a set of planes  $P_{X_i}$  with the four curves  $L_1, L_2, L_3$  and  $L_4$ . a)  $CV_1$  is the part, the + and - show the intersection layers and  $W_1$  is the part, the + and - show the intersection layers b) it is the same parts once jointed. Part  $CV_1$  above and part  $W_1$  below

through the bisector planes  $P_i$ .

As one of its main advantages, the side-cutting technique allows for the use of simple supports under the workpiece. It is not necessary for the edge to cantilever. The main limitation for this method is set by the geometry of the cutter and the tool holder: The inclination  $b$  of the tool must be limited to avoid a collision between the cutter and the wood panel. In consequence, this method can be applied to fold angles  $u$  within the range of  $90^\circ \pm b$ . With  $b = 40^\circ$  in our case, we are limited to folds up to  $u = 130^\circ$ . For the Connections  $CV_1 - CX$ , and  $CX - CV_2$ , each with fold angle  $167.2^\circ$ , we have generated the joints with the method described in Figure 3.5, but without a rotation about  $h$ , giving us a planar joint geometry. In order to cut the open slots of these joints, we used a saw blade-slicing technique instead (Figure 3.8, left side), making multiple vertical cuts for each slot. This method allows us to fabricate very obtuse folds on simple, non-cantilevering supports.

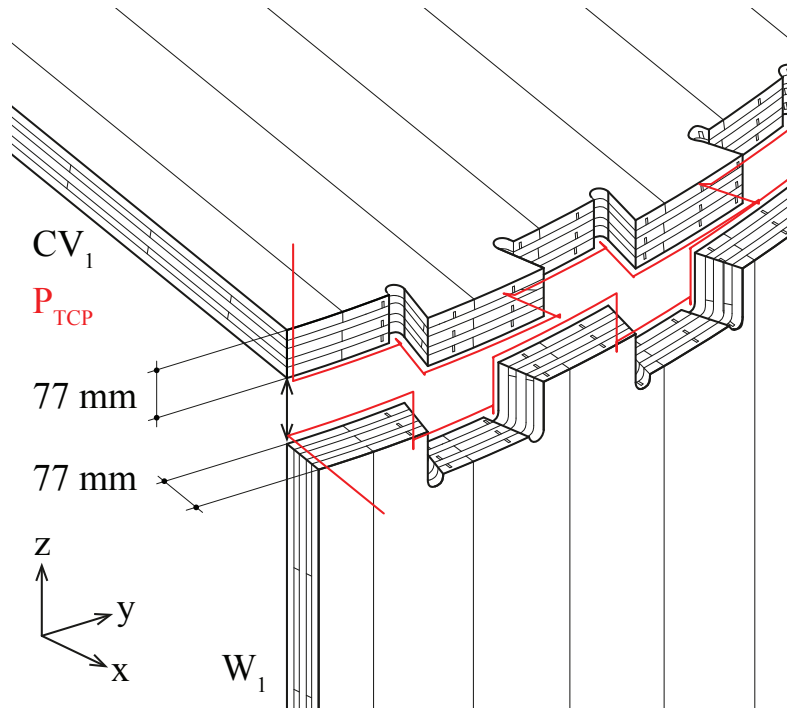


Figure 3.6 – Dovetail-type connections  $W_1 - CV_1$  and  $CV_2 - W_2$  on the full-scale prototype - Schematic drawing showing the CLT panels and joints including layers and stress cuts, Right principle of machine code generation on a curved joint, using parametric surface evaluation

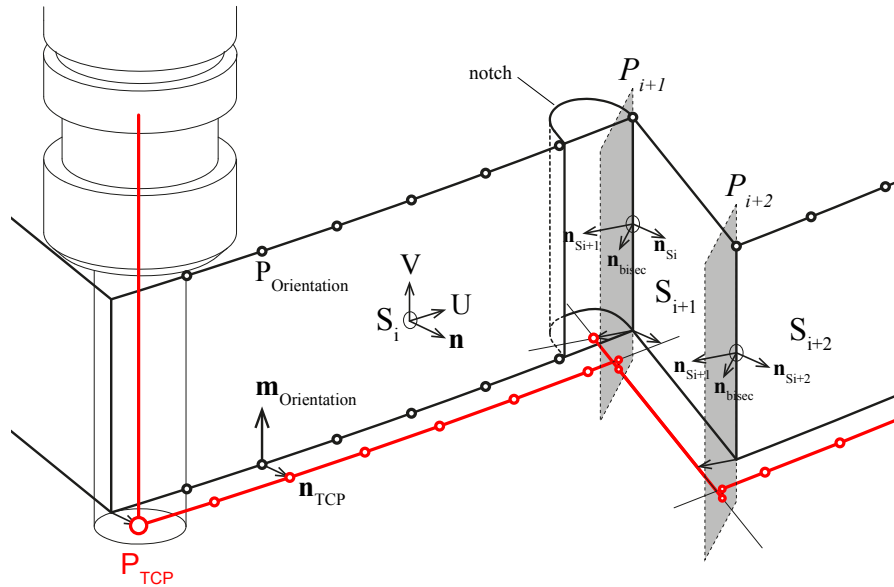


Figure 3.7 – Dovetail-type connections  $W_1 - CV_1$  and  $CV_2 - W_2$  on the full-scale prototype - Principle of machine code generation on a curved joint, using parametric surface evaluation

### Chapter 3. Design and Fabrication of Robot-Manufactured Joints for a Curved-Folded Thin-Shell Structure Made from CLT

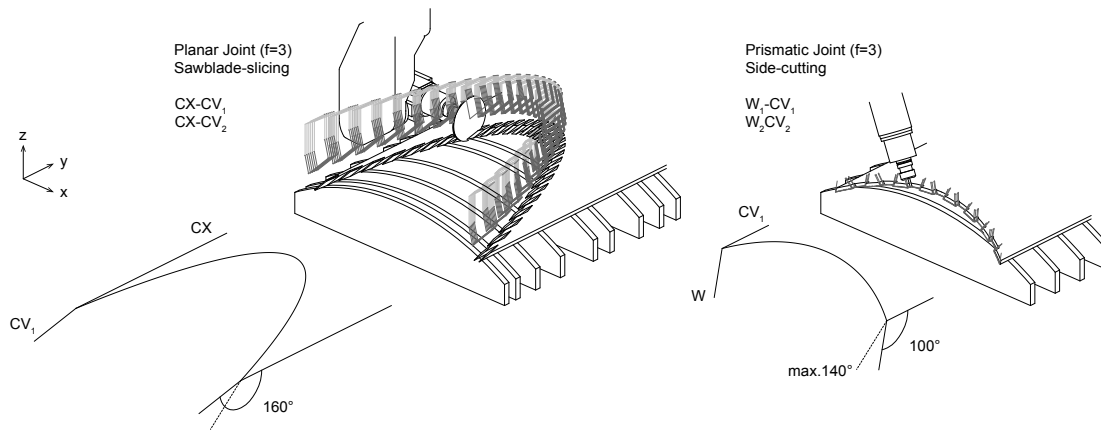


Figure 3.8 – Joint fabrication (tool path plot). Left planar finger-joint type connection (connections CV-CX), Right prismatic dovetail-type joint (connections W-CV)

### 3.5 Preliminary Structural Analysis

A preliminary structural analysis task has been performed in order to determine an initial value for the panel thickness and assess structural performance of the curved geometry to support relevant loads. Results from this primary engineering stage would let choose (or design) the appropriate laminate product as well as to ensure that enough degrees of freedom are linked in order to properly transmit structural effort between panels. A Finite Element shell model has been established from the mid-surface of panels, with local joints between curved panels simulated as rotational and translation links acting on local axis. For each joint the local axis  $x$  is the tangent to the joint 3D curve, the  $y$  axis is the bisector of two normal vectors of connecting mid-surfaces. The  $z$  axis is then defined by the right hand rule.

Panels at this preliminary structural design stage are considered as isotropic with Young Modulus  $E = 7.800 \text{ MPa}$  (a conservative value near to long term modulus of timber) and Poisson ratio  $m = 0.3$ . Structure is a temporary installation loaded for combination of self-weight and lateral as well as transversal wind load cases. Results for Ultimate Limit State and Service Limit State propose 77 mm thickness to be a safe initial size for the prototype (Figure 3.9). This preliminary dimension will be confirmed through a detailed model once connection technology and the panel laminate product have been selected through the investigations which would be carried out on the 1:5 scale prototype.

### 3.6 Prototype at Scale 1:5

The fabrication methods and the assembly of the parts were tested on a smaller prototype at scale 1:5 before applying it to the full-scale prototype. The curved CLT, which is not available at the scaled thickness, was replaced by a laminate of thin plywood panels. A MAKAMM7s 5-axis CNC router was used for the formatting of the panels and for the cutting of the joints.

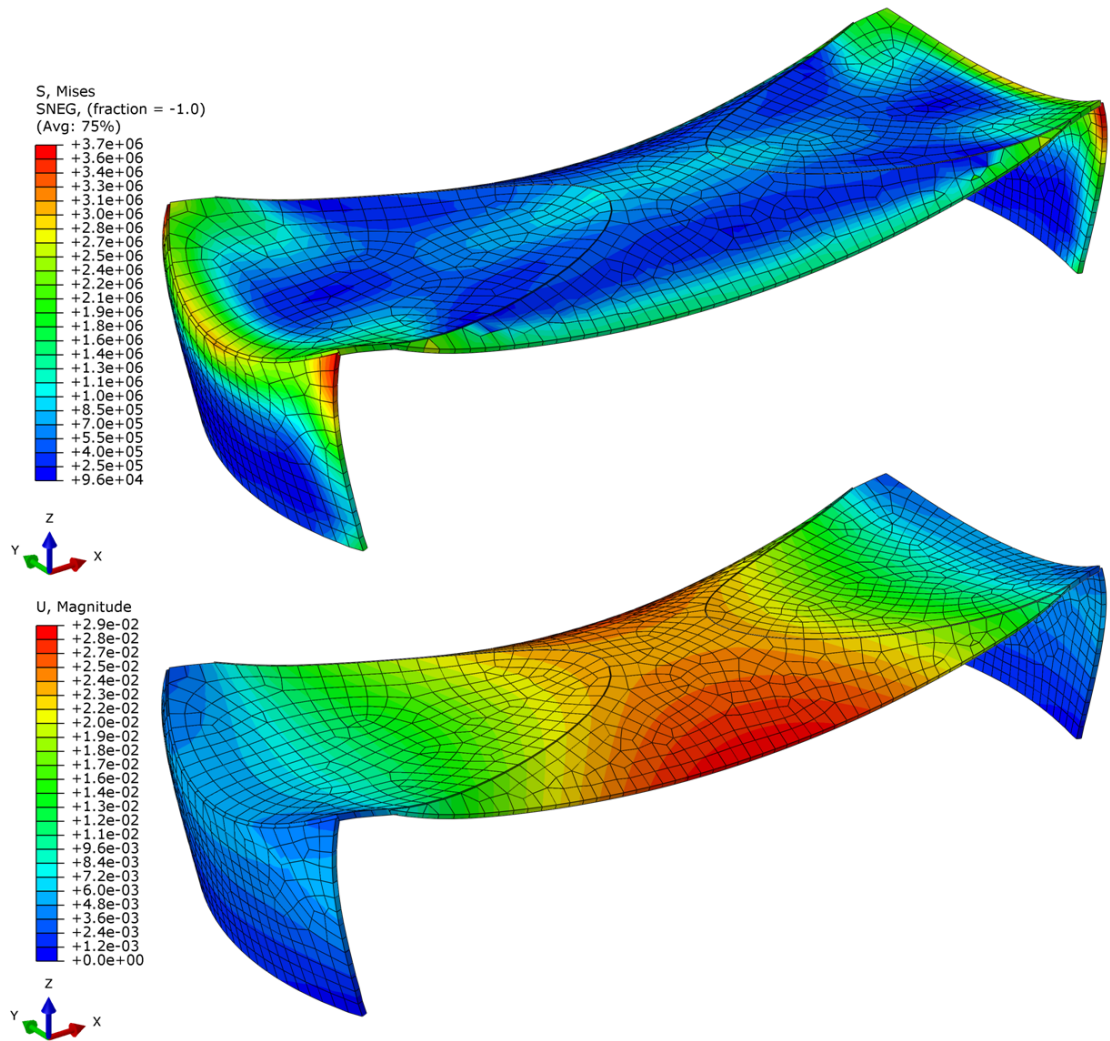


Figure 3.9 – Preliminary structural analysis results under the self-weight load case. Top Von-Mises stress distribution. Bottom total deformation

Due to the curved geometry of the parts, custom-made supports (Figure 3.10) were required for the curved panels, which served simultaneously as a mold for our curved laminate.

A convex support was built for the parts  $CX$ ,  $W_1$  and  $W_2$ , and a concave support for the parts  $CV_1$  and  $CV_2$ . An additional concave support was built for the saw blade-slicing technique, which requires access from above on the convex and the concave panel. The molds were fabricated from laminated veneer lumber panels (LVL) and assembled with half-lap joints. In order to provide a precise calibration of the supports, a previously added oversize was removed through spot facing along the ribs on the CNC-router. Figure 3.11 shows the assembly of the parts  $CX$  and  $CV_1$  on the small-scale prototype: The short segments of the planar joint provide a large contact area and gluing surface between the panels.



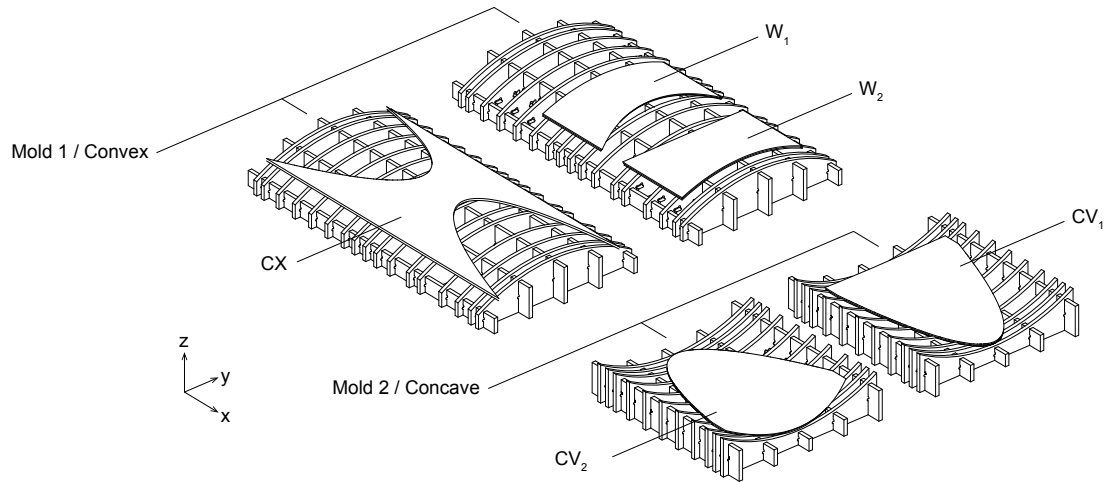


Figure 3.10 – Concave and convex mold for the lamination and formatting of the curved panels at scale 1:5

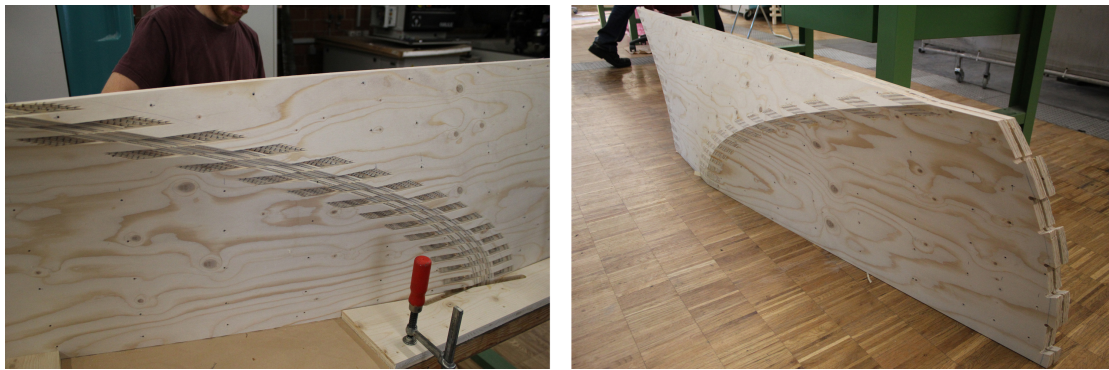


Figure 3.11 – Planar finger-type joints were used for the connections  $CV_1 - CX$  and  $CV_2 - CX$ . These joints were fabricated with a saw blade-slicing technique on a 5-axis CNC router

### 3.7 Full-Scale Prototype

With the initial thickness determined at the preliminary engineering stage (see Sect. 5), a special laminate product has been designed by the manufacturer to fulfill the requirement regarding the thickness/radius ratio. The selected CLT panels are five layer symmetric laminates with total thickness of 77 mm.

As the next step, a full three-dimensional Finite Element model has been developed with this precise layer configuration and the mechanical properties provided by the manufacturer. The glued areas over the connectors have been considered as surface tie constraints. The goal of this detailed engineering step was to investigate local panel interaction over the connectors as well as to confirm the thickness of the CLT panel regarding the structural safety. The structural



analysis confirmed the initial design thickness. The design issue was mainly to overcome deformation due to Service Limit State load combinations. The local and overall Von-Mises stress distribution is shown respectively in Figures 3.12 and 3.13.

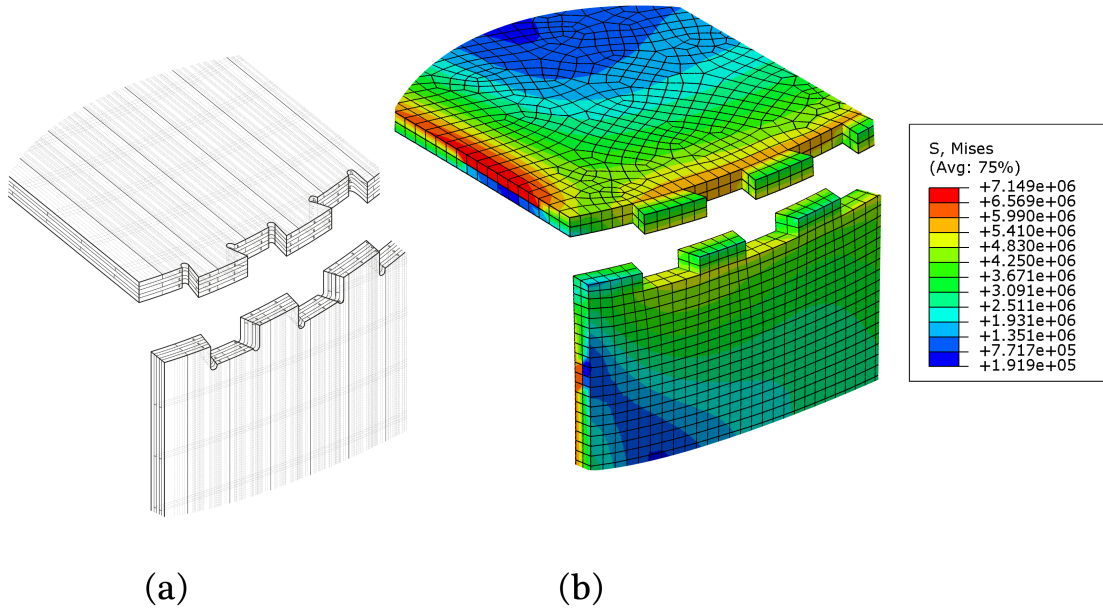


Figure 3.12 – Von-Mises stress distribution for Dovetail-type connections  $CV_1 - W_1$  and  $CV_2 - W_2$  on the full-scale prototype. Results are generated from a full three dimensional finite element simulation

Having verified the structural parameters of the full scale prototype through the detailed analysis, the fabrication process was carried out at the facilities of the manufacturer. Figure 3.14 shows the fabrication of the full-scale prototype at the CLT panel production and processing facilities. The KUKA KR250 robot router with an additional linear-axis table allowed for the precise 5-axis fabrication of the joints at full scale. Its large workspace with a length of more than 30 m was essential for the realization of the prototype. The sides of the curved CLT panels were formatted with an 800 mm saw blade (Figure 3.15) and the dovetail-type joints  $W_1 - CV_1$  and  $CV_2 - W_2$  were cut with a 25 mm turn-blade knife shank-type cutter.

For the joints  $CV_1 - CX$ ,  $CX - CV_2$ , a different joinery technique was used for the full-scale prototype: 30 slots, each with a width of 30 mm were cut into the curved panels to be connected. Subsequently, connector elements with rounded edges (Figure 3.17), were fabricated from cross-laminated spruce LVL with a Hundegger K1 joinery machine. During the assembly of the full-scale prototype, these connectors were first used to align the roof segments, before gluing them in with a 1K-PUR adhesive. This alternative technique was chosen to reduce the machining time at full-scale. The robot routers higher sensitivity to vibrations required a lower feed rate compared to the CNC portal router (factor 0.2), while the length of the tool paths increased by the factor 5 compared to the prototype at scale 1:5.

### Chapter 3. Design and Fabrication of Robot-Manufactured Joints for a Curved-Folded Thin-Shell Structure Made from CLT

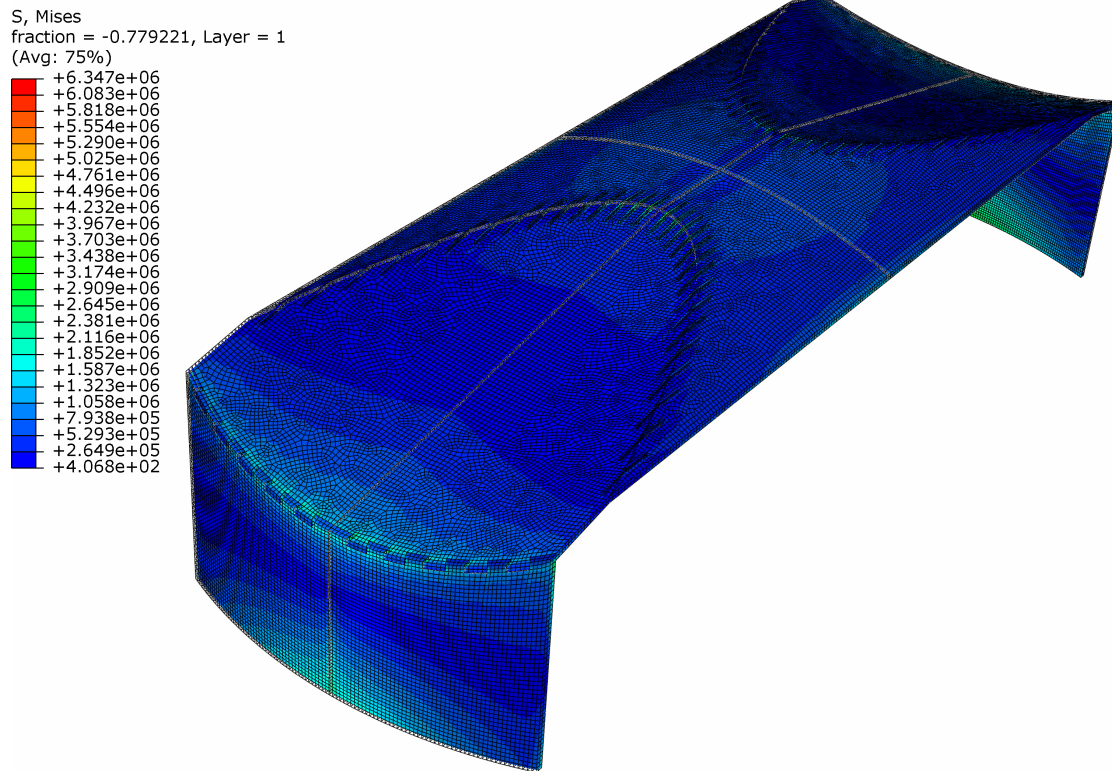


Figure 3.13 – Von-Mises stress distribution for detailed model

The slots for the LVL connectors could be fabricated without access from above on the concave panels  $CV_1$  and  $CV_2$ . This allowed for all formatting and joinery to be done on one convex support. An additional concave support was not necessary for the fabrication of the full-scale prototype.

After the panel formatting, the different parts of the pavilion were assembled. The three parts of the roof  $CV_1$ ,  $CX$  and  $CV_2$  were assembled in a first step and lifted with a portal crane. Afterwards, the vertical elements  $W_1$  and  $W_2$  were positioned and an adhesive was applied to the faces of the dovetail-type connections  $W_1 - CV$  and  $CV_2 - W_2$ . Finally the complete roof was lowered into position from above with a portal crane (Figure 3.18).

For weather protection, the entire shell has been treated with preservation for coniferous wood, before it was transported to its destination at the Academy of Architecture at the Università della Svizzera Italiana (USI). After its final assembly on site, the structure was presented to the public in September 2013. (Figure 3.20) To date, the temporary design is still exhibited on the campus of USI. Its exposure to the outdoor conditions is being documented.



Figure 3.14 – Robot fabrication of the full-scale prototype - fabrication of the joint  $CV_1 - CX$  using a 25 mm shank-type cutter

### 3.8 Conclusions/Towards an Integration of Joints

Instead of using additional stiffening elements, the thin-shell presented in this chapter achieves its wide span with an integrated approach. The design utilizes the geometry of curved CLT panels and combines it with the technique of curved- folding. The approach of integrated performance has been continued on the design of the joints: The connections were fabricated during the formatting of the panels and performed simultaneously as guides for the positioning and alignment of the pieces. The precise fabrication and the mono-material approach allowed for a visible application of the joints. This was not only useful for the aesthetic appearance of the prototype, but also for the simple monitoring of the condition of the joints. Three different techniques were used for the joinery, all of which take advantage of computational fabrication technology for the fabrication of the joints and utilize digital geometry processing tools for the generation of both the joint geometry and the machining code.

The side-cutting technique used for the fabrication of the dovetail-type W-CV joints demonstrates an integrated jointing method for the connection of curved CLT panels. Compared to a butt joint or miter joint geometry, it offers advantages such as a precise and fast alignment and the machining time is only slightly increased. The technique allows for the jointing of fold angles within a range of  $50^\circ$  and  $130^\circ$ .





Figure 3.15 – Robot fabrication of the full-scale prototype - formatting of the side of the panels using a saw blade with a diameter of 800 mm

The saw blade-slicing technique allows for the jointing of more obtuse fold angles, but it requires additional access from above on the concave side of one panel. Both a convex and a concave support are required. The number of saw blade cuts for the open slots of the joints results from the total edge length divided by the saw blade thickness. Fast routers with a high feed rate are beneficial for the fabrication of this type of joint.

The IVL connector technique demonstrates an alternative method for the jointing of curved-folds with obtuse fold angles  $\varphi$ . It allows for fast fabrication and all joints were cut on a single convex support, but the manual assembly of the IVL connectors is more time-consuming compared to the dovetail joints.

While each of the presented joinery techniques shows certain advantages and disadvantages, we found the side-cutting technique to be a particularly effective and universal method for the jointing of curved CLT panels with a robot router. In general, the robot-manufactured joints allowed for the realization of our prototype, but we believe the construction demonstrates only one of many possible applications for curved-folded CLT structures.



Figure 3.16 – Left assembly of the roof panels: shell prototype ready for the insertion of the IVL connectors. (connections *CV – CX*)

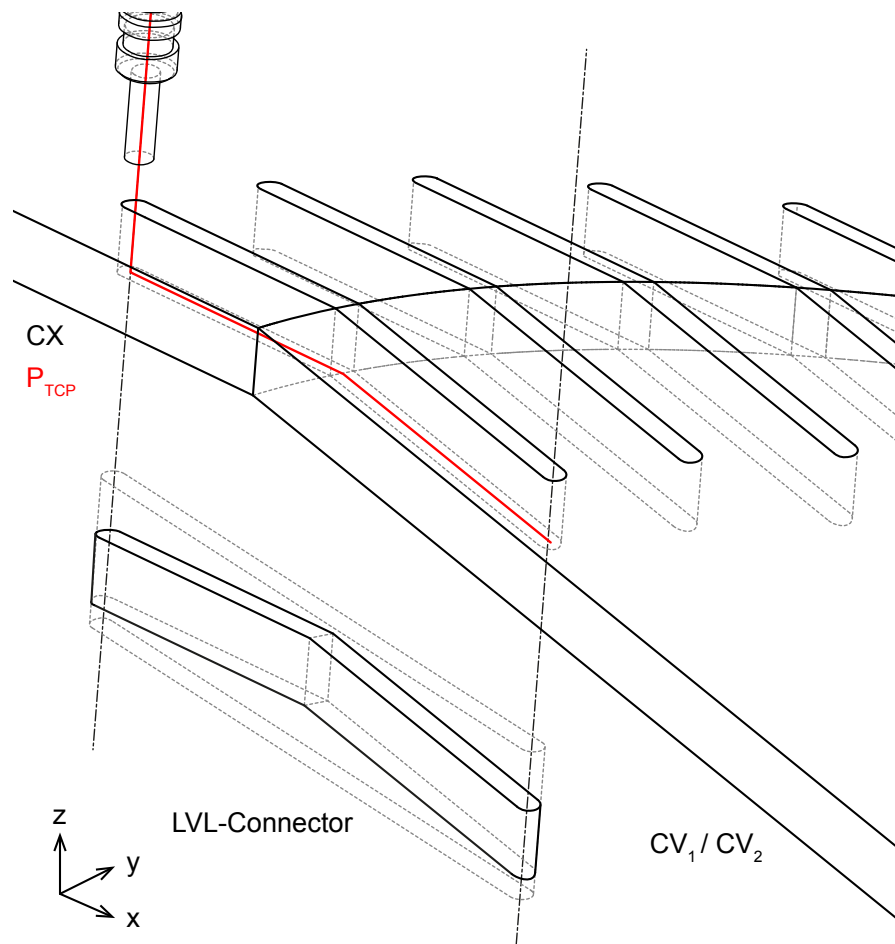


Figure 3.17 – Schematic Drawing of the Connector Elements made from Cross-laminated LVL Panels - The slots have been cut with a 30 mm shank-type turn blade-knife cutter



Figure 3.18 – Assembly of the Dovetail-type Connectors between the Wall Panels and the Roof Panels (Connections CV – CX)





Figure 3.19 – Robot-fabricated Dovetail Joints on a Curved CLT Panel





Figure 3.20 – Exhibition of the Completed Pavilion in Mendrisio, September 2013 63

## Additions and Remarks<sup>50</sup>

Two main innovations are presented in this chapter; the first implementation of CNC-fabricated (1DOF) dovetail joints in a full-scale building structure prototype, as well as the first implementation of integral plate-joints for CLT and curved CLT in particular. However, as mentioned in the conclusions, several observations were made in the process, which have suggested improvements related to the geometry of the joints and shell, fabrication techniques and technology used, as well as the choice of material.

### Benefits of Integral-Joints combined with Adhesive Bonding

After the delivery of the pavilion and its presentation to the public at the USI Academy for Architecture in Mendrisio, the shell was exhibited for a period of 6 months, from September 2013, to March 2014. A separate article was published about the advantages and disadvantages of the joints, including observations on the prototype and proposition for other applications within a wider context of CLT construction. [RHMW14]

The hybrid connection of form-fitting dovetail joints and adhesive bonding raises the question whether the joints were participating in the mechanical connection of the parts, or if they were just used for the precise and convenient assembly. While both uses would be legitimate, the aim of this thesis is to achieve a high level of *Integral Mechanical Attachment*, where the geometry of the joints is used as much as possible.

In the case of the curved-folded structure in this chapter, the joint geometry has played an important role beyond the assembly of the parts. However, the behaviour of the joints must be looked at in more detail to understand the role of its geometry in the connection of the parts.

Let us consider a flat, butt-jointed connection of the curved parts, with adhesive bonding, but without the dovetail joints. Two major problems would result from this simplified glued joint: [Neu94, 130] and [AGM05, 39] explain that such glued joints can not resist forces which are normal to the glued interface. However, this is clearly the case in many applications, including our prototype structure. Also, on one of the two panels, forces would be introduced across the wood fibers. This allows only for a very low rigidity of the connection.

In addition to these problems, any finger- or dovetail-jointed connection will increase the total contact area between the parts considerably. In the present case, the contact surfaces of the dovetail-jointed solution are 30% larger compared to a butt-joint.<sup>51</sup> This increased contact surface is highly beneficial, because the dimensioning of parts in timber construction

---

<sup>50</sup>This additional section was not included in the original publication.

<sup>51</sup>the loss of contact surface through stress-reduction notches has been considered in this calculation

is typically determined through the size of the contacts rather than the loading capacity of the parts. [BU07, 1-16]

Therefore, the dovetail joint geometry provides multiple benefits in a glued joint. Figure 3.21 provides a schematic illustration of the forces at the connection in our prototype. In addition to the faces parallel to the edge, the dovetail geometry now provides additional side-faces across the edge of the joint. Unlike the parallel contacts, these faces do not receive normal forces (red and blue arrows), but shear forces (green arrows), which can be resisted by the glue. The behaviour is illustrated in more detail through a simplified finite-elements model, which is shown in figure 3.22. Finally, Figure 3.23 shows the joints on the pavilion after six months. Only basic weather protection was applied to this structure, since it was planned only as a short-term exhibit. The image shows a delamination of the glued connection parallel to the edge, while the connections on the side faces were still connected. This corresponds to the behaviour illustrated in the Figures 3.21 and 3.22.

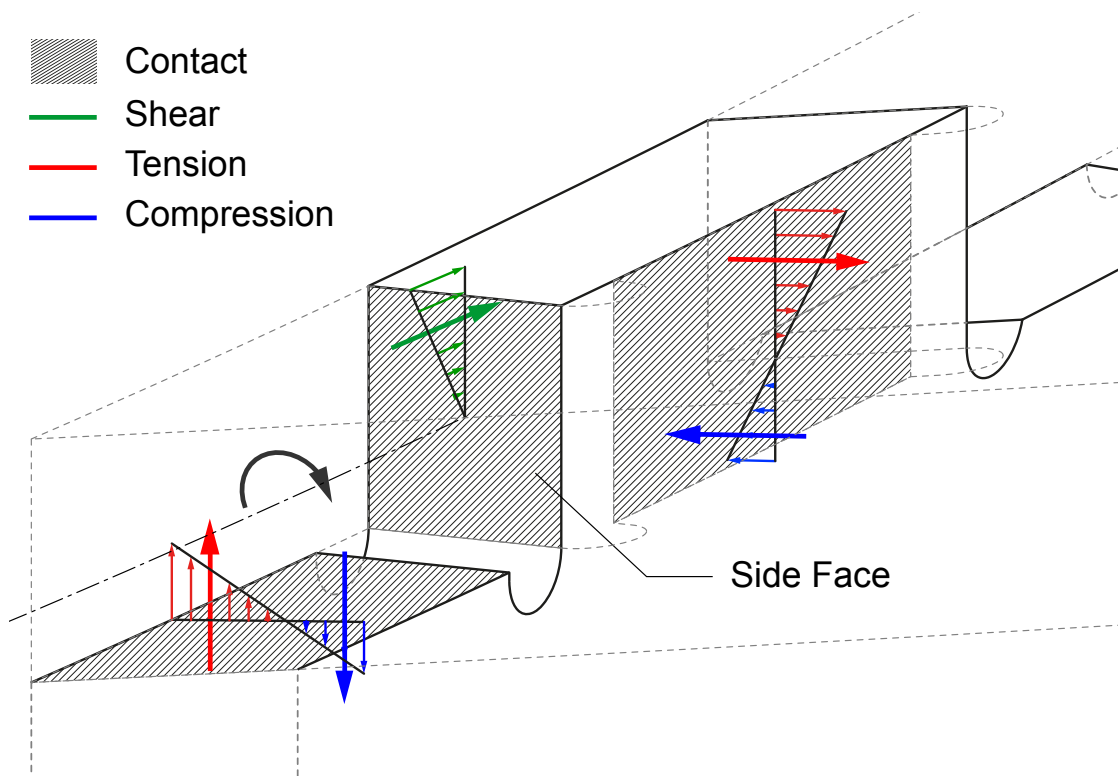


Figure 3.21 – IBOIS Curved CLT Pavilion 2013 - Adhesive bonding interfaces and distribution of forces. (connections  $W_1 - CV_1$  and  $W_2 - CV_2$ ) Large areas of the contacts along the edge receive forces normal to the interface. The contact areas across the edge receive only shear and compressive forces, which can be supported well by adhesive bonding.

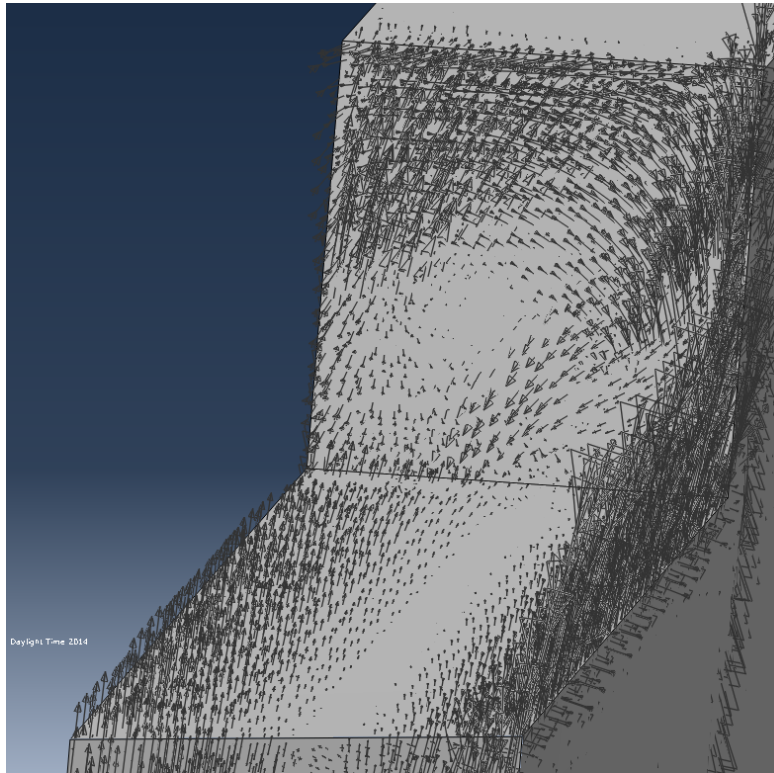


Figure 3.22 – Detailed Finite Elements Analysis of the Contact Surfaces on the Dovetail Joints. (connections  $W_1 - CV_1$  and  $W_2 - CV_2$ ). A vertical force has been applied to observe the general load distribution of the joint under bending.

#### Joint Optimization

As explained in the previous section, the additional side faces play an important role in the structural performance of the dovetail-jointed and glued connection. A higher resistance to bending moments can therefore be achieved through a larger amount of dovetail joints with a shorter individual length. However, two disadvantages result from this modification. The machining time will increase slightly for a larger amount of joints. Also, as explained in [RHMW14], the resistance to bending moments will be higher, but the shear-resistance of the joints will decrease with a shorter joint length. Depending on the specific use and location within a design, a compromise must be found between these parameters. This can be considered a strength of the proposed solution, since a parametric model allows for such adaptations.

An even more specific optimization might be achieved through the variation of the joint length within one edge. Information on this behavior, based of the prototype in this chapter has been provided by Lianne Tas, who collaborated as an Intern during the early stages of the development of the curved-folded pavilion, and later completed a Masters Thesis in Civil Engineering on curved folded structures. This thesis provides force-distribution curves along the curved-folded and edges. [Tas13, p.109-114] While the joints in this thesis are distributed



Figure 3.23 – Connection  $W_1 - CV_1$  Before the Removal of the Temporary Curved CLT Pavilion - After being exposed to outdoor conditions for a 6-month period, partial debonding was observed on the adhesive bonding interfaces along the edges  $W_1 - CV_1$  and  $W_2 - CV_2$ . The interfaces across the edge were still intact.

with a constant distance or spacing along the edges, this analysis illustrates the actual, non-linear distribution of the moments. This information could be used for a corresponding, non-linear spacing of the dovetail joints. A narrow spacing would be applied in areas with high bending moments, while a wider spacing is applied in areas with lower bending moments, which could be implemented relatively easily with the algorithms used for the design of the prototype in this chapter. An adaptive distribution of joints along the edge would not only allow for a more efficient and faster production of the joint, but also for a more specific response to local, structural requirements of the connection.

#### **Disadvantages of Integral-Joints combined with Adhesive Bonding**

Advantages of a hybrid glued-integral joint for timber panels were explained in the previous section, however there are also some disadvantages of such a combination. The full-scale prototype demonstrated the transportation problems that may result from large and bulky components, which have been pre-assembled in a factory. The two halves of the shell were, despite their very low weight of only 1.500kg each, transported with two separate trucks. An assembly of the joints on site would have simplified the transport and lowered the overall cost of the project considerably. However, with few exemptions<sup>52</sup>, a glued assembly on site is typically not possible. This provided a motivation for the developments in the following chapters, which aim at a higher degree of integral mechanical attachment, trying to achieve a

---

<sup>52</sup>For examples for in-situ adhesive bonding, see [HES14] and page 29

### Chapter 3. Design and Fabrication of Robot-Manufactured Joints for a Curved-Folded Thin-Shell Structure Made from CLT

---

connection of the parts without additional adhesive bonding, but rather through features in the geometry of the parts.

#### Disadvantages of CLT

While laminated veneer lumber (LVL) and plywood consist of layers of wood veneer, cross-laminated timber panels are built from timber boards, typically with a width of about 20cm per piece. Due to the fabrication process of these panels, the boards are usually not glued along their edges or side-faces, but only along their top and bottom. Additionally, there are stress-cuts along these boards, which allow for certain dimensional changes, for example due to humidity. These cuts are found up to every 8 or 10 cm, with about 80-90 % depth of the total height of the boards.<sup>53</sup> As a result of both the unconnected sides of these boards and the stress-cuts, precise details such as dovetail joints must be carefully planned not to collide with any of these details.

During the fabrication of the full-scale prototype presented in this chapter, some damage due to “chipping” was observed on the corners of the dovetail joints. These defects could be repaired, however these problems should be considered in the design of integral joints for CLT panels. Similar problems may result from knots, holes and other defects, which are common inside CLT panels. The joint geometries which are presented in the following chapters 4 and 5 have been designed for LVL panels, which are very homogenous and therefore ideal for the design of integral joints. The geometry of these joints could not be used with CLT, however geometrical modifications could be made to achieve similar joint functions on CLT panels.

#### Jointing of Elastically Bent Panels

It was mentioned in the foreword of this chapter, that the curved folded wood pavilion was originally intended to be built with elastically deformed panels. From the point of view of integral joint design, the choice of either pre-curved or elastically bent panels has consequences for the fabrication of the joints: The pre-curved multi-layer panels can, as described in section 3.6., only be formatted and fitted with joints after their lamination, which means that the joints must be cut on the already curved panels. This requires a more complicated setup for the fabrication process, including custom-made supports for the machining of the parts. (see Figures 3.8, 3.10 and 3.14)

Alternatively, when working with elastically bent panels, the formatting and fabrication of the joints can be carried out on the flat panels, before they are bent into their curved shape. However, the flat-cut joints will deform when the panel is bent. So, in order to obtain a precise joint geometry on an elastically bent panel, this deformation must be considered.

Figure 3.24 illustrates this problem and demonstrates a solution: According to the *Euler-*

---

<sup>53</sup>The stress-cuts and side-connections of the boards within the CLT are illustrated in Figure clt4a



### 3.8. Conclusions/Towards an Integration of Joints

---

*Bernoulli Elastic Beam Theory*, points on the upper and lower layer will always remain perpendicular to the *Neutral Layer* (Figure 3.24, blue curve). We can therefore project points on the flank of the dovetail joint normal onto this neutral layer (Figure 3.24a, red lines). The curve segments between these projected points represent the unrolled segments of the flattened part, which is illustrated in Figure 3.24b. It is to be noted that the original flank angle  $\theta$  and the shape of the dovetail joint have changed through the elastic deformation. The originally planar flank of the joint has turned into a slightly curved surface. Measuring from its center point,  $\theta'$  is smaller than  $\theta$ , and  $\theta''$  is larger than  $\theta$ .

When working with elastically bent panels, the described method of projecting the points on the upper and lower layer to the neutral plane, and then unrolling these points to a flat plane, will compensate for the deformation of the joints and result in a higher accuracy of the connection.

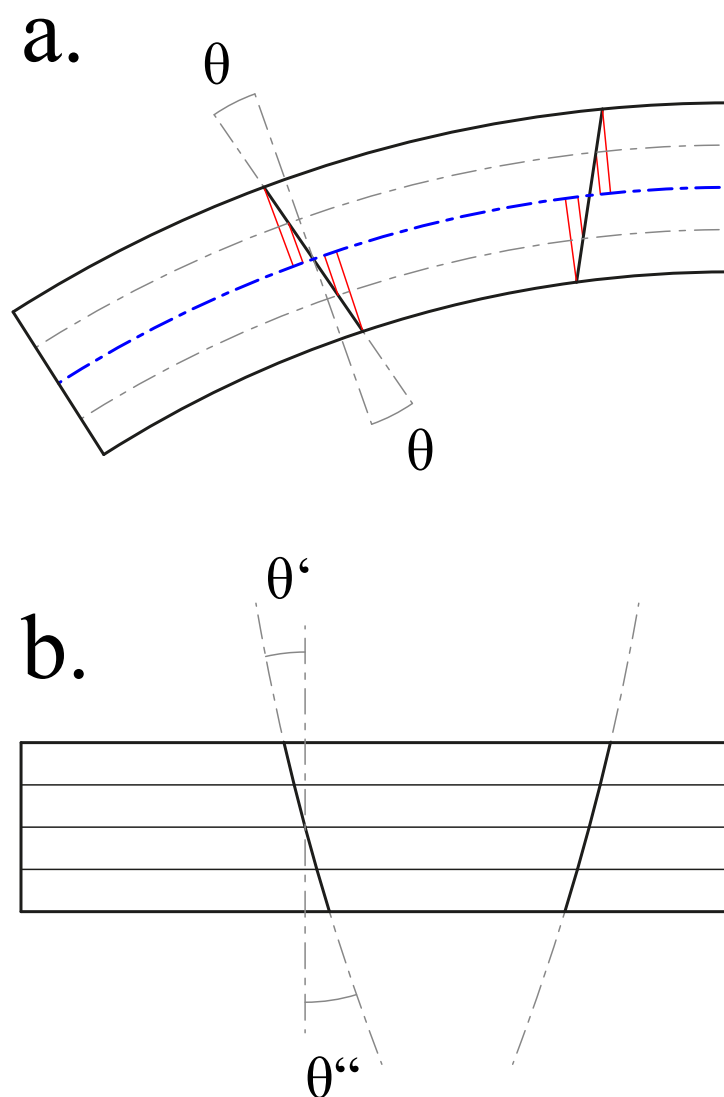


Figure 3.24 – Joint Deformation During Elastic Bending - For elastically bent panels, the joint deformation during the bending must be considered. In order to fabricate the bent joint illustrated in *a.*, the deformed angles  $\theta'$  and  $\theta''$  must be cut on the flat panel.



## Bibliography

- [AGM05] Heinz Ambrozy and Zuzana Giertlova-Merk. *Planungshandbuch Holzwerkstoffe: Technologie, Konstruktion, Anwendung*. Springer Verlag, 2005.
- [BSW11] Hans-Ulrich Buri, Yvo Stotz, and Yves Weinand. Curved folded plate timber structures. In *IABSE-IASS 2011 London Symposium*, 2011.
- [BU07] Hans-Joachim Blaß and Thomas Uibel. Tragfähigkeit von stiftförmigen verbindungsmitteln in brettsperrholz. In *Karlsruher Berichte zum Ingenieurholzbau*, volume 8, 2007.
- [BW10] Hani Buri and Yves Weinand. *Origami aus brettsperrholz*, 2010.
- [EN104] EN1995. *DIN EN 1995 (Eurocode 5) - Design of timber structures -part 1-1: General-common rules and rules for buildings*. DIN Deutsches Institut für Normung e. V., 2004.
- [fB11] Deutsches Institut für Bautechnik. Allgemeine bauaufsichtliche zulassung, z-9.1-100: Furnierschichthölzer kerto-s und kerto-q, 2011.
- [fB13] Deutsches Institut für Bautechnik. European technical approval, eta-10/0241: LENO cross-laminated timber, 2013.
- [HES14] HESS. Hess limitless, 2014. <http://www.hess-timber.com/de/produkte/>.
- [HU13] Holzbau-Unterrainer. Holzbau-unterrainer, 2013. <http://www.holzbau-unterrainer.at/Hallenbau>.
- [KFC<sup>+</sup>08] Martin Kilian, Simon Flory, Zhonggui Chen, Niloy Mitra, Alla Sheffer, and Helmut Pottmann. Curved folding. In *ACM Trans Graph* 27, pages 1–9, 2008.
- [lMea13] Riccardo la Magna et al. From nature to fabrication: Biomimetic design principles for the production of complex spatial structures. *International Journal of Spatial Structures*, Vol. 28 No. 1:27–39, 2013.
- [Neu94] Helmuth Neuhaus. *Ingenieurholzbau: Tragende geklebte Verbindungen im Holzbau*. Teubner Verlag, 1994.
- [RHMW14] Christopher Robeller, Benjamin Hahn, Paul Mayencourt, and Yves Weinand. Cnc-gefraeste Schwalbenschanzzinken für die Verbindung von vorgefertigten Bauteilen aus Brettsperrholz. *Bauingenieur*, 89:487–490, 2014.
- [SS10] Milan Simek and Vaclav Sebera. Traditional furniture joinery from the point of view of advanced technologies. In *Proceedings of the International Convention of Society of Wood Science and Technology and United Nations Economic Commission for Europe, Geneva, Switzerland*, 2010.

### **Chapter 3. Design and Fabrication of Robot-Manufactured Joints for a Curved-Folded Thin-Shell Structure Made from CLT**

---

- [Tas13] Lianne Tas. Curved folded timber plate structures -numerical and geometrical reserach into the structural behaviour of curved folded systems. Master's thesis, University of Eindhoven, 2013. Master Thesis 0620699.

## 4 Interlocking Folded Plate - Integrated Mechanical Attachment for Structural Timber Panels

Christopher Robeller, Andrea Stitic, Paul Mayencourt, Yves Weinand

Peer-reviewed and published as a chapter in: N. Mitra and P. Block (eds.), *Advances in Architectural Geometry 2014*, DOI: 10.1007/978-3-319-11418-7\_18, pp 281-294, Springer International Publishing Switzerland 2015

**Abstract** Automatic joinery has become a common technique for the jointing of beams in timber framing and roofing. It has revived traditional, integrated joints such as mortise and tenon connections. Similarly, but only recently, the automatic fabrication of traditional cabinetmaking joints has been introduced for the assembly of timber panel shell structures. First prototypes have used such integrated joints for the alignment and assembly of components, while additional adhesive bonding was used for the load-bearing connection. However, glued joints cannot be assembled on site, which results in several design constraints.

In this paper, we propose the use of dovetail joints without adhesive bonding, on the case study of a timber folded plate structure. Through their single-degree-of-freedom (1DOF) geometry, these joints block the relative movement of two parts in all but one direction. This presents the opportunity for an interlocking connection of plates, as well as a challenge for the assembly of folded plate shells, where multiple non-parallel edges per plate must be jointed simultaneously.

### Foreword<sup>54</sup>

#### Geometrical Interlocking

While the previous chapter demonstrated some clear advantages of integral joints for structural wood panels, such as the much improved assembly of prefabricated components with irregular shapes, there were also some major disadvantages observed in the process. The necessity to add adhesive bonding to the joints, in order to provide a sufficient stiffness and rigidity, did in consequence not allow for an on-site assembly of the components. The structure had to be transported with the joints already assembled. The potential flat-pack-ability of the design was therefore lost and transportation cost was increased considerably.

This chapter follows up on the previous investigation, investigating an integral connection of structural timber panels without the use of adhesive bonding. A possible technique for such joints is presented by the *mutual blocking*<sup>55</sup> of the relative movements between components. This is possible through the use of a single-degree-of-freedom joint geometry, which was already introduced in the previous chapter. Without the use of glue, the mutual blocking presents an entirely integral attachment solution, in contrast to the joints presented in the previous chapter, which must be considered a hybrid integral / adhesive-jointed solution.

Figure 4.1 illustrates the concept of mutual blocking: The left side of the figure provides a simple example where a drawer, representing a typical traditional application of such joints, is assembled from four parts  $P_1$ ,  $P_2$ ,  $P_3$  and  $P_4$ . In this configuration,  $P_1$  and  $P_3$  are blocked. They cannot be removed without removing  $P_2$  or  $P_4$  before. Above these four parts, there is another component  $P_5$ , which connects to the parts  $P_2$  and  $P_4$  simultaneously. Once  $P_5$  is inserted, it blocks the parts  $P_2$  and  $P_4$  in their single remaining degree of freedom. Due to the hierarchy of this assembly, and the different assembly directions, a single component  $P_5$  can block all other parts.

The right side of figure 4.1 shows a (non-directional) *blocking graph*<sup>56</sup> for this assembly. Components which are connected with two arrows are blocked, connections with only one arrow can be removed. The concept introduced in this figure is based on the assembly of components with multiple connections. If the removal or assembly of a part requires the simultaneous operation of two or more joints, this is only possible if a common vector for the insertion of the part can be found. This vector must then lie within the degrees-of-freedom of all the joints that are involved.

---

<sup>54</sup>This additional section was not included in the original publication.

<sup>55</sup>the mutual blocking of intersecting planar pieces with *half-lap joints* has been demonstrated by [SP13]

<sup>56</sup>for blocking graph theory, directional- and non-directional blocking graphs, see [WL94]

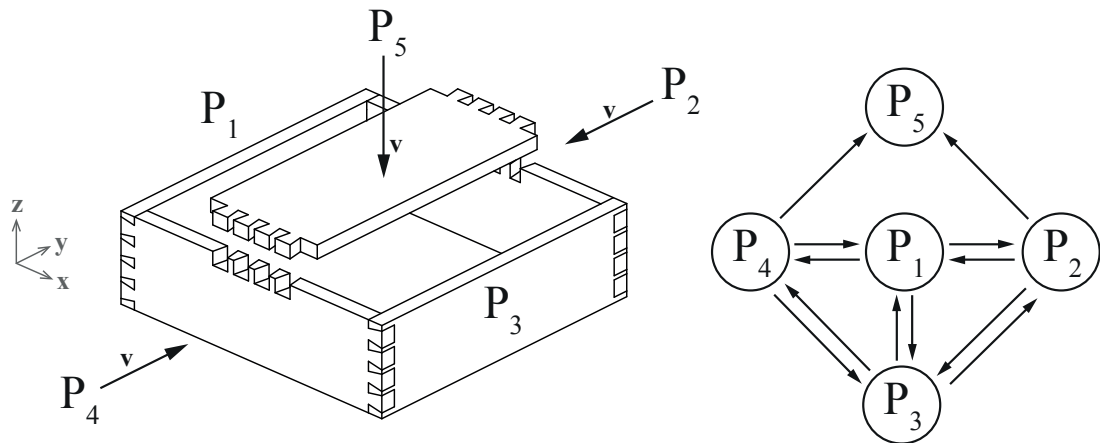


Figure 4.1 – This figure illustrates the mutual and hierarchical blocking of an assembly of multiple components through integral dovetail joints with only one degree of freedom.

### Bidirectionally Folded Surfaces

The curved-folded plate structure presented in the previous chapter demonstrated a design, in which all folds are folded to the same side, forming a frame (or an arch). Its transversal cross-section profile is a segmented half circle. With an increasing number of segments on this half-circle, which may be necessary in order to reduce the size of the individual components, the dihedral angles  $\varphi$  between the plates will become increasingly obtuse, which presents a problem for the design of integral 1DOF joints. It was explained in the previous chapter, that jointing techniques for dihedral angles larger than  $140^\circ$  can be developed, but significant compromises need to be made, compared to the more efficient side-cutting technique presented in Section 3.4 (see figure 3.7, page 51).

Furthermore, the prototype presented in the previous chapter was folded in only one direction. The static-height in its transversal cross-section was not achieved through folding, but through the arc-height of the curved CLT panels. However, in a purely folded surface structure with planar faces, the static height will be determined only through the width-to-height ratio of the folds  $w/h$ , or respectively the dihedral angles  $\varphi$ . Therefore, dihedral angles between  $50^\circ$  and  $140^\circ$  will not only satisfy the fabrication constraints of the side-cutting technique. This range of dihedral angles is also ideal for the design of structurally efficient folded plates, which makes the combination of the dovetail joints and the folded-plate geometry a complementary combination.

In traditional “through-type” folded plate structures<sup>57</sup>, plates are folded in an alternating up-and-down manner. In paper folding, this is also called zig-zag, concertina or accordion folding. This principle of up-and-down folding can also be applied to *bidirectionally* folded surfaces, which are simultaneously folded in two different directions. Well known examples

<sup>57</sup> see page 26

## Chapter 4. Interlocking Folded Plate - Integrated Mechanical Attachment for Structural Timber Panels

are the Japanese *Origami* paper folding techniques, such as the Miura-Ori or the Yoshimura fold. The same geometry used for these paper folds has also been used for architectural applications, for example the so-called *Antiprismatic Shell Structures*, some of which were researched and built during the 1970s. These surface-active structures allow for the assembly of structurally efficient curved shells from small planar components. They provide a relatively large and continuous static height  $h$ , and small dihedral angles  $\varphi$  for all folds.<sup>58</sup>

The antiprismatic shells that were studied in the 1970s were cylindrical (singly-curved) shells. Figure 4.2a shows a design that was studied by Zygmunt Stanislaw Makowski's group. Figure 4.2b shows the geometry of an individual component of this shell in its cross-section. The structural benefits of this particular shape are explained in Figure 4.3. The illustration shows a span between two supports, which is bridged by three discrete elements. This system is being stabilized through the diagonal cross-bracing, which connects every *second* point. The antiprismatic folded plate shells work in a very similar way. A detailed description has been provided by [Huy72] and [Huy01].

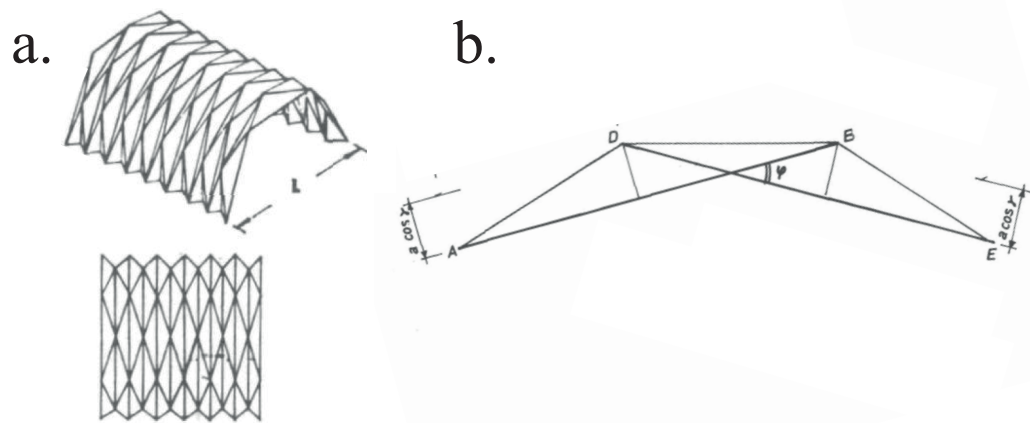


Figure 4.2 – Antiprismatic Folded Plate Shell - a. shows a cylindrical shell studied by Zygmunt Stanislaw Makowski, b. shows a cross-section of a component of this structure. Drawings taken from [Huy72, p.38(a)/p.48(b)]

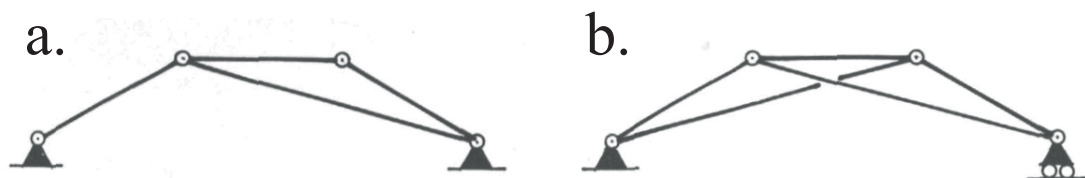


Figure 4.3 – Structural Principle of an Antiprismatic Folded Plate - An arch of discrete planar elements is being stabilized by diagonal struts, which connect every second point and provide cross-bracing for the structure. (Figure taken from [Huy72, p.45])

<sup>58</sup>A detailed description of the angles on antiprismatic shells is provided on page 94

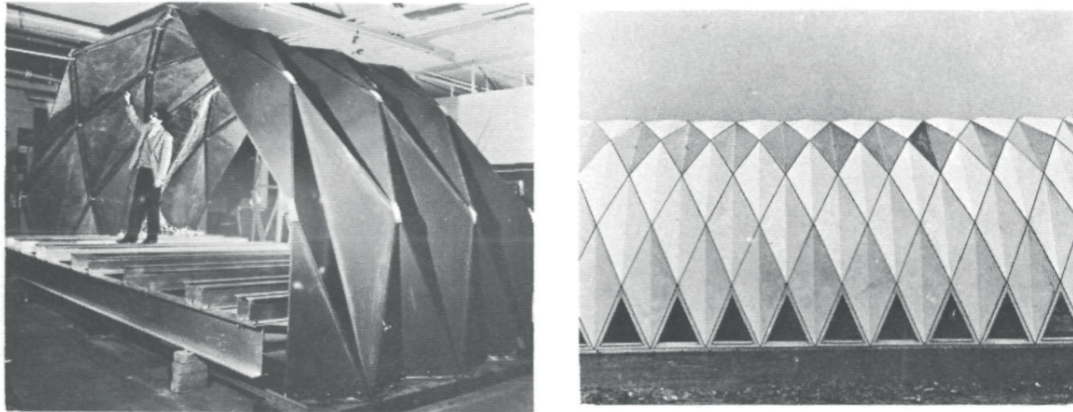


Figure 4.4 – Several Antiprismatic Folded Plate Shells were built with fiber-reinforced plastics in the 1960s and 1970s - The left side of this figure shows an experimental prototype, which was studied by J.Ensor in 1962. The image on the right side shows a permanent structure designed by renzo Piano for a sulfur extraction factory in Italy in 1966.

## Contributions

The finite element simulations (fig 4.8 and fig 4.9) have been created by the co-authors of the publication, Andrea Stitic and Paul Mayencourt. The purpose of these illustrations is to provide basic information about the prevalent forces in an antiprismatic folded plate shell, rather than providing conclusive information or optimizations. Instead, a detailed analysis is provided in a separate publication [SRW15]. A general understanding of the prevalent forces and their distribution along the edges is crucial for the choice of a jointing technique and its specific design, which always presents a compromise between multiple constraints such as fabrication, assembly, architectural and structural functions. The co-authors have also conducted the two load-tests (fig 4.14 and fig 4.19) of the prototypes presented in this chapter. Similar to the finite element illustrations, these load-test were not aimed at specific

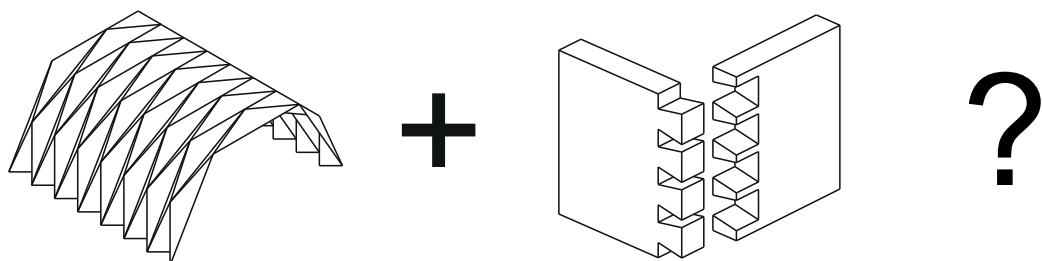


Figure 4.5 – Can an Antiprismatic Folded Plate be assembled with single-degree-of-freedom (1DOF) joints, combining the advantages of the shell geometry with those of the joints?

#### **Chapter 4. Interlocking Folded Plate - Integrated Mechanical Attachment for Structural Timber Panels**

---

optimizations or comparisons, they rather provided some fundamental knowledge about the load-bearing capabilities, deflections and the failure of these new glue-less jointed structures.



## 4.1 Introduction

Architectural designs have often been inspired by folded shapes such as origami, however the folding principle can rarely be applied to building structures directly. Alternatively, folded plates can be cast as concrete thin-shells [TB09], which requires complex formwork and an elaborate vertical support structure, or realized as cladded space-frames built from metal plates [Piz03] or tubular steel.

A prefabricated folded plate built from cross-laminated timber panels has been proposed by [Bur10]. It combines the elegant and efficient shape of folded plate shells with the advantages of structural timber panels, such as CO<sub>2</sub> storage and a low weight-to-strength ratio. However, a major challenge in the design of a timber folded plate is presented by the joints: Since timber panels cannot be folded, a large amount of edgewise joints has to provide two main functions. One of these functions is the load-bearing behaviour, where *Connector features* of the joints must provide a sufficient stiffness and rigidity. The second main function of the joints is the assembly of the parts, where *Locator features* of the joints are essential for a precise and fast positioning and alignment of the parts.

[Hah09] examined the structural behaviour of a first timber folded plate shell built from plywood and assembled with screwed miter joints, concluding that the load-bearing performance could be improved significantly with more resistant connections.

Inspiration for such improvements may be found in *integral mechanical attachment* techniques, the oldest known technique for the jointing of parts, where the geometry of the parts themselves blocks their relative movements [Mes06]. Such integrated joints have recently been re-discovered by the timber construction industry. Beginning in 1985, mortise-and-tenon joints have been repatriated in timberframe and roof constructions [Hun14]. Only very recently, integrated joints have also been proposed for the edgewise jointing of timber panels. [lMea13] and [KCC<sup>+</sup>14] have applied finger joints to plywood panels and [RNW14] have demonstrated an application of dovetail joints for cross-laminated timber panels (CLT). In these prototype structures, the integrated joints have played an important role for the assembly of the components. They have also participated in the load-bearing connection of the parts, but additional adhesive bonding was needed. With few exceptions [HES14], such glued joints cannot be assembled on site, because they require a curing period with a specific temperature and humidity [Pur11]. Therefore, their application is limited to off-site assembly of larger components, which complicates both transport and handling while still requiring additional connectors for the final assembly.

In this paper, we propose the use of dovetail joints without additional adhesive bonding, on the case study of a timber folded plate shell. (Figure 4.6).

Through their single-degree-of-freedom (1DOF) geometry, these joints block the relative movement of two parts in all but one direction. This presents the opportunity for an interlocking connection of plates, as well as a challenge for the assembly of folded plate shells, where



Figure 4.6 – Timber folded plate built from 21mm LVL panels, assembled with single-degree-of-freedom dovetail joints without adhesive bonding. Components interlock with one another

multiple non-parallel edges per plate must be jointed simultaneously.

## 4.2 Dovetail Joint Geometry and Mechanical Performance

Using polygon mesh processing, we describe an edgewise joint based on its edge  $E$ . From the mesh connectivity, we obtain the edge vertices  $p$  and  $q$  and the adjacent faces  $F_0$  and  $F_1$  with their face normals  $n_0, n_1$ . We use the polygon mesh to represent the mid-layer of timber panels with a thickness  $t$  and offset  $F_1$  and  $F_2$  at  $\pm \frac{t}{2}$  to obtain the lines  $L$  (Figure 4.7a). From a division of  $E$ , we obtain the points  $X_j$  for a set of reference frames  $\{u_1, u_2, u_3\}$ , where  $u_1 \parallel \vec{pq}$  and  $u_2 \parallel n_0$  (Figure 4.7b). A finger joint geometry is obtained from an intersection of planes located at  $X_j$ , normal to  $u_1$ , with the four lines  $L$ .

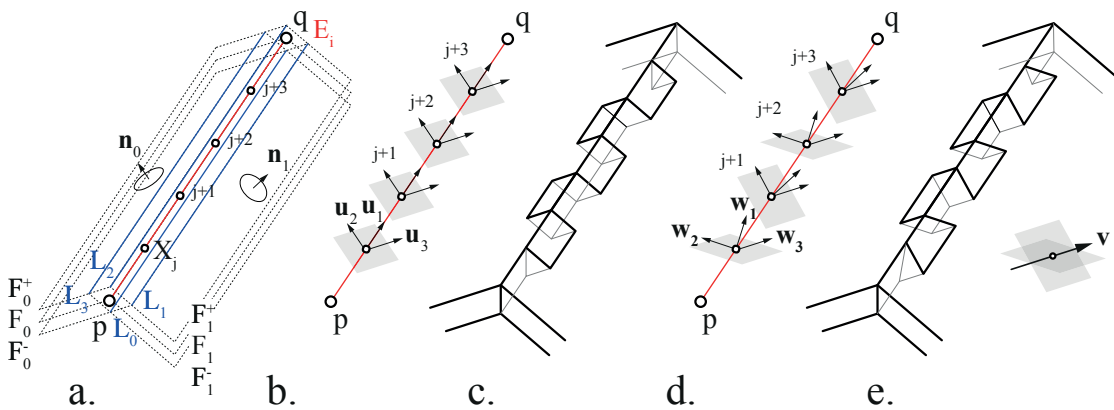


Figure 4.7 – Joint geometry. a: Basic parameters, b: Intersection planes (grey) normal to  $\vec{pq}$ , c: 3DOF joint, d: Rotated intersection planes (grey) normal to  $\vec{w}_j$ , e: 1DOF joint

Without additional connectors, finger joints are *planar joints* with three degrees of freedom

(3DOF). They can resist shear forces parallel to the edge and in-plane compressive forces. However depending on the plate geometry, thickness and most of all rotational stiffness of the connection detail, bending moments are also transferred between the plates. Also, due to the rotation of the plate edge caused by bending, in-plane traction forces perpendicular to the edge line appear and their magnitude increases under asymmetrical loads. Such forces, which occur as a result of out-of-plane loading, cannot be supported only by shear and in-plane compression resistant joints.

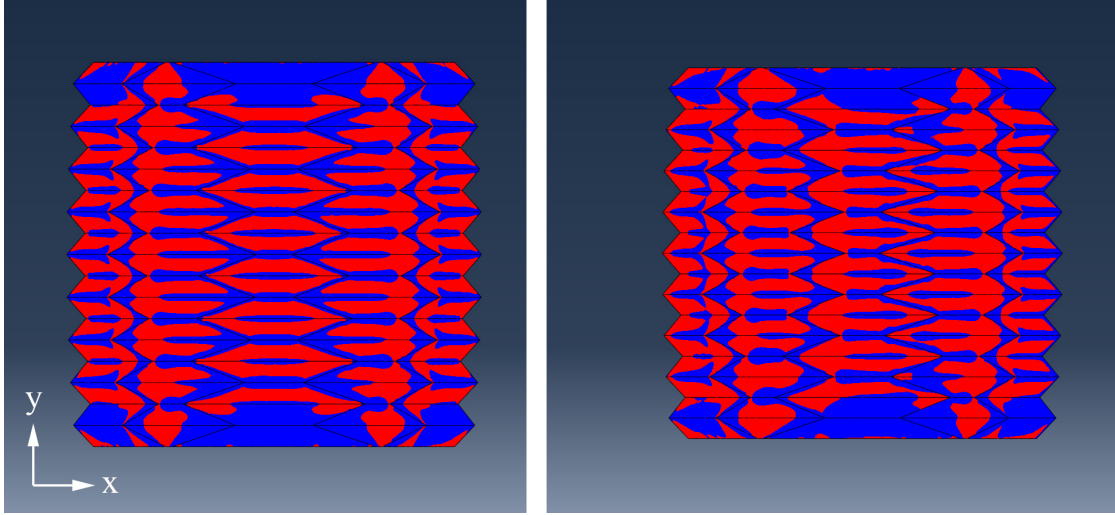


Figure 4.8 – FEM analysis (top view) of a 3x3m, 21mm Kerto-Q folded plate thin shell assuming fully stiff joints. Distribution of traction (red) and compression (blue) stresses in the y direction. Left side: gravity load case. Right side: asymmetric snow load.

On a dovetail joint (Figure 4.7d,e), the intersection planes on the points  $X_j$  are normal to a rotated vector  $w_1$ . It is obtained from a rotation of the reference frame  $\{u_1, u_2, u_3\}$  about  $u_3$  at an alternating angle  $\pm\theta_3$ . The resulting rotated side faces reduce the dovetail joints degrees of freedom to one translation  $\vec{w}_3$  (1DOF). [SS10] have suggested  $\theta_3 = 15^\circ$  for spruce plywood panels. Such prismatic joints can only be assembled or disassembled along one assembly direction  $\vec{v} = \vec{w}_3$ . In addition to the finger joints resistance to shear and compressive forces, dovetail joints can, without adhesive bonding, also resist bending moments and traction forces which are not parallel to  $\vec{v}$ . Due to the inclination of the side faces of the joint, resistance to these forces can be improved significantly. In that way the inclined faces take over the role that the glue would have in a finger joint. (Figure4.9)

### 4.3 Fabrication Constraints

One of the main reasons for the resurgence of finger and dovetail joints is the possibility of automatic fabrication. However, the mechanical performance of the joints depends on fabrication precision. At the same time, fast machine feed rates are important for a time-efficient production. We have fabricated such joints with a robot router and a gantry router,

## Chapter 4. Interlocking Folded Plate - Integrated Mechanical Attachment for Structural Timber Panels

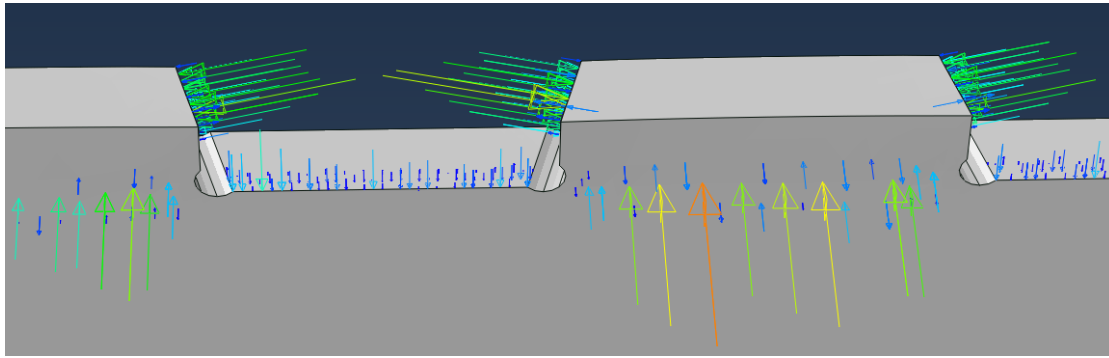


Figure 4.9 – FEM simulation of bending on a dovetail joint connecting two Kerto-Q 21mm LVL panels. The bending moment applied is transformed into compression, normal and shear forces parallel to the inclined contact faces.

achieving higher precision with the gantry machine, which is more stiff and provides a higher repeat accuracy.

The variability of the machine-fabricated joints is enabled by the 5-axis capability of modern routers: Although traditional edgewise joints in cabinetmaking were used for orthogonal assemblies, both the finger and dovetail joint can also be applied for non-orthogonal fold angles, which was essential for the reference projects mentioned before. However, there are certain fabrication-related constraints for machine-fabricated dovetail joints. In order to integrate the joint fabrication directly with the panel formatting, we use a side-cutting technique [Koc64], which is limited to a tool inclination  $\beta_{max}$ . We obtain this limit from the specific geometry of the tool, tool-holder and spindle used for the joint fabrication. (Figure 4.10)

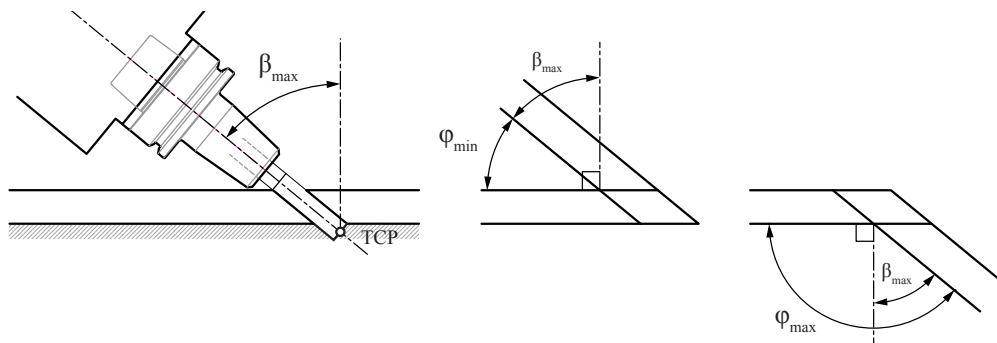


Figure 4.10 – Fabrication Constraints. Side-cutting technique used for the automated fabrication of 1DOF edgewise joints with common 5-axis CNC routers. The maximum tool inclination  $\beta_{max}$  results from the tool and the tool holder geometry. From this we obtain the range of possible fold angles  $\pm\varphi$  between panels.

The parts can be assembled in two ways, as shown in figure 4.10, which allows to address a

larger range of interior fold angles  $\varphi$ .

$$\varphi = \arccos \frac{(\vec{n}_0 \times \vec{p}q) \cdot (\vec{n}_1 \times \vec{p}q)}{\|(\vec{n}_0 \times \vec{p}q)\| \cdot \|(\vec{n}_1 \times \vec{p}q)\|}$$

From this we obtain the fabrication-constrained most acute fold  $\varphi_{min} = 90^\circ - \beta_{max}$  and most obtuse fold  $\varphi_{max} = 90^\circ + \beta_{max}$ . With standard routing tools, this technique allows for the jointing of acute folds up to  $\varphi = 50^\circ$ , which is ideal for folded plate structures. Very obtuse fold angles  $\varphi \geq 140^\circ$ , which might be required for small-tiled geodesic dome structures, cannot be fabricated with this method.

#### 4.3.1 Simultaneous Assembly of Multiple Edges

The assembly of doubly-corrugated folded plates requires the *simultaneous* jointing of multiple edges per component (Figure 4.11), which has implications on both the shell and the joint geometry.

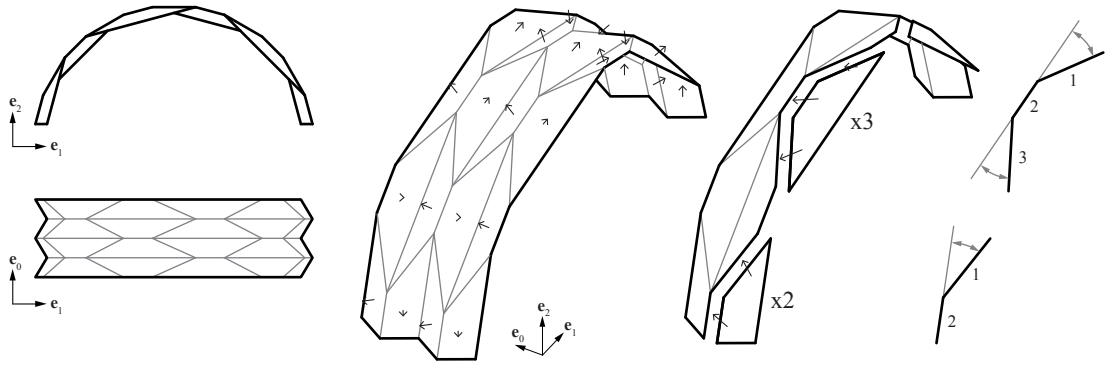


Figure 4.11 – The assembly of a folded plate from discrete elements (left side) requires the *simultaneous* assembly of non-parallel edges. (right side) We rotate the insertion direction of our 1DOF joints, to make the insertion vectors of simultaneously jointed edges parallel. We chose a hexagon reverse fold pattern which requires only moderate rotations.

For multiple 1DOF-jointed edges  $E$ , simultaneous assembly is only possible if the individual assembly directions  $\vec{v}$  are parallel. With a normal dovetail joint geometry, where  $\vec{v} = \vec{n}_0 \times \vec{p}q$  (Figure 4.7d,e), this is not the case: A simultaneous assembly is only possible for parallel edges, which allows only for rectangular assemblies, such as drawers or a cabinets.

In order to simultaneously join non-parallel edges, we must rotate the assembly direction  $\vec{v}$  of the joints to make them parallel. This possibility is known from Japanese cabinetmaking [Tet07], where certain joints, like the Nejiri Arigata Joint are assembled along the external bisector of the fold.

We extend the Japanese technique to a cardan rotation of the frames  $\{u_1, u_2, u_3\}$  about  $u_1$  at the angle  $\theta_1$  and about  $u_2$  at the angle  $\theta_2$  (Figure 4.12a). Each of these rotations is constrained

to a maximum value.  $\theta_{1,max}$  is set by the fold interior angle  $180^\circ - \varphi_i$ . The range is large for acute fold angles and small for obtuse fold angles.  $\theta_{2,max}$  is fabrication-constrained through the maximum tool inclination  $\beta_{max}$  (Figure 4.10). The specific limit relates to  $\varphi$  and  $\theta_3$ . For our setup,  $\theta_{2,max}$  was approximately  $\pm 20^\circ$ . From these constraints, we obtain a pyramid-shaped window  $S$  for every edge  $E$  (Figure 4.12b). This window illustrates all possible assembly directions for  $E$ .

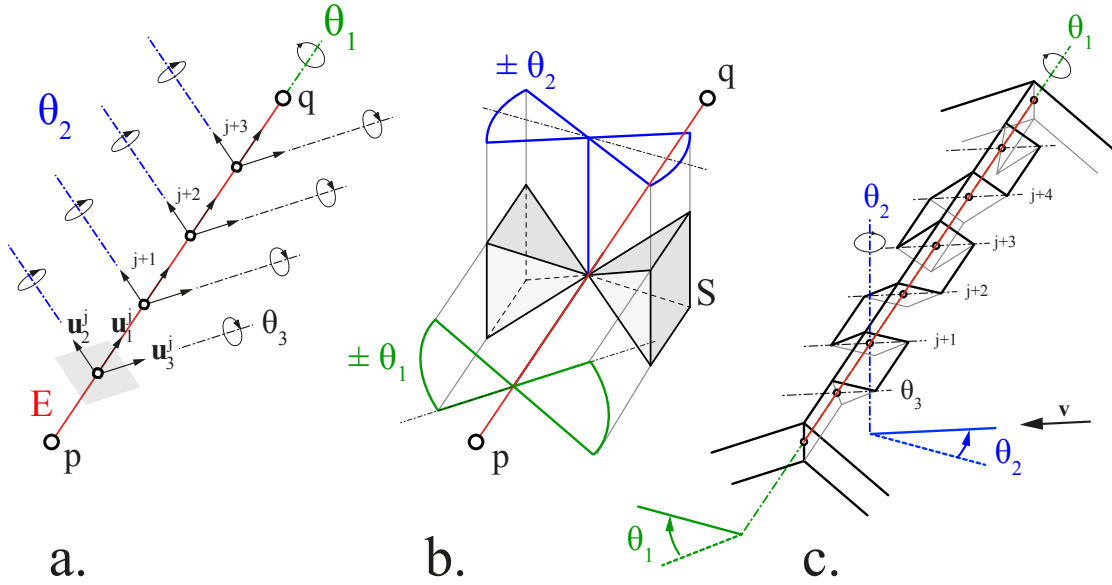


Figure 4.12 – a: Rotation of the frames  $\{u_1, u_2, u_3\}$  about the three Euler angles  $\theta_1$  (green),  $\theta_2$  (blue), and  $\theta_3$ . b: Rotation window  $S$ , illustrating all possible assembly directions. c: Dovetail joint with assembly direction rotated about  $\theta_1 = 20^\circ$  and  $\theta_2 = 20^\circ$ .

For the simultaneous jointing of three edges  $E_1, E_2, E_3$ , we overlay the three rotation windows  $S_1, S_2, S_3$ . If there is an intersection  $S_1 \cap S_2 \cap S_3$  the edges can be jointed simultaneously. The assembly direction must be chosen within the intersection. As a result of these limited rotations, the angle between neighbouring, simultaneously jointed edges cannot be very acute. Folded plate patterns like the Herringbone, the Diamond, or the Hexagon pattern, which we chose for our prototypes, [Bur10] (Figure 4.11) work well for our joining technique. Another essential feature provided by these reverse-folds are the acute fold angles, which easily satisfies the fabrication-constrained range of  $\varphi_{min} = 50^\circ$  to  $\varphi_{max} = 140^\circ$ .

#### 4.4 Interlocking Arch Prototype

In an assembly of multiple components (Figure 4.13), a step-by-step sequence must be planned for the assembly of the parts. The completed structure can only be disassembled piecewise in the reverse order of assembly. In this way, the elements interlock with one another like a burr puzzle [Wya28].





Figure 4.13 – Folded-plate arch prototype built from 12mm birch plywood (9-layer, I-I-I-I-I). Assembled without adhesive bonding or metal fasteners. Span 1.65m, self-weight 9.8kg.

Each joint consists of two parts, which must be parallel during assembly. We therefore chose a folded plate geometry with relatively short edges. The manual assembly of long edges may be more difficult but can be simplified with a modified joint geometry. It is important to know the approximate direction of insertion for each part, as this is not easily visible through the joint geometry. Deformations of the arch during the assembly should be minimised. We have assembled this first prototype lying on the side. However larger assembly may require temporary punctual supports. Although the in-plane dimensional stability of the Kerto-Q panels is very high, panels may be slightly warped and some force may be necessary during assembly. While we have simply used a rubber hammer, more advanced techniques could be applied.

To understand the mechanical behaviour of the built prototype, we have applied a vertical load at mid-span of the arch and measured the vertical deflection at the same point. The total load of 821N was applied in two identical load cycles consisting of four loading/unloading sub-cycles. First, a vertical load of 117N was applied in seven steps, after which the load of the last four steps was removed. The loading and unloading of the last four steps was repeated three more times, after which the complete load was removed and the residual deflection was measured. (Figure 4.14)

Under a vertical load equal to the arch's dead weight of 9.8kg (98N), the deflection measured at mid-span was 2mm. From this we obtain a span-to-deflection-ratio of  $L/750$  and the arch's structural efficiency which reaches 8.6 when loaded with 821N (ratio of the maximal load over the dead weight of the arch).

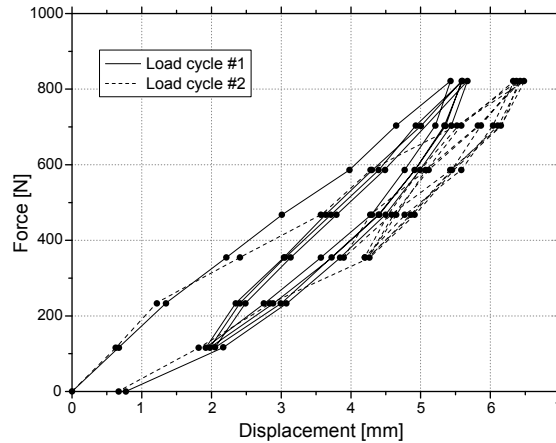


Figure 4.14 – Series of 3-point flexural tests on the small scale interlocking arch prototype built from Metsawood 12mm birch plywood panels.

## 4.5 Interlocking Shell Prototype

### 4.5.1 Automatic Geometry Processing

Using the RhinoPython application programming interface, we have developed a computational tool which lets us instantly generate both the geometry of the individual components and the machine G-Code required for fabrication. The tool processes arbitrary polygon meshes, and generates 1DOF joints for all non-naked edges where the fold angle  $\varphi$  is larger than  $\varphi_{min}$  and smaller than  $\varphi_{max}$  shown in figure 4.10 (non-smooth meshes). It also requires an input of edge identifier tuples identifying those edges which must be jointed simultaneously, as well as the thickness of the LVL panels. Exploiting this geometrical freedom, we have tested our computational tool on the design of a folded plate shell prototype with an alternating convex-concave longitudinal curvature. The shell spans over 3m at a thickness of 21mm, using Kerto-Q structural grade LVL panels (7-layer, I-III-I). (Figure 4.15)

Comparing this doubly-curved folded plate with a straight extrusion (as tested by [Bur10]), it can be concluded that the slight double-curvature proves to be very beneficial when it comes to global deflections, for example those caused by wind loads. Deflections for the doubly-curved shell geometry in the vertical direction are up to 39% smaller and up to 13% smaller in the lateral direction than the ones for the straight extrusion one.

### 4.5.2 Assembly

Figure 4.16 shows a part of the connectivity graph of the doubly-curved folded plate shell prototype. It illustrates the hierarchy, direction and order in which the 107 components with their 239 edgewise 1DOF joints must be assembled.

Figure 4.17 shows the components from figure 4.16 in 3D, demonstrating how the component



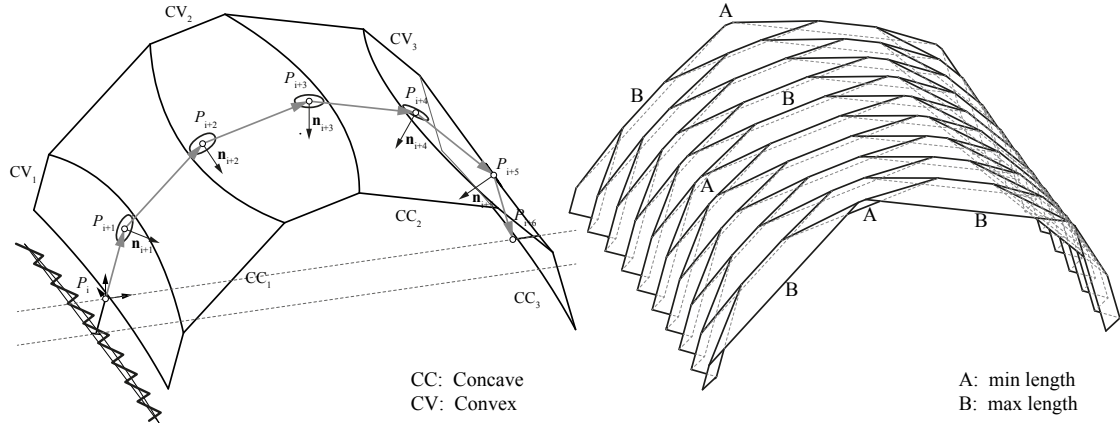


Figure 4.15 – Doubly-curved folded-plate: The radius ( $R = 17m$ ) of the transversal curvature is determined by the folded plates maximum amplitude  $h$  [Bur10], which is inversely proportional to the number of segments  $m$  of the cross-section polyline (grey). We obtain this polyline from a circular arc divided into segments of equal length. The interior angle  $\gamma = ((m - 2) * 180) - m$  of this polyline is proportional to all fold angles  $\varphi$ . The geometry of our prototype was fabrication-constrained to a maximum component length  $B \leq 2.5m$

based on mesh face  $F_{86}$  is being inserted. Its three edgewise joints  $E_{41}$ ,  $E_{68}$  and  $E_{89}$  must be assembled simultaneously. The three assembly vectors of the edges  $\vec{v}_{41}$ ,  $\vec{v}_{68}$  and  $\vec{v}_{89}$  have been rotated to be parallel. The same applies for the adjacent edges on the left side of the faces  $F_{67}$ ,  $F_{69}$ ,  $F_{88}$ ,  $F_{103}$  and  $F_{105}$  (see figure 4.16: all faces with multiple outgoing arrows). The roman numerals on top of figure 4.16 show the interlocking sequence. All joints marked with I. ( $E_{18}$ ,  $E_{99}$ ,  $E_{100}$ ,  $E_{44}$ ,  $E_{66}$ ,  $E_{91}$ ,  $E_{59}$ ,  $E_{43}$ ) can be assembled individually and independently in a first step. Within the rotation window of the edge, we can freely rotate  $\vec{v}$  for these edges (the greater the angle between  $\vec{v}$  and the main direction of traction  $e_1$ , the better). After the connection of the joints marked II. ( $E_{35}$ ,  $E_{65}$ ,  $E_{98}$ ), all connections left of this point cannot be disassembled any more without disconnecting II. The components interlock with one another, similar to a burr puzzle [Wya28]. The rest of the assembly follows the same logic.

### 4.5.3 Completed Shell Prototype and Load Test

Figure 4.18 shows the completed folded plate prototype, with a span of 3m and a shell thickness of 21mm. Boundary conditions that restrain displacements of the supports in every direction, but allow rotations, were applied on both sides. A longitudinal line load was introduced along the top of the shell and vertical displacement was measured at center point. (Figure 4.19)

The prototype structure was also modelled in FE analysis software (Abaqus) and loaded in the same way. The plates were modeled using shell elements, where the mid-surface is used to represent the 3D plate and transverse shearing strains are neglected. Connections between the plates were considered as completely rigid in order to obtain minimal displacements of the structure. By comparing the displacements of the structure with infinitely stiff joints with

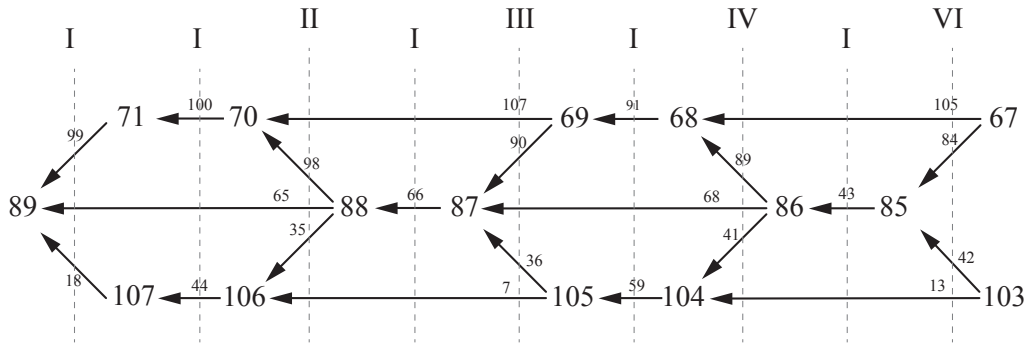


Figure 4.16 – Partial connectivity graph of the folded plate shell prototype. (Left-to-right side assembly) Large numbers represent mesh Faces  $F$ , small numbers represent mesh edges  $E$ . Roman numerals illustrate the interlocking hierarchy

the ones measured on the prototype, we obtained information about the actual semi-rigidity of the joints. The results obtained from the testing of the large scale prototype showed that the load of 25kN, that corresponds to the proportional limit of the load-displacement curve, causes a vertical displacement of 23mm. In the FE model, the load applied in the same manner caused a vertical displacement of 2.6mm.

## 4.6 Conclusion

A timber folded plate shell combines the structural advantages of timber panels with the efficiency of folded plates. However, in such discrete element assemblies, a large amount of semi-rigid joints must provide sufficient support for the adjacent plates in order to ensure an efficient load-bearing system. This remains a challenge with much potential for improvements [Hah09].

Integrated edgewise joints present an interesting addition and an alternative to state-of-the-art connectors: Compared to adhesive bonding, such joints can be assembled rapidly on site. Also, compared to costly metal plates and fasteners, which are typically required in large quantities [Neu04], the fabrication of integrated joints is not more expensive. The replacement or reduction of metal fasteners with an integrated mono-material connection includes advantages such as improved aesthetics, ease-of recycling or a homogeneous thermal conductivity of the parts, which can reduce condensation and decay. [Gra86] Another particular advantage is the possibility to join thin panels: The current technical approval for the Kerto-Q panels does not permit screwed joints on panels with a thickness of less than 60mm. [DIB11]

Recent experimental projects, which we introduced in section 4.1, have already demonstrated first applications of integrated edgewise joints for timber panels. This paper followed up on these projects, examining the particular advantages, potential and challenges of 1DOF joints for timber folded plate shells. We have demonstrated how this joint geometry helps

resisting the forces which occur in such structures. In addition to the load-bearing connector features, the joints provide locator features, which allow for precise positioning and alignment of the parts through the joint geometry. This improves both accuracy and ease of assembly. Furthermore, we have presented a solution for the simultaneous assembly of multiple edges per panel, which is essential for the application of 1DOF joints in a folded plate shell structure. The per edge "rotation window" introduced in section 4.3.1 integrates the joint constraints related to assembly and fabrication. It can be processed algorithmically and give instant feedback on whether or not a set of non-parallel edges can be jointed simultaneously. This provides a tool for the exploration of a variety of alternative folded plate shell geometries.

The prototypes presented in this paper already suggest possible patterns and demonstrate the reciprocal relationship between the geometry of the plates and the joints. Two built structures allowed us to test and verify the proposed methods for fabrication and assembly while providing valuable information about the load-bearing capacity of the integrated joints.

For the application in a large-scale building structure, further research is required to determine if the integrated joints can replace additional connectors entirely or reduce their amount. A possible combination of integrated joints with additional metal fasteners has been demonstrated recently in the LaGa Exhibition Hall [ICD14]. Another possibility would be a combination of the 1DOF joints with integrated elastic interlocks. [RMW14]

## 4.7 Acknowledgments

We would like to thank Stéphane Nicolas Roche for the discussions, as well as Gabriel Tschanz for assisting with the fabrication and assembly of the prototypes. We also thank Jouni Hakkarainen and the Metsa Group for the supply of information and materials.

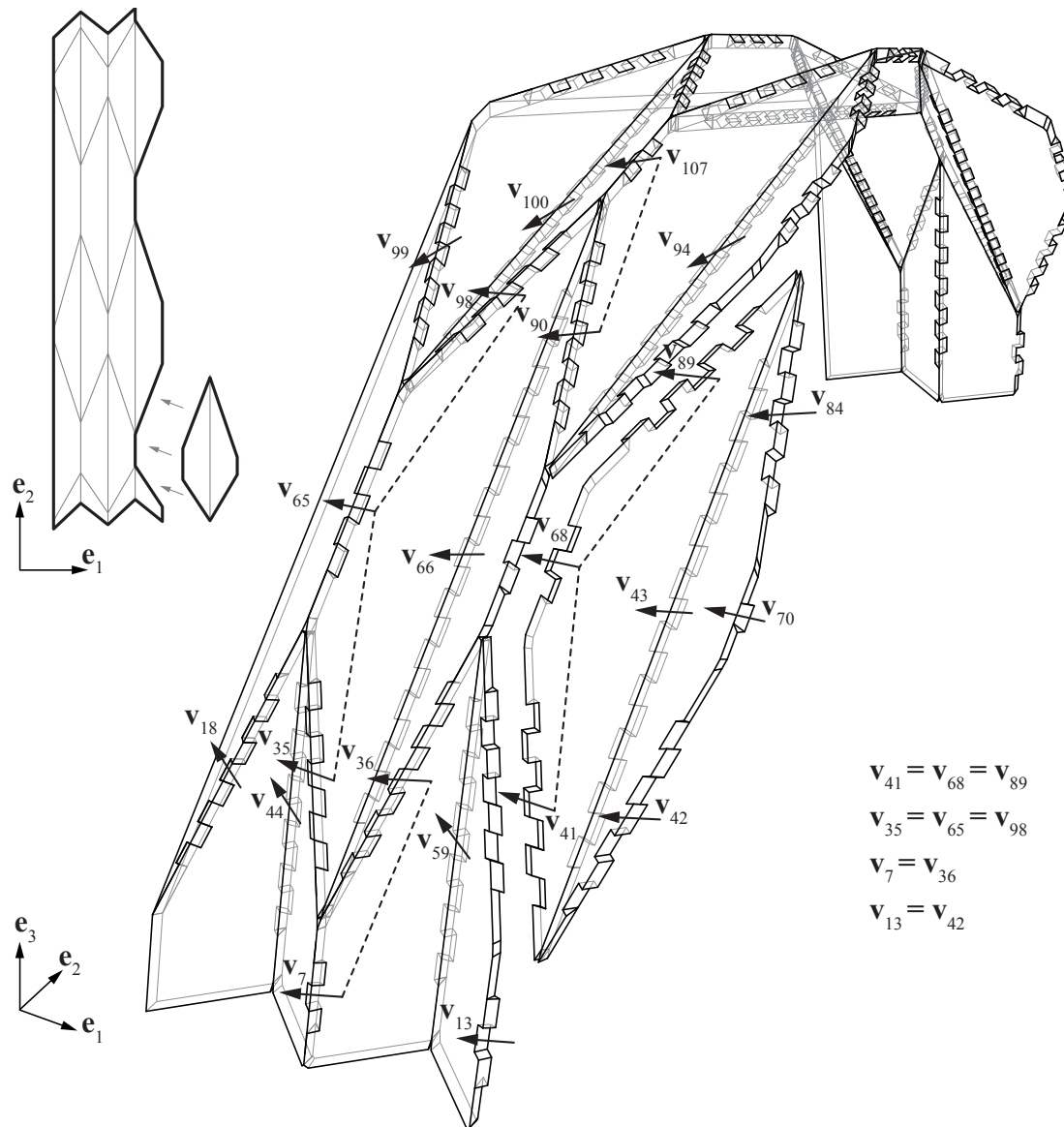


Figure 4.17 – Left-to-right-side assembly of the Interlocking folded plate shell prototype. Built from Kerto-Q structural grade LVL panels (7-layer, I-III-I)



Figure 4.18 – Folded-plate shell prototype, built from 21mm LVL panels. With a self-weight of 192kg, the prototype with a span of 3m was tested with a line-load up to 45kN.

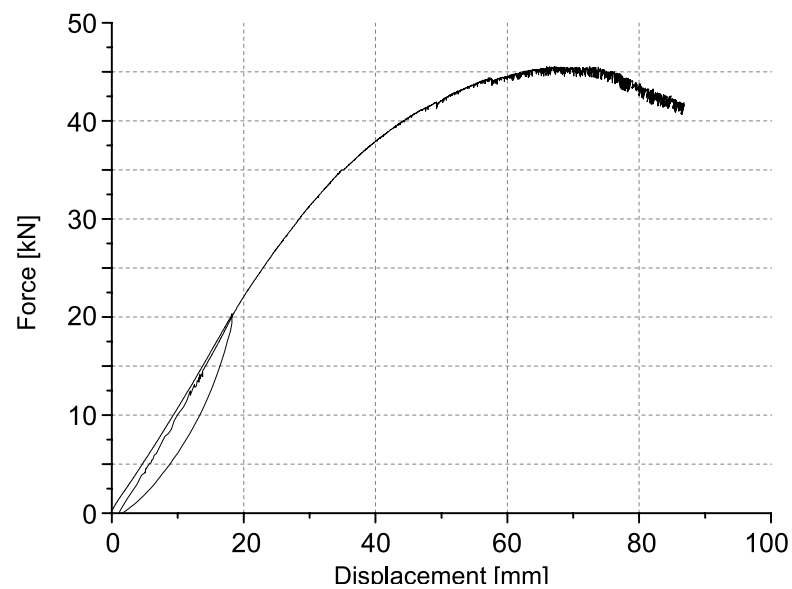


Figure 4.19 – Load-displacement curve of the shell prototype. A longitudinal line load was introduced along the top of the shell. Vertical displacement was measured at the center point.





Figure 4.20 – Doubly-curved Prototype, Folded in 2 Directions - Interior View 1





Figure 4.21 – Doubly-curved Prototype, Folded in 2 Directions - Interior View 2

## Additions and Remarks<sup>59</sup>

### Antiprismatic Folded Plate Geometry

While the publication was primarily focused on the jointing solution, its geometry and interlocking sequence, this section will provide additional information on the important complementary role of the antiprismatic folded plate geometry, and the detailed choices and compromises that were made for the prototypes in this chapter.

It was already briefly mentioned in the foreword (see page 4) and in section 4.3.1, that the antiprismatic shell geometry provides not only an efficient shape from a structural point of view, but also a bidirectionally folded surface geometry with only small dihedral angles (fold angles)  $\varphi$  between all plates. Figure 4.22a shows how the geometry of regular Antiprismatic Folded Plates can be described with only three parameters: The width  $w$  and height  $h$  of the folds determine the transversal fold angles  $\varphi_{trans} = \tan(w/h)$ . The additional cross-section angle  $\gamma$  determines the base length of the modules.  $L_{base} = \frac{\cot(\gamma)}{h} 2$ . The antiprismatic folded plate is now generated through the reflection of modules about the plane  $P$  between the high- and low points of two neighboring faces.

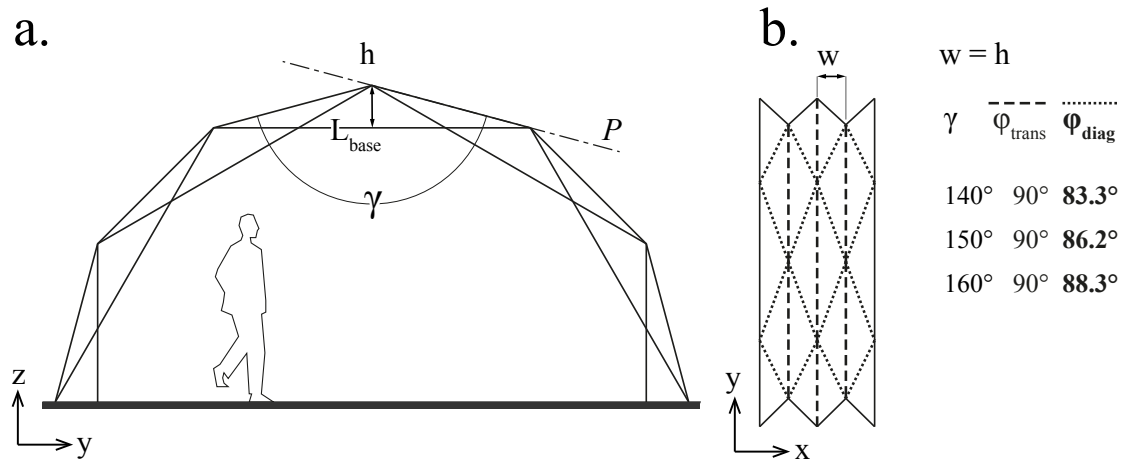


Figure 4.22 – Antiprismatic Folded Plate Geometry - a. Parameters, and b. Illustration of transversal and diagonal dihedral angles in top view. The table shows the resulting diagonal angles  $\varphi_{diag}$  for a configuration with  $w = h$ , for three different values of  $\gamma$

The now created diagonal dihedral angles  $\varphi_{diag}$  are illustrated in figure 4.22b. In the shown configuration, where  $w = h$ , all transversal dihedral angles<sup>60</sup> are 90°. The resulting diagonal angles are shown on the right side, for three variations of the cross-section angle  $\gamma = 140^\circ, 150^\circ$

<sup>59</sup>This additional section was not included in the original publication.

<sup>60</sup>the dihedral angles on edges which are parallel to the y-axis (Figure 4.22)



and  $160^\circ$ . The list shows that for a folded plate configuration with good transversal dihedral angles, from the point of view of joint fabrication, assembly and structural performance, the diagonal dihedral angles  $\varphi_{diag}$  will be only slightly smaller.<sup>61</sup>

These geometric rules apply both to regular Antiprismatic shells, as shown by [Huy72] and illustrated in figure 4.2a and 4.4, as well as to the doubly-curved irregular version introduced in section 4.5 of this chapter. While in regular configurations the cross-section angle  $\gamma$  is constant throughout the folded plate, the double-curved version obtains its double-curvature through different cross-section angles  $\gamma$ , segment lengths  $L_{base}$ , and fold height  $h$ . However, while the variations of the segment lengths are large, those of the fold height are minimal, which allows for a constant static height of the structure. The fold width was kept constant in the prototype in section 4.5.

A general disadvantage of the antiprismatic geometry lies in its restriction to curved surfaces: All vertices of a regular antiprismatic folded plate lie on a smooth cylindrical surface (see figure 4.23a). The folded geometry is created through the alternating connection of these points (illustrated in figure 4.3). If this topology is applied to a flat surface, it will also be completely flat, with a fold height  $h = 0$  and  $\gamma = \varphi_{trans} = \varphi_{diag} = 0^\circ$ . In consequence, the static height  $h$  of an antiprismatic folded plate is highly dependant on the surface curvature. This must be considered for architectural applications which may sometimes require a low shell curvature. One measure that can be taken, in order to counteract the loss of static height is an increase of the segment lengths  $L_{base}$ . This however will increase the size of components, which reduces the ease-of-handling and assembly and is typically also constrained by the maximum dimensions for transport and sometimes also fabrication.

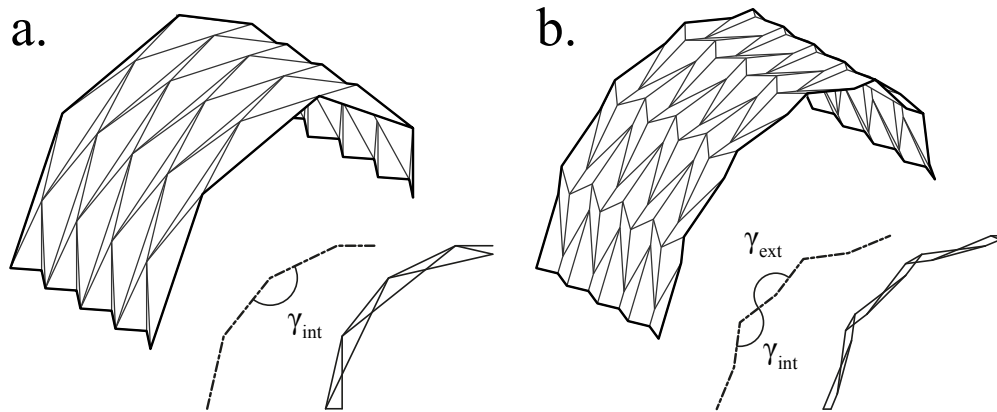


Figure 4.23 – Comparison of an Antiprismatic (a.) and Miura-Ori (b.) Cylindrical Shell, designed by [BW06], including cross-section schematics and projected cross-sections.

An alternative type of folded plate, which equally satisfies the joints fabrication and assembly constraints, but is not restricted to curved surfaces, is presented by the Miura-Ori paper-fold

<sup>61</sup> the diagonal dihedral angle of an Antiprismatic configuration through  $w$ ,  $h$  and  $\gamma$  is found on a plane through the mid-point of  $L_{base}$ , which is normal to one of the diagonal edges.

## Chapter 4. Interlocking Folded Plate - Integrated Mechanical Attachment for Structural Timber Panels

---

geometry (Figure 4.23b). It was briefly introduced as an alternative bidirectionally folded topology in the foreword of this chapter, and it was also previously used for the first timber folded plate prototype designed and built by H. Buri in 2006 [BW06] and studied by [Hah09]. The vertices of the Miura-Ori type manifold shown in figure 4.23b do not lie on one common cylindrical surface, but on two concentric ones with different radii. In contrast to the Antiprismatic Folded Plate, which has only interior cross-section angles  $\gamma$ , there are interior angles  $\gamma_{int}$  and exterior angles  $\gamma_{ext}$  in the cross section of curved Miura-Ori Folded Plates. It results from the curvature that the angles  $\gamma_{ext}$  are larger than  $\gamma_{int}$ , but the principle also works for flat surfaces, where  $\gamma_{int} = \gamma_{ext}$ .

The main disadvantage of this geometry is visible on the lower right side of Figure 4.23b: The projected cross-section of the Miura-Ori Version from [BW06] shows kinks, away from the structurally ideal smooth cylindrical shell surface. In contrast to this, the comparable Antiprismatic version shown in figure 4.23a shows a much smoother cross-section. However, the kinks in 4.23b are not necessarily due to the geometrical principle, but rather to the parameters used in the configuration of [BW06]. A relatively smooth cross-section can be achieved by collapsing all transversal short edges in the manifold. This however will result in problematic angles  $\lambda$  (see section Transition Segments in this chapter).

### Edge-to-edge connectivity

It is the intention of this thesis to use integral connections not only for their benefits when it comes to precise assembly and efficient production of timber folded plates, but also for the rigid connection between plates. The determination of the detailed mechanical behaviour of the joint geometry is not part of this thesis, but a parallel, ongoing investigation of this behaviour is being carried out at the Timber Construction laboratory IBOIS. A first analysis of the joint rigidity and stiffness has been performed in a series of flexural test with dovetail-jointed box girders built from laminated veneer lumber. [RRHW15] The joint's resistance to moments, which has been discussed and illustrated in figure 4.9, has been the subject of a second study. [RGW15] The aim of these publications is to determine the exact behaviour of the joints in relation to various interrelated geometrical parameters. The results will be used to propose simplified models for the calculation and dimensioning of integral joints for timber folded plates.

It is already clear from these investigations, that the integral joints generally demonstrate a so-called *semi-rigid* mechanical behaviour, similar to other state-of-the-art connections for the edgewise jointing of timber plates, such as screws or other metal fasteners. This means that the joints are not completely rigid and stiff, instead they introduce a certain weakness in a structure. This weakness must be counteracted primarily through a sufficient dimensioning of the joint, but it is also being influenced by the geometry and topology of a folded plate structure.

Figure 4.24a shows the topology of a regular antiprismatic folded plate. The diagram below

shows the edge-to-edge connections between the faces: While all faces are connected in the horizontal direction, only every second face connects to its vertical neighbor. Figure 4.24b shows the same folding pattern, only additional straight-extruded segments (folded in one direction) have been introduced, changing the faces from triangles to quadrilaterals and the manifold's valence from 6 to 4. The diagram below shows that this modification also changes the edge-to-edge connectivity of the faces: Now all faces connect to their horizontal and vertical neighboring faces. Considering the semi-rigid behaviour of the connections, this improved connectivity between the plates presents an effective improvement of the folded plate's overall structural performance.

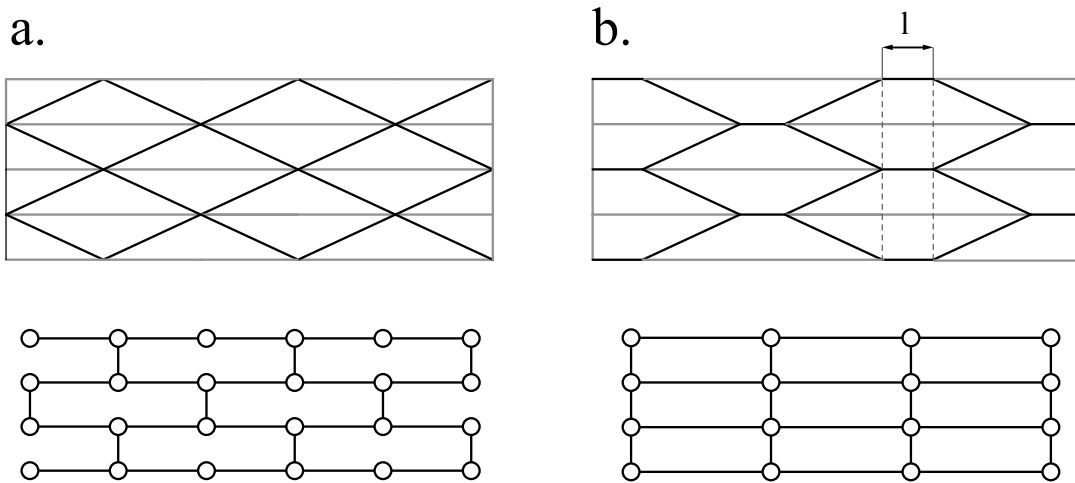


Figure 4.24 – Edge-to-edge connectivity between the faces of a regular Antiprismatic Folded Plate (a.) and a quadrilateral version with additional straight-extruded segments (b.).

### Nejiri Arigata Joint Geometry

In section 4.3, it was mentioned that the diagonal assembly of plate-shaped timber elements with 1DOF joints is known from Japanese Cabinetmaking joints. This technique is essential for the out-of-plane 1DOF assembly of panels presented in this chapter. This section will explain the origin and the geometry of the Japanese joints, as well as the geometric principle that was derived from this joint. Nejiri Arigata Joints have often been used for the assembly of donation boxes, which are exhibited in the Japanese Shinto Shrines<sup>62</sup>. Numerous geometrical variations of this type of joint are known, mostly for decorative purposes. An overview of these joints is provided in [Tet07].

Figure 4.25 shows a *Nejiri Arigata Joint* on the right side, compared to a dovetail joint on the left side. The projected cross-section profile of the pins illustrates the different directions of assembly  $\vec{v}$  for the two joints. The dovetail joint (Figure 4.25a) is being assembled along a vector that lies on the plane of the right plate, perpendicular to the edge. During the assembly,

<sup>62</sup>a well known example is exhibited in front of the Fukuchizan Shuzenji Temple

## Chapter 4. Interlocking Folded Plate - Integrated Mechanical Attachment for Structural Timber Panels

there are two sets of surfaces in contact: The faces *along* the edge and the faces *across* the edge (illustrated in figure 4.25).

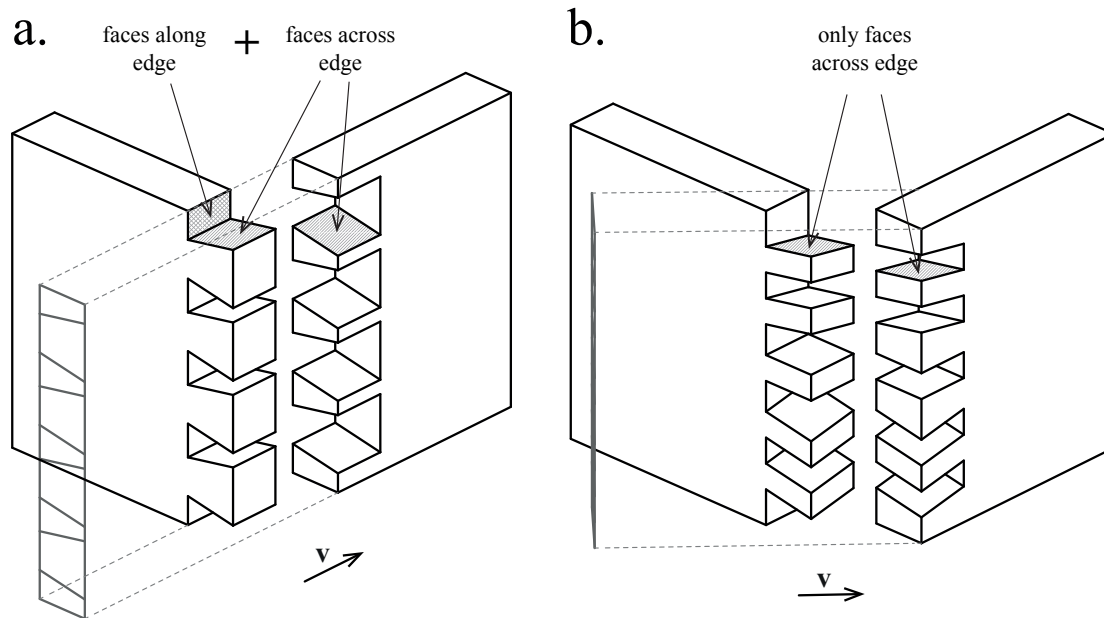


Figure 4.25 – European Dovetail joint geometry (a.), compared to a Nejiri Arigata joint (b.)

The Nejiri Arigata Joint however is being assembled along a vector that does not lie on either one of the two plates. Instead, the assembly vector of these Japanese joints is the exterior bisector of the dihedral angle between the plates. As a consequence of this, only the faces across the edge are in contact during the assembly of these joints. These faces are rotated at different angles, but about a set of lines which are parallel to the assembly direction. The other surfaces along the edge will only be in contact when the joint is fully assembled. However, although the Nejiri Arigata Joint has only the faces across its edge in contact during the assembly, it is still a connection with only one degree of freedom. This is possible only through the shape of the pins, which is different from the the shape of the pins on a dovetail joint. If the pins on the diagonally assembled joint in figure 4.25b were shaped like the dovetails in figure 4.25a, it would result in a joint where none of the faces would be in contact during the assembly.

The reason why the Nejiri Arigata Joint can be assembled along directions that do not lie on either one of the two connected plates is that it uses *multiple* pins to block all relative movements, expect for the assembly direction. The dovetail joint illustrated in figure 4.25a needs only one single pin to become a *prismatic* connection. The prism is shaped between two faces across the edge, and two faces along the edge. The Nejiri Arigata Joint however needs at least two pins to block all movements expect for the assembly direction. Also this works only with two types of quadrilateral-based cross-section shapes: While the pins of a dovetail joint are *Isocles Trapezoids* (Figure 4.26b) in their cross-section, the Nejiri Arigata

Joint uses at least two mirrored *Parallelograms* (Figure 4.26f). Each of these pins creates a planar (3-degree-of-freedom) joint, which could still rotate or translate about the plane of the side faces across the jointed edge. Together however, two of these 3DOF-pins will create a joint with only one remaining degree of freedom.

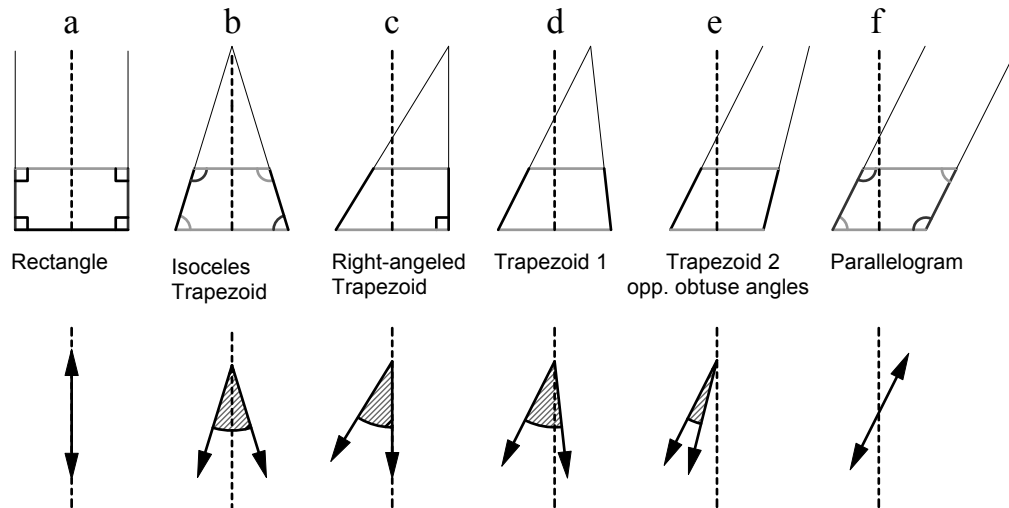


Figure 4.26 – Quadrilateral Pin Cross-section Shapes for Tab-and-Slot Joints - While European dovetail-joints use Isosceles Trapezoid shaped pins (b), Japanese Nejiri Arigata Joints use Parallelogram (e) or Trapezoid-with-opposite-obtuse-angle shaped pins (f).

Some variations of the Nejiri Arigata Joints are using a second possible pin-cross-section geometry: Trapezoids with opposite obtuse angles (Figure 4.26e) work in the same way like the parallelograms do, provided that there is no intersection between their two 2D ranges of assembly vectors (Figure 4.26, bottom diagrams). For all other pin shapes in figure 4.26, there will always be an intersection between these ranges, which is why they can not be used for tab-and-slot joints with an assembly direction that does not lie on either one of the two plates.

### Assembly Vector Rotation Windows

In Section 4.3.1, it was described that the geometrical principle of the previously described Nejiri Arigata Joints can be used not only for the assembly along the external bisector of the dihedral angle, but for a 3-dimensional, pyramid-shaped *Rotation Window*  $S_i$ , which is defined by two assembly- and fabrication constrained maximum rotations of the assembly vector  $\vec{v}$ :  $\theta_{1,max}$  and  $\theta_{2,max}$ . In a folded plate assembly, these rotation windows are generated for every edge and then overlaid (on the pyramid tips) to check for intersections. If an intersection is found, the two corresponding edges can be jointed simultaneously. This additional section will provide detailed information about the maximum rotations  $\theta_{1,max}$  and  $\theta_{2,max}$ , their interrelation with each other and other parameters, the intersection of these maximum ranges, as well as the algorithm that was used for the automatic processing.

## Chapter 4. Interlocking Folded Plate - Integrated Mechanical Attachment for Structural Timber Panels

Figure 4.27 illustrates how  $\theta_{1,max}$  is obtained from the dihedral angle  $\varphi$  between the plates: Single-degree-of-freedom tab-and-slot joints, such as dovetail-joints or nejiri-arigata joints, can only be assembled sideways, within the range illustrated in figure 4.27. Showing three joints with dihedral angles of  $50^\circ$ ,  $90^\circ$  and  $130^\circ$ , the figure also visualizes that  $\theta_{1,max}$  will be large for acute dihedral angles and small for obtuse dihedral angles.

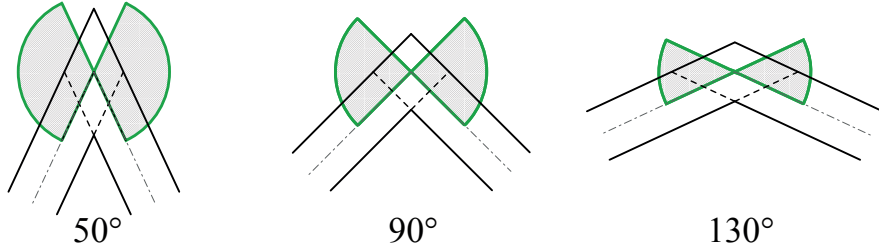


Figure 4.27 – 2D Rotation of Assembly Vector

Figure 4.28 shows an important consequence of obtuse dihedral angles and the resulting small values for  $\theta_{1,max}$ . When multiple edges must be jointed simultaneously (for example  $E_1$  and  $E_2$  in fig 4.28), an intersection must be found between their possible assembly-vector rotations. The possibility of finding a common intersection is much reduced when any obtuse fold angles are involved.

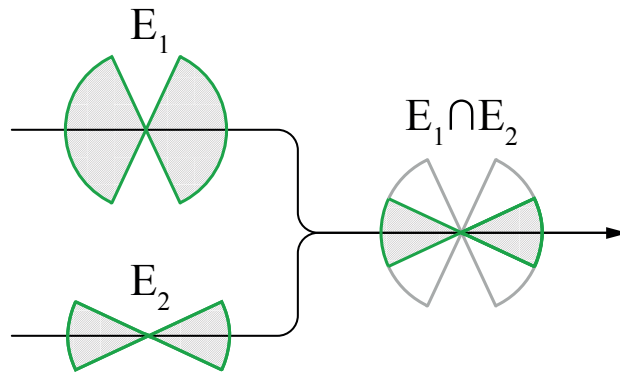


Figure 4.28 – Simultaneous Assembly

Finally, the 3-dimensional range of possible assembly-vector rotations (a pyramid spanned by four vectors) is defined by a second angle,  $\theta_{2,max}$ . It was explained in 4.3.1 that a global value of  $\pm 20^\circ$  was used for the prototypes. This was a sufficient value for the prototypes in this chapter, because intersections were found between all windows that represented simultaneously assembled edges. The exact value for  $\theta_{2,max}$  can not be obtained easily because of interrelations between multiple parameters, as illustrated in figure 4.29. These parameters include two fixed values, the dihedral angle  $\varphi$  and the maximum tool rotation  $\beta_{max}$ , as well as two variable parameters, the previously mentioned rotation  $\theta_1$  and the alternating rotation of the joints side faces across the edge  $\theta_3$ . For example, a larger value for  $\theta_3$  will result in a

smaller possible range for  $\theta_{2,max}$ .<sup>63</sup>

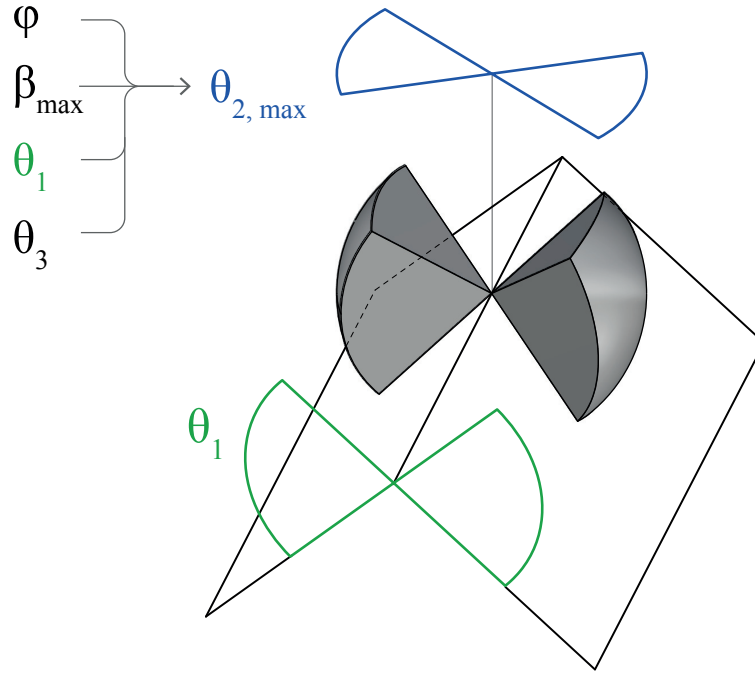


Figure 4.29 – 3-dimensional Rotation Window

The pseudo-code algorithm 1 shows how the rotation windows were generated with a Rhino-Python Script. It receives a simplified, fixed value for  $\theta_{2,max}$  as an input, and iterates over the edges of a polygon mesh. First, the script checks for naked edges with only one neighboring face, since the next step will require two neighboring faces. Then, the two edge vertices and the normals of the two neighboring faces are obtained from a previously generated list. In the next step, two vectors  $c\vec{p}_1$  and  $c\vec{p}_0$  on the neighboring faces, perpendicular to the edge are obtained through a cross-product between the edge vector and the face normals.<sup>64</sup> Then the dihedral angle  $\varphi$  is calculated, as well as its bisector  $\vec{n}_2$ . Now the two vectors  $c\vec{p}_1$  and  $c\vec{p}_0$  are rotated about  $\vec{n}_2$  at the angle  $\pm\theta_{2,max}$ . The resulting four vectors span the rotation window that defines all possible rotations of the joints assembly vector.

For the prototypes presented in this chapter, the pyramid-shaped windows were generated automatically, using the algorithm 1, however they were checked for intersections only manually. The principle is illustrated in figure 4.30, where three edges  $E_1$ ,  $E_2$  and  $E_3$  are checked for a possible simultaneous assembly. The resulting rotation windows  $S_1$ ,  $S_2$  and  $S_3$  are then overlaid at the pyramid tips, showing the common intersection (grey-colored solid).

A manual check for intersections may be feasible for smaller assemblies, especially when

<sup>63</sup>for more information on the interrelations between these parameters, see page 155. An analysis in Maple is provided by [Mat14]

<sup>64</sup>the reverse vectors are obtained to create a mirrored rotation window. This method simplifies the comparison of multiple windows in a poly mesh, because it is independent from the directions of the edges

## Chapter 4. Interlocking Folded Plate - Integrated Mechanical Attachment for Structural Timber Panels

---

### Algorithm 1 Define Rotation Window per Edge

---

```

1: function ROTATIONWINDOWS(Mesh,  $\theta_{2,max}$ )                                ▷ input Mesh,  $\theta_{2,max}$ 
2:   _mTEs ← Mesh.TopologyEdges                                           ▷ edge list
3:   _mFNs ← Mesh.FaceNormals                                             ▷ normals list
4:   for  $i$  in _mTEs do                                                    ▷ iterate over topology edges
5:     get _mTEs.ConnectedFaceIndices( $i$ )
6:     if ConnectedFaceIndices  $\neq$  1: then                                  ▷ skip naked edges
7:        $EdgeLine \leftarrow$  _mTEs.EdgeLine( $i$ )                             ▷ get vertex points
8:        $p_0 \leftarrow$  EdgeLine.PointAt(0)
9:        $p_1 \leftarrow$  EdgeLine.PointAt(1)
10:       $n_0 \leftarrow$  _mFNs[ConnectedFaceIndices[0]]                      ▷ get face normals
11:       $n_1 \leftarrow$  _mFNs[ConnectedFaceIndices[1]]
12:       $cp_0 \leftarrow n_0 \times (p_0 - p_1)$                                 ▷ perp to edge (panel 0)
13:       $cp_1 \leftarrow n_1 \times (p_1 - p_0)$                                 ▷ perp to edge (panel 1)
14:       $cp_{1c} \leftarrow n_1 \times (p_0 - p_1)$                             ▷ perp to edge (panel 1 reverse)
15:       $cp_{0c} \leftarrow n_0 \times (p_1 - p_0)$                             ▷ perp to edge (panel 0 reverse)
16:       $\varphi \leftarrow$  VectorAngle( $cp_0, cp_1$ )                             ▷ dihedral angle
17:      if  $\varphi \leq 90^\circ - \beta$  and  $\varphi \geq 90^\circ + \beta$  and  $\varphi \neq 180^\circ$  then  ▷ fabrication constraints
18:         $n_2 \leftarrow$  Bisector( $n_0, n_1$ )                                ▷ dihedral angle bisector
19:         $n_2$ .Unitize()
20:         $cp_0$ .Rotate( $\frac{\theta_{2,max}}{2}, n_2$ )                                     ▷ rotation window boundary (1)
21:         $cp_1$ .Rotate( $\frac{\theta_{2,max}}{2}, n_2$ )                                     ▷ rotation window boundary (2)
22:         $cp_{0c}$ .Rotate( $(\frac{\theta_{2,max}}{2}) * -1, n_2$ )                            ▷ rotation window boundary (3)
23:         $cp_{1c}$ .Rotate( $(\frac{\theta_{2,max}}{2}) * -1, n_2$ )                            ▷ rotation window boundary (4)
24:      end if
25:    end if
26:  end for
27: end function

```

---



the dihedral angles are relatively small and large intersections are found. An algorithmic implementation is missing for this step. Figure 4.29 shows a possible approach, intersecting a BREP-object representing the rotation window with a mesh sphere. The resulting intersection could be mapped into a 2D space and compared with other edges.

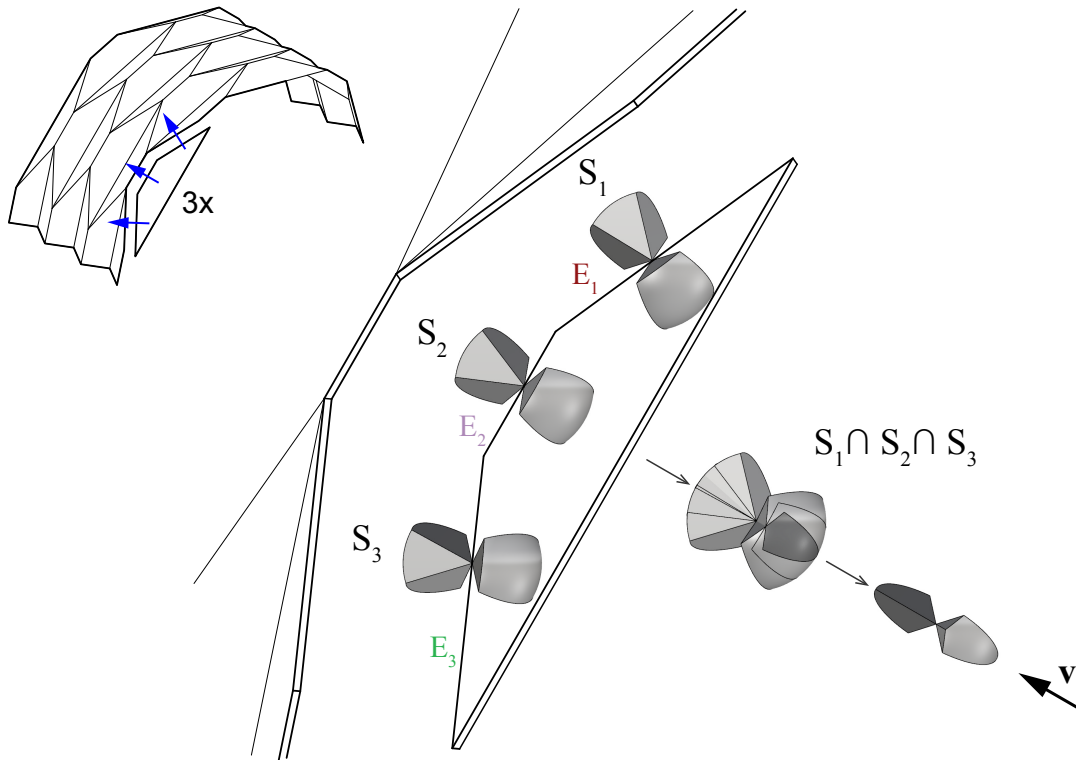


Figure 4.30 – Common assembly rotation window for three edges  $E_1$ ,  $E_2$  and  $E_3$ . The possible assembly vectors are visualized as Rotation Window solids  $S_1$ ,  $S_2$  and  $S_3$ .

### Joint Fabrication Algorithm

The doubly-curved shell prototype presented in this chapter takes advantage of the automatic processing of information through algorithms. provided a parametric component and joint geometry, including the relevant constraints, large sets of parts of the same type, but each with an individual geometry can be processed automatically.<sup>65</sup> This allows for the design of irregular shapes which cannot be realized through manual drawing or manual machine programming respectively.

This section will provide detailed information on the algorithms which were used in this chapter. The figure 4.31 gives an overview over three important steps in one drawing, illustrated in a sequence from the right to the left side of the figure: 1. the generation of the joint geometry, which was introduced previously in figure 4.7, 2. the automatic generation of the toolpath

<sup>65</sup>In other industry sectors the principle is often referred to as *Mass Customization*

## Chapter 4. Interlocking Folded Plate - Integrated Mechanical Attachment for Structural Timber Panels

for the 5-axis CNC router, and 3. the resulting geometry of the part, which however is not generated by any of the algorithms.

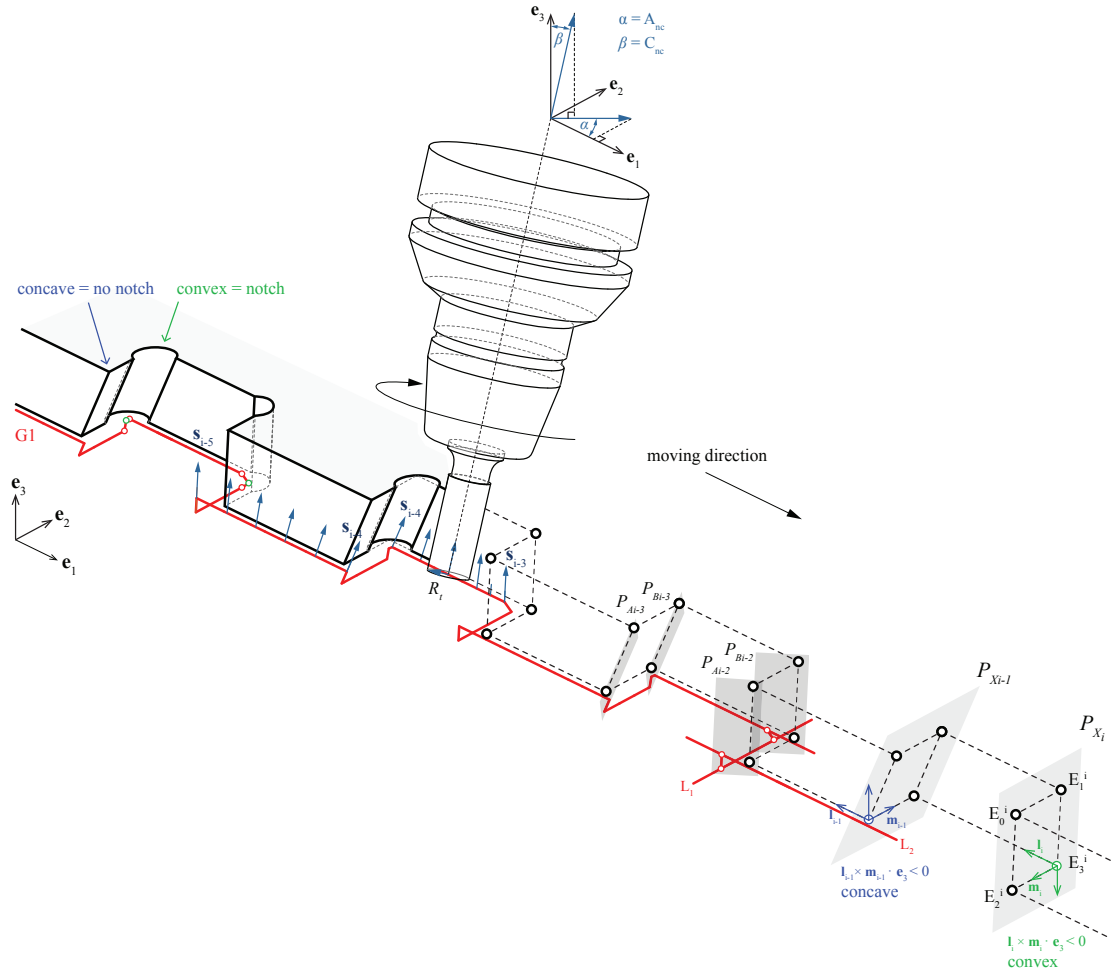


Figure 4.31 – Algorithmic generation of the joint geometry and the machine code - The figure shows multiple algorithms used in this chapter in one illustration: From the right bottom to the left side, it starts with the generation of the joint geometry, followed by the tool-path generation and the final part geometry. At the top, the conversion of the tool vector into the cardan rotations of the CNC router is shown.

A first algorithm is used for the generation of the joint geometry. It will generate the four sets of Points  $E_0^i, E_1^i, E_2^i, E_3^i$  from a polygon mesh edge, as explained in figure 4.7<sup>67</sup>. Then, two polylines are generated, connecting alternating segments between the points:  $E_0^i, E_1^i, E_1^{i+1}, E_0^{i+1}$  for the top of the panel and  $E_2^i, E_3^i, E_3^{i+1}, E_2^{i+1}$  for the bottom of the panel. These polylines define the geometry of the dovetail joint, which can be obtained through a loft-surface between these two polylines.

<sup>66</sup> see the G-Code sample in listing 4.1

<sup>67</sup> for the automatic joint generation on polygon meshes, see lines 1-11 in the algorithm 1

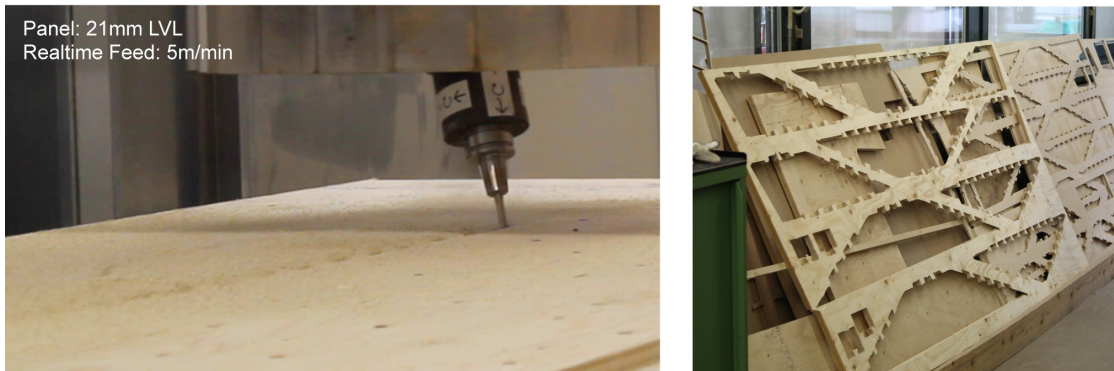


Figure 4.32 – Joint Fabrication - The left image shows the fabrication of the parts with a MAKAMM7s 5-axis CNC router, operating with a 12mm-diameter shank-type nesting cutter, at a target feed rate of 5m per minute and a tool rotation of 16.000 revolutions per minute.<sup>66</sup> The right image shows the nesting of the components on a waste part. The left bottom of this image also shows small key parts, with one dovetail joint each. These parts were used for the calibration of the machine. A certain tool wear and variations in the thickness of the panels could be partially compensated through adaptations of the tool offset parameter.

For the joint fabrication however a 3-dimensional surface is not required. The machine code will rather be generated through the two polylines provided by the joint generation algorithm. The fabrication algorithm will iterate over the corresponding vertices of the two polylines. The correct alignment of the start-points of the two curves is important, because the tool orientation vectors  $n^i$  are obtained through subtraction of the upper point from the corresponding lower point.<sup>68</sup> For the polyline segments along the axis  $e_2$  of the figures coordinate system, the orientation of the tool vector is the same for the start and the end point of the segment. However for the segments along axis  $e_1$ , the vectors are different due to the dovetail flank rotations. From the machining point of view, this means that the tool has to simultaneously translate and rotate during this cut, which is called *Simultaneous Machining*.<sup>6970</sup> A smooth and synchronized transition between the two vectors is assured through the sub-division of these segments (by the same number for the top and bottom segment).

in the previous paragraph, all tool-rotation vectors were obtained directly through the vertices of the two polylines of the joint. Next, the corresponding tool center points  $TCP_i$  will be generated as an offset of the vertices on the lower polyline. This offset must be made due to the radius  $r_{tool}$  of the rotating tool of the CNC router. For each segment of the dovetail joint, the offset must always be normal to the vertical joint face. However, due to the different inclinations of these faces, the offset tool center points will not lie on the same horizontal

<sup>68</sup>the conversion of these vectors into the Euler angle rotations required by the CNC machine are explained in the algorithm 2

<sup>69</sup>for 5-axis simultaneous machining, see [Wei05, p.505]

<sup>70</sup>An early application of 5-axis simultaneous machining for the fabrication of furniture was presented by the chair *Flankenschnittstuhl F/01* in 2008. [Sch09, p.211-213]

## Chapter 4. Interlocking Folded Plate - Integrated Mechanical Attachment for Structural Timber Panels

---

plane in the coordinate system  $e_1, e_2, e_3$ . Figure 4.31 shows a solution for this problem: the red lines  $L_1$  and  $L_2$  have been offset normal to their corresponding vertical joint faces. since these lines do not intersect, an additional intersection plane  $P_{Ai-2}$  is generated. This intersection plane is obtained from the bisector of the normals of the two neighboring vertical planes. Now, the two lines  $L_1$  and  $L_2$  are intersected with the intersection plane. The resulting two intersection points provide a *transition line*, on which the tool will transit from one cut to the next.

### Notches at Convex Corners

Another feature that must be added automatically are the *notches* on the interior corners of the dovetail joint. Since the CNC router will cut the parts with a rotating tool, sharp interior corners which are found on traditional dovetail joints from cabinetmaking cannot be cut. At the same time, sharp notches would not be beneficial for the load bearing behaviour of the joints. A stress concentration would occur at such sharp corners<sup>71</sup>. However, the rounded interior corners that result from the regular offset toolpath do not allow for the assembly of the parts. A solution for this problem are additional notches, which are cut into the corners as far as necessary for the assembly of the parts.

The radius of the notches is equal to the radius  $r_{tool}$  which is typically determined by the density and thickness of the material, as well as the machine's spindle parameters. However there are two possible geometries for such cuts, both of which were applied in the prototypes in this thesis: Option 1 is an extension of the cuts on the joint's vertical side faces (extension of the poyline segments parallel to the axis  $e_2$ , illustrated in figure 4.31). This notch geometry has been applied to the joints of the curved folded structure in chapter 3. The main advantage of this method is that the contact surface of the joint's vertical side faces will not be reduced. The technique allows to make a per-interior-edge choice of positioning the notch on either one of the two neighboring faces. Option 2 are *tangential notches*, which are illustrated on the left side of figure 4.31. This type of notch is the smallest possible notch for a given tool radius, however some contact surface will be lost on both neighboring faces. The geometry of the tangential notches is obtained as follows: A bisector-vector is generated from the normals of the two neighboring faces. This vector is then unitized and multiplied by  $r_{tool}$ . Now, the center-axis of the cylindrical notch can be obtained from two points: The first point is found through a translation of one of the joints interior corner points along the previously generated vector, the second point is found through a translation of the first point along the corresponding tool vector. Finally the additional tool center point on this tangential notch cylinder axis is determined, depending on the corresponding tool inclination.<sup>72</sup>

Both types of the before mentioned notches are only required on the joints interior edges. These points are being recognized automatically by the fabrication algorithm illustrated in

---

<sup>71</sup>see Notch Stress Reduction (Kerbspannung)

<sup>72</sup>The tool-center-point of tangential notches must extend below the machining table surface, unless the tool is oriented normal to the table.

figure 4.31: While the algorithm iterates over the vertices of the dovetail joints lower polyline ( $E_2^i, E_3^i, E_3^{i+1}, E_2^{i+1} \dots$ ), interior corners are identified through a cross-product of a forward looking vector and a backward-looking vector. A positive cross-product indicates an interior corner. The result will depend on the orientation of the polyline, however this algorithm was only applied to closed polylines (representing the quad-based components of the folded plate), with a constant clockwise orientation.<sup>73</sup>

In the previous steps of this section, the information required for the joint fabrication was obtained: A list of tool center points  $TCP$ , including sub-division points for segments with simultaneous translations and rotations, notch points and the tool orientation vectors  $n$ . However, the 5-axis CNC router requires G-Code<sup>74</sup> for its operation, in which the orientation of the tool is described through two Euler Angles  $A$ , for the primary rotation about the world Z-axis (yaw-angle)<sup>75</sup> and  $B$ , for the secondary rotation about the world X-axis (pitch-angle)<sup>76</sup>.

### Conversion from tool vector to machine axis rotations

There are different methods for this conversion, depending on the fabrication technique. This algorithm requires 5-axis *simultaneous machining*, where the two machine axis  $A$  and  $B$  rotate continuously during the cutting. However, CNC 5-axis routers can not rotate endlessly around any of their axes. In the case of the MAKAM7s router that was used for the prototypes in this thesis, the primary  $A$ -axis is constrained to a continuous movement of  $\pm 270^\circ$ . Once the physical endpoint is reached (e.g. moving from  $A = 0^\circ$  to  $A = 360^\circ$  clockwise), the router will stop at  $A = 270^\circ$ . In order to complete the circle, it must rotate a full  $360^\circ$  counterclockwise, to arrive  $A = -90^\circ$ . Only now, the cut can be finished moving from  $A = -90^\circ$  to  $A = 0^\circ$ . The reverse-rotation that was necessary in this example, must be performed away from the workpiece (above). Such situations must be foreseen by the algorithm: The tool must be

<sup>73</sup>the clockwise rotation, in combination with typical clockwise tool geometries of the cutters that were used, will result in so-called *regular cutting*, as opposed to the inverted *climb cutting*. Due to a different force diagram, the two cutting directions will result in different qualities of the machines surfaces.[Koc64]

<sup>74</sup>for more information see ISO standard number ISO6983

<sup>75</sup>the ISO6983-letter for this rotation is C, but some routers may use different notations

<sup>76</sup>the ISO6983-letter for this rotation is A, but some routers may use different notations

---

#### Algorithm 2 Conversion from tool vector to machine axis rotations

---

1: <b>function</b> __AB180( $n$ )	▷ input tool orientation vector
2: $a_1 \leftarrow \text{atan2}(n[0], n[1])$	▷ arctangent function with signs
3:   convert $a_1$ to degrees	
4: $A \leftarrow \text{round}(a_1) * -1$	▷ output primary $A$ -axis rotation (yaw)
5: $b_1 \leftarrow \sqrt{n[0] * n[0] + n[1] * n[1]}$	
6: $b_2 \leftarrow \text{atan2}(b_1, n[2])$	▷ arctangent function with signs
7:   convert $b_2$ to degrees	
8: $B \leftarrow \text{round}(b_2) * -1$	▷ output secondary $B$ -axis rotation (pitch)
9: <b>end function</b>	

---

## Chapter 4. Interlocking Folded Plate - Integrated Mechanical Attachment for Structural Timber Panels

retreated along its orientation vector  $n$ , and then, after the routers reverse-rotation, returned to its previous position, along the same orientation axis.

The fabrication algorithm used throughout this thesis (Algorithm 2) uses the `atan2()` arctangent function with two arguments, provided by python's math module, which is a common method for the conversion of Euler-angles in algorithms. It will divide the primary, horizontal rotation (machine- $A$ -axis) into two circle segments of 0 to  $180^\circ$  (for  $n.Y > 0$ ), and 0 to  $-180^\circ$  (for  $n.Y < 0$ ). Together with a  $B$ -axis rotation of 0 to  $-90^\circ$ , a conversion is possible for any tool orientation vector  $n$  into the Euler Angles  $A$  and  $B$ .

The algorithm watches out for the endpoint at  $A = 180^\circ$ . A continuous movement that crosses this boundary, will interrupted before the endpoint is reached. Then, the tool will be retreated, reverse-rotated and then returned to finish the cut, as described above.<sup>77</sup> A G-code example, where an endpoint is reached, is shown in listing 4.1, lines 18-22.

### G-Code File Generation

With the previously generated tool center points and the corresponding Euler Angle rotations, a G-code file (Listing 4.1<sup>78</sup>) is being generated by the algorithm. After a set of initial preparative commands (Figure 4.1, lines 1-10) for the file name (P8766268), tool selection (Tool 27), startposition(A:0, B:0), start of the machine (M3 - clockwise), spindle speed (S=13.000 rpm) and workpiece coordinate system (G55), separate lines are added for each tool center point the machine should move to.

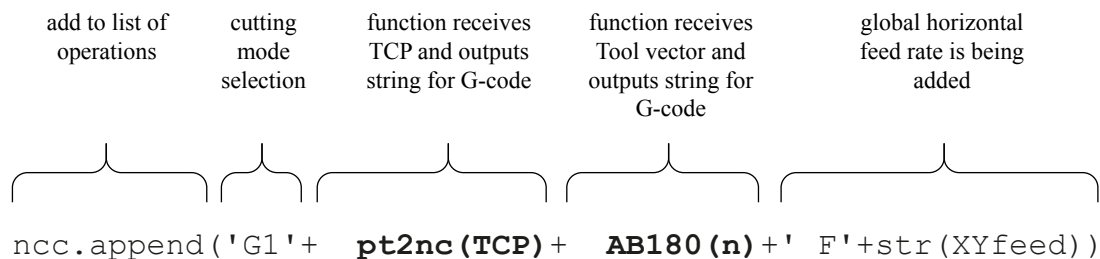


Figure 4.33 – Python script assembly of a line of G-Code during cutting.

Figure 4.33 shows how the lines are assembled and appended to a list. First, a mode of movement is selected at the beginning of the line. This is either G1, for linear cutting, or G0 for rapid positioning outside of the workpiece, followed by the two main geometry parameters.

<sup>77</sup>Note that the problem with endpoints described in this paragraph applies only to *5-axis simultaneous machining*, where the tool simultaneously rotates and translates. For applications where a tool translates with a permanent rotation, the fabrication process can be carried out faster with a tool vector conversion in four horizontal quadrants, where the  $B$ -axis sign is inverted. This avoids the otherwise necessary, time-consuming  $360^\circ$ -rotation of the  $A$ -Axis.

<sup>78</sup>The code sample shows the fabrication of the prototype presented in section 4.5. The part  $F_{24}$  is being cut on sheet number 12. With 10 parts per sheet, there are about 1.700 lines of 5-axis G-Code per part, which underlines the necessity of automatic G-Code Generation

The function `__pt2nc(TCP)` converts the cartesian coordinates of each tool center point into a text string (X,Y,Z), and the function `__AB180(n)` converts the tool vectors  $n$  into a text string with the Euler angles (see 4.31) (A,B). Finally, a linear *feed rate*, in millimeter per minute, is added to each movement. A distinction is made between regular, horizontal cutting movements, for which a global value (XYfeed) is used, and vertical cutting, for which a global reduced value (Zfeed) is used. Finally certain *comments* (Listing 4.1, in parenthesis / blue color) for better readability are being inserted automatically by the algorithm, highlighting events such as endpoints (lines 18 to 22), and providing information about the file origin and content (lines 2 and 3).

Listing 4.1 – G-Code Sample for Maka mm7s CNC Router

```

1 P8766268
2 (***** 17682 commands to process *****)
3 (***** masterfile y:/P8766268_5x_jointing_2014-3-6_11-35-13 *****)
4 N10 G47
5 N20 T27 M6
6 N30 G47 A0 B0 F8000
7 N40 S13000 M3
8 N50 G49 G55
9 N60 P4010:0 (lower aspiration)
10 N70 (dual infeed mode)
11 N80 G0 X0 Y0 Z70 (startpos)
12 N90 G0 X945.959 Y1530.901 Z66.308 A109.306 B-40.447 (safe)
13 N100 G1 X993.829 Y1547.671 Z6.808 A109.306 B-40.447 F5000
14 N110 G1 X997.514 Y1539.217 Z6.808 A112.656 B-40.373 F5000
15 ...
16 N260 G1 X1034.094 Y1464.454 Z8.753 A160.451 B-26.853 F5000
17 N270 G1 X1035.013 Y1465.004 Z8.753 A169.049 B-23.399 F5000
18 N280 (** turn **)
19 N290 G0 X1033.574 Y1457.57 Z26.253 A169.049 B-23.399 (retreat)
20 N300 G0 A-179.229 B-20.435 (new ab)
21 N310 G1 X1035.013 Y1465.004 Z8.753 A-179.229 B-20.435 F1500 (back)
22 N320 (** end turn **)
23 N330 G1 X1035.932 Y1465.555 Z8.753 A-179.229 B-20.435 F5000
24 N340 G1 X1036.85 Y1466.106 Z8.753 A-163.936 B-18.433 F5000
25 ...
26 N176800 G1 X287.948 Y495.574 Z-3.692 A-109.618 B-40.436 F5000
27 N176810 G1 X291.586 Y503.919 Z-3.692 A-110.418 B-40.412 F5000
28 N176820 G0 X347.44 Y483.127 Z66.308 (safety)
29 N176830 G0 X0 Y3700 Z70 (endpos)
30 N176840 M5
31 N176850 M30
32 #

```

### Miter-jointed Transition Segments

Tab-and-slot-joints such as Finger-joints, Dovetail-joints, Nejiri-Arigata-joints or the variations used for the prototypes in this chapter, interlock two neighbouring plates with one another through their common intersection solid. This space is being split up between the plates in an alternating manner. For example, every even segment is assigned to plate A and every odd segment is assigned to plate B.

In a polygon-mesh based assembly of multiple plates, such as the timber folded plates presented in this chapter, there is a conflict around the vertices: The intersection solids of two neighboring plates may partially intersect with those of other edges which are connected to the same vertex. Figure 4.34a illustrates the problem on a set of parts from the doubly-curved folded plate prototype: The two edges  $E_{188}$  and  $E_{174}$  are connected to the same vertex. Due to the acute angle  $\lambda$  between these edges, the intersection solids between the two adjacent plates  $F_{34}/F_{35}$  will collide with those of the plates  $F_{35}/F_{17}$ , when they approach the common vertex.

In the present prototypes, this conflict has been solved through miter-jointed start and end segments for all edges. A global length of  $\frac{L_{edge}}{10}$  has been applied for all of these segments, where the intersection solid between the two neighboring plates is being divided equally, at the bisector of their dihedral angle. The necessary length of these *transition segments* is dependent on the minimum angle  $\lambda_{min}$  between neighboring edges. The lower this angle, the longer transition segments are required to avoid conflicts. This compromise however is directly linked to the rotation windows of the joints: In order to join multiple edges simultaneously, as it is necessary for the edges  $E_{187}$  and  $E_{188}$  in figure 4.34a, the angle  $\lambda$  between these two edges must be obtuse, otherwise there will be no intersection found between their two rotation windows<sup>79</sup>. Therefore, the configuration shown in figure 4.34a presents a compromise between these requirements.

The problem that results from these transition segments is that in a certain proximity to the vertices of the mesh, there is no connection between the plates, because the geometrical interlock is only created through the tab-and-slot joints. Figure 4.34b shows the resulting behaviour under loads.<sup>80</sup> Larger deformations will occur in these unconnected regions, while the tab-and-slot-joints are still fully intact.

A relatively simple solution for the improvement of this problem could be implemented by an adaptive length of the transition segments: Figure 4.34a shows that there are several unnecessary long transition segments, which is due to the global value for their length. For example, the transition segments on the edges  $E_{187}$ ,  $E_{188}$  and  $E_{193}$ , towards their shared vertex, could be shortened, as long as the segment on edge  $E_{174}$  remains at its length of  $\frac{L_{edge}}{10}$ .

---

<sup>79</sup>for Details see Section 4.3.1

<sup>80</sup>the photo was taken during the load test of the doubly-curved folded plate prototype described in section 4.5.3



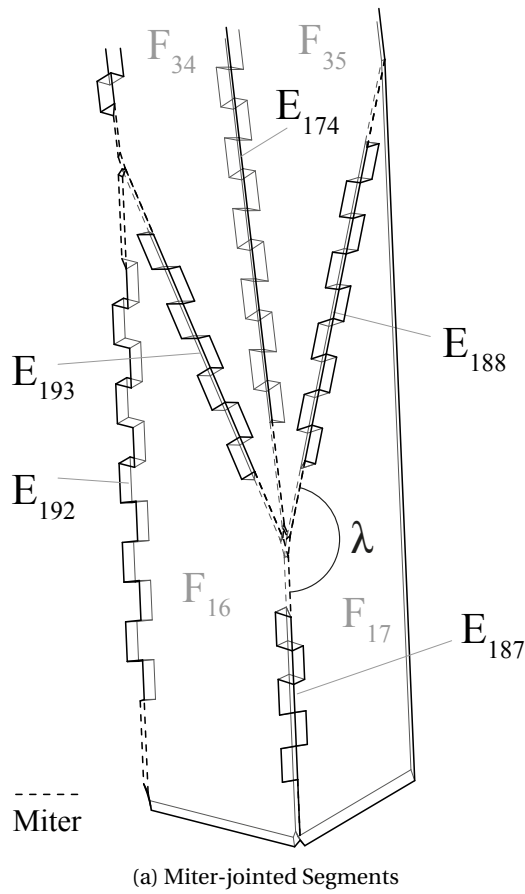


Figure 4.34 – Miter-jointed Transition Segments - Towards the vertices, the last segment of the tab-and-slot-joints is generated as a miter joint geometry. For the prototypes in this chapter, a fixed start/end segment length of  $\frac{L_{edge}}{10}$  was applied to all non-naked edges.

### Grasshopper Component

The complete joint geometry generation (including the miter segments) has been integrated into a “component” for the Rhino3D CAD visual programming plug-in Grasshopper, written in Python using GhPython. This component receives a polygon mesh as input, as well as a parameter for the thickness of the plates, and a list with edge identifiers<sup>81</sup> and corresponding custom assembly vectors. Edges that are not in this ID list will be processed as regular dovetail joints. Short edges and edges with dihedral angles which are too acute ( $\varphi < 90^\circ - \beta_{max}$ ) or too obtuse ( $\varphi > 90^\circ + \beta_{max}$ ) will be processed as miter joints.

<sup>81</sup>edge IDs will be displayed on the input polygon mesh

## **Bibliography**

- [Bur10] Hani Buri. *Origami - Folded Plate Structures*. PhD thesis, EPFL, Lausanne, 2010. EPFL Doctoral Thesis No. 4714.
- [BW06] Hani Buri and Yves Weinand. BSP Visionen - Faltwerkkonstruktionen aus BSP-Elementen. In *Grazer Holzbau-Fachtage*, 2006.
- [DIB11] DIBt. *Allgemeine bauaufsichtliche Zulassung Kerto-Q Z-9.1-100, Paragraph 4.2 and Attachment No 7, Table 5*. Deutsches Institut für Bautechnik, 2011.
- [Gra86] Wolfram Graubner. *Holzverbindungen, Gegenüberstellung von Holzverbindungen Holz in Holz und mit Metallteilen*. Deutsche Verlags-Anstalt Stuttgart, 1986.
- [Hah09] Benjamin Hahn. Analyse und beschreibung eines räumlichen tragwerks aus massivholzplatten. Master's thesis, EPFL, Lausanne, 2009. Master Thesis.
- [HES14] HESS. Hess limitless, 2014. <http://www.hess-timber.com/de/produkte/>.
- [Hun14] Hundegger. Hans Hundegger Maschinenbau GmbH, Hawangen, Germany, 2014. <http://www.hundegger.de/en/machine-building/company/our-history.html>.
- [Huy72] Pieter Huybers. *See-through Structuring - A method for large span plastics roofs*. PhD thesis, Technische Hogeschool Delft, 1972.
- [Huy01] P. Huybers. Prism based structural forms. *Engineering Structures*, 23(1):12 – 21, 2001.
- [ICD14] ICD/ITKE. Laga exhibition hall, 2014. <http://icd.uni-stuttgart.de/?p=11173>.
- [KCC<sup>+</sup>14] Oliver David Krieg, Zachary Christian, David Correa, Achim Menges, Steffen Reichert, Katja Rinderspacher, and Tobias Schwinn. Hygroskin: Meteorosensitive pavilion. In *Fabricate 2014 Conference Zurich*, pages 272–279, 2014.
- [Koc64] Peter Koch. *Wood Machining Processes*. Wood Processing. Carl Hanser Verlag GmbH & Co. KG, 1964.
- [lMea13] Riccardo la Magna et al. From nature to fabrication: Biomimetic design principles for the production of complex spatial structures. *International Journal of Spatial Structures*, Vol. 28 No. 1:27–39, 2013.
- [Mat14] Geoffrey Mattoni. Folded plate structure - design and analysis of woodworking joints for structural timber panels. Master's thesis, Ecole Nationale es Ponts et Chaussees, 2014. Master Thesis.
- [Mes06] Robert W. Messler. *Integral Mechanical Attachment: A Resurgence of the Oldest Method of Joining*. Butterworth Heinemann, 2006.

- [Neu04] Helmuth Neuhaus. *DIN EN 1995 (Eurocode 5) - Design of timber structures*. DIN Deutsches Institut für Normung e. V., 2004.
- [Piz03] Emilio Pizzi. *Renzo Piano*. Birkhaeuser, Basel, 2003.
- [Pur11] Purbond. *National Technical Approval Z-9.1-711 / Single-component polyurethane adhesive for the manufacture of engineered wood products*. Deutsches Institut für Bautechnik, 2011.
- [RGW15] Stephane Roche, Mattoni Geoffrey, and Yves Weinand. Rotational stiffness at ridges in folded plate structures. In *Elegance of Structures: IABSE-IASS Symposium 2015 Nara*. 2015, 2015.
- [RMW14] Christopher Robeller, Paul Mayencourt, and Yves Weinand. Snap-fit joints: Integrated mechanical attachment of structural timber panels. In *Proceedings of the 34th International Conference of the Association of Computer-aided Design in Architecture ACADIA, Los Angeles, USA*. Riverside Architectural Press, 2014.
- [RNW14] Christopher Robeller, SeyedSina Nabaei, and Yves Weinand. Design and fabrication of robot-manufactured joints for a curved-folded thin-shell structure made from clt. In Wes McGee and Monica Ponce de Leon, editors, *Robotic Fabrication in Architecture, Art and Design 2014*, pages 67–81. Springer International Publishing, 2014.
- [RRHW15] Stephane Roche, Christopher Robeller, Laurent Humbert, and Yves Weinand. On the Semi-rigidity of Dovetail Joints for the Joinery of LVL Panels. *European Journal of Wood Products*, 0:0, Submitted Sept. 2015.
- [Sch09] Christoph Schindler. *Ein architektonisches Periodisierungsmodell anhand fertigungstechnischer Kriterien, dargestellt am Beispiel des Holzbaus*. PhD thesis, ETH Zurich, 2009. DISS. ETH Nr. 1860.
- [SP13] Yuliy Schwartzburg and Mark Pauly. Fabrication-aware design with intersecting planar pieces. In *Computer Graphics Forum*, volume 32, pages 317–326. Wiley Online Library, 2013.
- [SRW15] Andrea Stitic, Christopher Robeller, and Yves Weinand. Form exploration of folded plate timber structures based on performance criteria. In *Elegance of Structures: IABSE-IASS Symposium 2015 Nara*. 2015, 2015.
- [SS10] Vaclav Sebera and Milan Simek. Finite element analysis of dovetail joint made with the use of cnc technology. *Acta Universitatis Agriculturae Et Silviculturae Mendelianae Brunensis*, Volume LVIII:321–328, 2010.
- [TB09] Martin Trautz and Peter Von Buelow. The application of folded plate principles on spatial structures with regular, irregular and free-form geometries. In *IASS - Evolution and Trends in Design, Analysis and Construction of Shell and Spatial Structures, Valencia*, 2009.

#### Chapter 4. Interlocking Folded Plate - Integrated Mechanical Attachment for Structural Timber Panels

---

- [Tet07] Kōndo Tetsuya. *Dento kanehozo kumitsugi : Sekkei to seisaku no jissai*. LLP Gijutsushi Shuppankai, Tokyo : Seiunsha, 2007.
- [Wei05] K. Weinert. *Spanende Fertigung: Prozesse, Innovationen, Werkstoffe*. Number Bd. 10 in *Spanende Fertigung: Prozesse, Innovationen, Werkstoffe*. Vulkan-Verlag, 2005.
- [WL94] Randall H. Wilson and Jean-Claude Latombe. Geometric reasoning about mechanical assembly. *Artificial Intelligence*, 71(2):371 – 396, 1994.
- [Wya28] Edwin Wyatt. *Puzzles in Wood*. Bruce Publishing Co., 1928.

## 5 Snap-fit joints - CNC fabricated, Integrated Mechanical Attachment for Structural Timber Panels

Christopher Robeller, Paul Mayencourt and Yves Weinand

Peer-reviewed and published in: D. Gerber, A. Huang and J. Sanchez (eds.), ACADIA 2014 Design Agency: Proceedings of the 34th Annual Conference of the Association for Computer Aided Design in Architecture (ACADIA), pp. 189-198, ISBN: 978-1926724478, Riverside Architectural Press 2014

**Abstract** This paper describes the design and potential applications of *CNC* fabricated *Snap-fit joints* for *cross-laminated veneer lumber panels (LVL)*. These joints are new to the building construction sector, but commonly used in other domains such as the automotive or consumer electronics industry. We explain our application of existing knowledge about the design and dimensioning of such joints, as well as several adaptations that we have made in order to optimize the connectors for the jointing of structural wood panels. This was necessary due to the materials and fabrication processes in timber construction, which are different from those in the sectors of origin of the *Snap-fit joints*. We propose applications, including two case studies with physical prototypes: 1. a box girder prototype on which we introduce the combination of *Snap-fit joints* with shear-resistant tab-and-slot joints and test the mechanical performance of the joints. 2: A double-layer arch prototype with non-orthogonal, 5-axis *CNC*-fabricated joints.

Foreword<sup>82</sup>

Blocking of the Assembly Direction in 1DOF joints

The geometry of the joints that were discussed in the previous chapters is blocking all but one relative movement between the connected parts. The single remaining direction  $\vec{v}$  is needed for the assembly. However, for the applications presented in this thesis, this single remaining degree of freedom must be blocked once the joints are assembled. This is necessary in order to resist the various possible directions of forces in a building structure.

Two different techniques for the blocking of the assembly direction were presented in the previous chapters: 1. The hybrid integral and adhesive-bonded connection, where the glue blocks the assembly vector and provides additional stiffness, and 2. the mutual blocking of multiple connected components with different individual assembly directions which are blocking each other. A third option is introduced in this chapter, however it is a complementary solution rather than an alternative to the techniques that were discussed previously.

Elastic Interlocks

In a taxonomy of Integral Mechanical Attachment techniques, both of the previously discussed jointing techniques fall into the category of so-called *Rigid Interlocks* (see table 5.1) [Mes06, 55], where the connection is established only through geometric features of a pair of parts.

Rigid Interlocks	Elastic Interlocks	Plastic Interlocks
Tongues-and-grooves	Integral spring tabs	Setting and staking
Dovetails-and-grooves	Snap slides and clips	Stitching and Clinching
Rabbets or Dados	Clamps and clamp fasteners	Crimping and hemming
...	...	...

Table 5.1 – Taxonomy of Integral Mechanical Attachment techniques [Mes06, p.15]

Instead, the joints introduced in this chapter fall into the so-called group of *Elastic Interlocks*, where one of two parts in the pair to be jointed, called the *snap* will deflect elastically during the assembly with the so-called *latch* on its counterpart. The deflection movement is typically created through the geometry at the interface between snap and latch, which transforms the force applied for the assembly of the parts into the necessary assembly force for deflection. Once the parts are in their final position, the snap will recover from this deflection back into a stress-free state, in which it is now geometrically blocking the other part in the pair from

<sup>82</sup>This additional section was not included in the original publication.

disassembly. In such a configuration, there is no remaining degree of freedom.

Such Elastic Interlocks are very common connectors in mass-produced objects as they are found in industry sectors such as the automotive industry or the consumer electronics sector. In contrast to the joints that were previously discussed in this thesis, the design and application of elastic interlocks is based not only on geometrical parameters, but also on certain *material parameters*, such as the maximum permissible strain and the elasticity modulus, which determine the parameters of the joint cantilever, and the materials friction coefficient, which plays a role in the determination of the joints deflection force, along with the so-called insertion angle  $\alpha$  of the snap. Figure 5.1 show various different version of integral, elastic snap-fit joints. This chapter is focusing on an adaptation of the very common cantilever-snap which is illustrated in the middle of the figure.

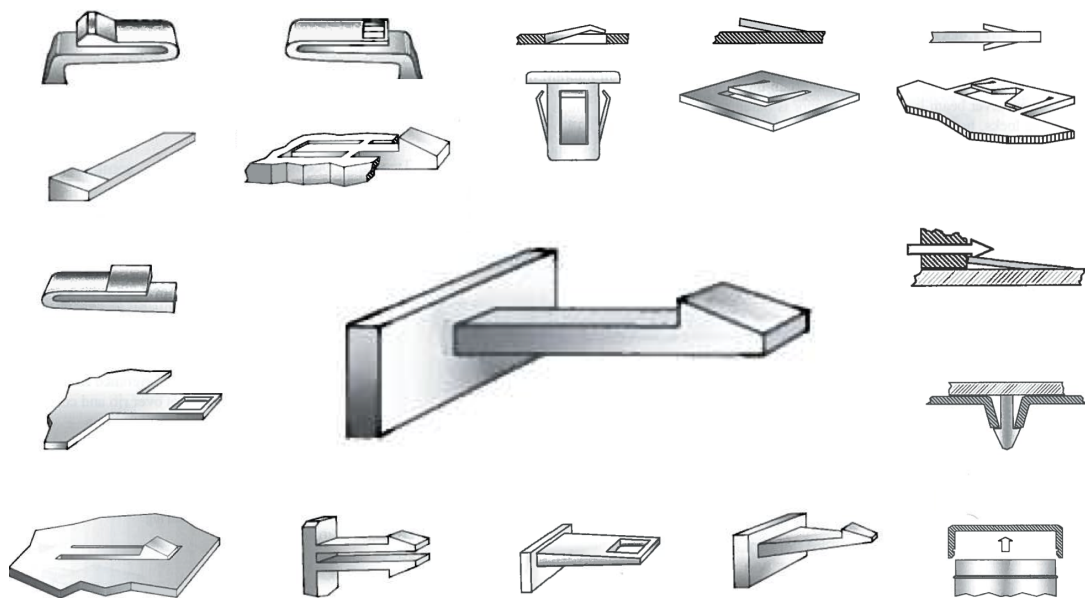


Figure 5.1 – Variations of Elastic Cantilever Locks for Plastics - Illustrations taken from [Bon05]

## Double-layer Structures

Beginning with the Curved-folded Wood Pavilion in Chapter 3, the development of a double-layered timber folded plate structure was pursued. The cross-laminated veneer lumber (LVL) panels in particular provide a high strength even for thin panels, which is ideal for the design of lightweight, double-layered components. Existing Applications with a regular, orthogonal geometry demonstrate the efficiency of such solutions [fTA13]. However, in a timber folded plate the joints are more complex. The previous two chapters have shown a variety of fabrication- and assembly-related constraints which must be considered in the design of integral joints for timber folded plate structures. The following chapter will build directly upon these investigations and add geometrical features and techniques that allow for the

completely integral assembly of a double-layered timber folded plate.

### **Contributions**

Aiming at the joints application in building structures, the input of a civil engineer was essential for the evaluation and development of the snap-fit joints. Paul Mayencourt, co-author of the following publication, has provided valuable information about the mechanical behaviour of the joint in section 5.5 and contributed the numerical model in section Section 5.7 and the Finite Element model shown in Figure 5.6.



## 5.1 Introduction

In 2010 the building sector was responsible for nearly a third (32 per cent) of the global final energy use. The embodied energy in buildings can be significantly reduced with materials which require less energy in their production, such as wood products [oCC14]. Typical building certified spruce *laminated veneer lumber* (LVL) panels are made from more than 90 per cent renewable materials and store 450g of carbon per kg. Following the combustion conditions provided by the manufacturer, these panels can be recycled into energy production.

Generally, due to its low weight-to-strength ratio, timber is an ideal material for the production of prefabricated building components, where ease-of-transport, handling and assembly have a great impact on the construction footprint, cost and timespan. In this context, LVL panels offer particular advantages: Compared to *cross-laminated timber* panels (CLT), considerably thinner cross-sections are possible with the more homogenous and mechanically strong peeled-veneer laminate components, such as the *Kerto RIPA* rib or box elements [fTA13].

In the context of shell and spatial structures, timber panels machine easily into irregular shapes, and prefabrication simplifies the use of advanced techniques and technology. However, while LVL panels offer numerous advantages for such constructions, design constraints result from limitations in the edgewise jointing of the thin panels. Geometrically simple, orthogonal components such as the *Kerto RIPA* elements can be prefabricated with glued butt joints. On site, metal plates or fasteners are used for the final assembly. Gluing is not possible due to a lack of constant conditions for the curing of the adhesive. For more complex timber panel assemblies, such as folded plate structures [Bur10], the assembly of large amounts of angular edgewise joints becomes very challenging with state-of-the-art metal fasteners. Previous studies have also demonstrated that the structural performance of such designs could be increased considerably through improved joints [Hah09].

Inspiration for improvements can be taken from Integral mechanical attachment, the oldest known method of joining (Messler 2006). Rigid interlocks form one category of this general concept, including connections like mortise-and-tenon-, finger- or dovetail joints, which were common handcrafted joining techniques in traditional carpentry and cabinetmaking. However, with the industrialization and its proliferation of machine-tool-technology (Schindler 2009), these joints were widely replaced by mass-produced metal plate connectors and fasteners. Only recently, the increasing use of information-tool-technology in timber construction companies and Application Programming Interfaces for the algorithmic generation, analysis of integrated joints, has caused a resurgence of integral mechanical attachment techniques.

First examples of integrated line-joints for wood panels have been demonstrated on the ICD/ITKE Research Pavilion 2011 [lMea13] and the Curved-folded CLT Pavilion [RNW14], as well as the recent ICD/ITKE LaGa Exhibition Hall [ICD14]. In these projects, form-fitting joints integrate locator features for the fast and precise positioning of elements, which enables and simplifies complex assemblies. Simultaneously, the joints participate in the load-bearing connection of the components through their connector features. Additional metal fasteners

## Chapter 5. Snap-fit joints - CNC fabricated, Integrated Mechanical Attachment for Structural Timber Panels

or adhesive bonding are necessary to receive forces and to retain elements in their remaining degrees of freedom.

A possible solution for the jointing of structural wood panels without additional fasteners or adhesive bonding may be found in *elastic interlocks*, another category of integral mechanical attachment techniques. So-called *Snap-fit joints* provide an integrated locking feature to connect the parts. While *Snap-fit joints* are a common attachment technique in the consumer electronics or automotive industry, possible applications for the jointing of timber panel structures have yet to be studied.

### 5.2 Concept

*Snap-fit joints* are widely used in the industry as a simple, economical and quick way of connecting two parts. The joints consist of one male and one female part. The temporary bending of the cantilever hook allows the fit of two pieces, using the material's elasticity property. After the joining operation, the pieces return to a stress-free state. The geometrical parameters of the parts define the force needed to assemble or disassemble it and the separable or inseparable characters of the joints. The joint is mainly designed according to the mechanical load during assembly and its corresponding assembly force (Figure 5.2).

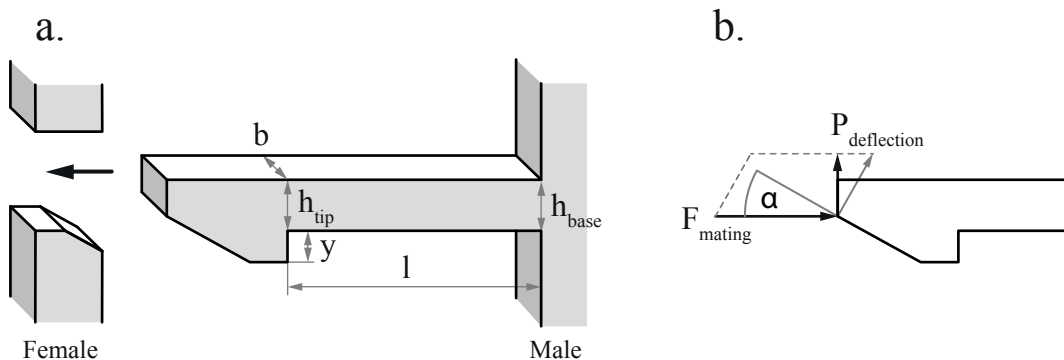


Figure 5.2 – Basic Cantilever Hook Nomenclature - (a) Geometrical parameters of the two parts. (b) Mating force  $F_{mating}$  in relation to the insertion angle  $\alpha$  and the deflection force  $P_{deflection}$

#### 5.2.1 General Joint Design

Rudimentary design is provided by the snap-fit manufacturers such as BASF [Com07] or Bayer [LLC00]. Based on the assumption of the Euler-Bernoulli beam theory, the design variables for the joints are the following:

- height of the cantilever beam  $h$ ,
- length of the cantilever  $l$ ,

- undercut  $y$ .

Given the maximal permissible strain of the material  $\epsilon$ , the maximal deflection for a cantilever with rectangular and constant cross section is:

$$y_{max} = \frac{b_1 + b_2}{2b_1 + b_2} \frac{\epsilon l^2}{h_{base}} \quad (5.1)$$

For a cantilever snap joint with decreasing height to one-half at the tip over the length the 0.67 factor becomes 1.09.

During the assembly, the deflection force  $P$  at the tip of the cantilever at  $y_{max}$  is given by:

$$P_{deflection} = \frac{bh^2}{6} \cdot \frac{E\epsilon}{l} \quad (5.2)$$

Where  $E$  is the E-modulus of the material,  $b$  the width of cantilever. More information on the design of cantilever snap joint with other geometry such as trapezoid section can be found at [Com07] or derived from the beam theory of a cantilever beam with point load at the tip (Figure 5.3).

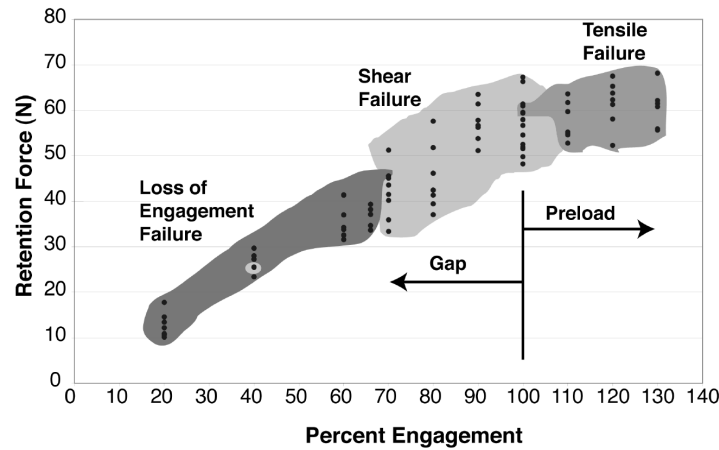


Figure 5.3 – Retention Force Diagram (Courtesy of A. Luscher)

The force necessary to assemble the joint, called mating force, depends on the friction coefficient of the material  $\phi$ , the insertion angle and the deflection force. Both the deflection and friction force have to be overcome by the mating force:

$$F_{mating} = P \frac{\mu + \tan(\alpha)}{1 - \mu \tan(\alpha)} \quad (5.3)$$

## Chapter 5. Snap-fit joints - CNC fabricated, Integrated Mechanical Attachment for Structural Timber Panels

---

The same equation can be used to determine the separation force of the joint where the insertion angle  $\alpha$  has to be replaced by the retention angle  $\beta$ . A value of  $90^\circ$  for the retention angle gives the maximal retention force.

Furthermore, a study from Luscher [Lus95] shows that the retention force not only depends on the retention angle but on the *Percentage of Engagement (PE)* as well. The engagement is the depth of insertion in the undercut of the mating part. A hook fully in contact with its mating part would have a *PE* of 100 per cent. The *PE* defines the failure mode and thus the maximal retention force. Figure 1 shows that a *Percentage of Engagement* of 100 per cent or higher is preferable. Finally, the stress concentration at the root of the cantilever should be reduced by adding a fillet radius.

### 5.2.2 Adaptation to Fabrication and Materials in Timber Construction

(Figure 5.4) shows our design for a CNC-fabricated snap-fit joint. For the production of our prototypes, we have used a MAK A MM7s 5-axis router equipped with a cemented carbide shank-type cutter with a radius of 6mm, operated at a feed rate of 6-8m per minute and a rotational speed of 17.000 revolutions per minute.

The elasticity of the wood allows to design a cantilevering hook for the jointing of two panels of wood. For a given panel thickness  $t$  and an undercut  $y$  the cantilever length  $l$  and height  $h$  can be chosen to correspond to the material's limits:

- maximal permissible elastic strain in the bending direction,
- maximal compressive strength at the hook contact to avoid fiber crushing

During the joining operation, the hook will be bent. This implies bending moment at the base of the cantilever and a deflection force against the mating panel. For a given undercut, the length and height of the cantilever have been chosen to limit the strain at the base in its elastic range and to avoid the crushing of the fibers at the tip of the hook and the top layer of the mating part, due to the deflection force. The undercut is the displacement constraint imposed to the hook during insertion. A smaller height gives a larger flexibility of the cantilever, smaller strain at the base ( $h$ ) and a smaller deflection force ( $h^2$ ). In case of the use of the retention resistance and an engagement of the hook higher than 100 per cent, the section of the cantilever have to be sized sufficiently for the disassembly tensile force.

### 5.3 Combination with Tab-and-slot Joints

While *Snap-fit joints* can resist a certain retention force, they do not provide any shear resistance. In order to use this joint as a load-bearing connection for building components, we combine the snap-fit joint with prismatic tab-and-slot joints, which receive the majority of the

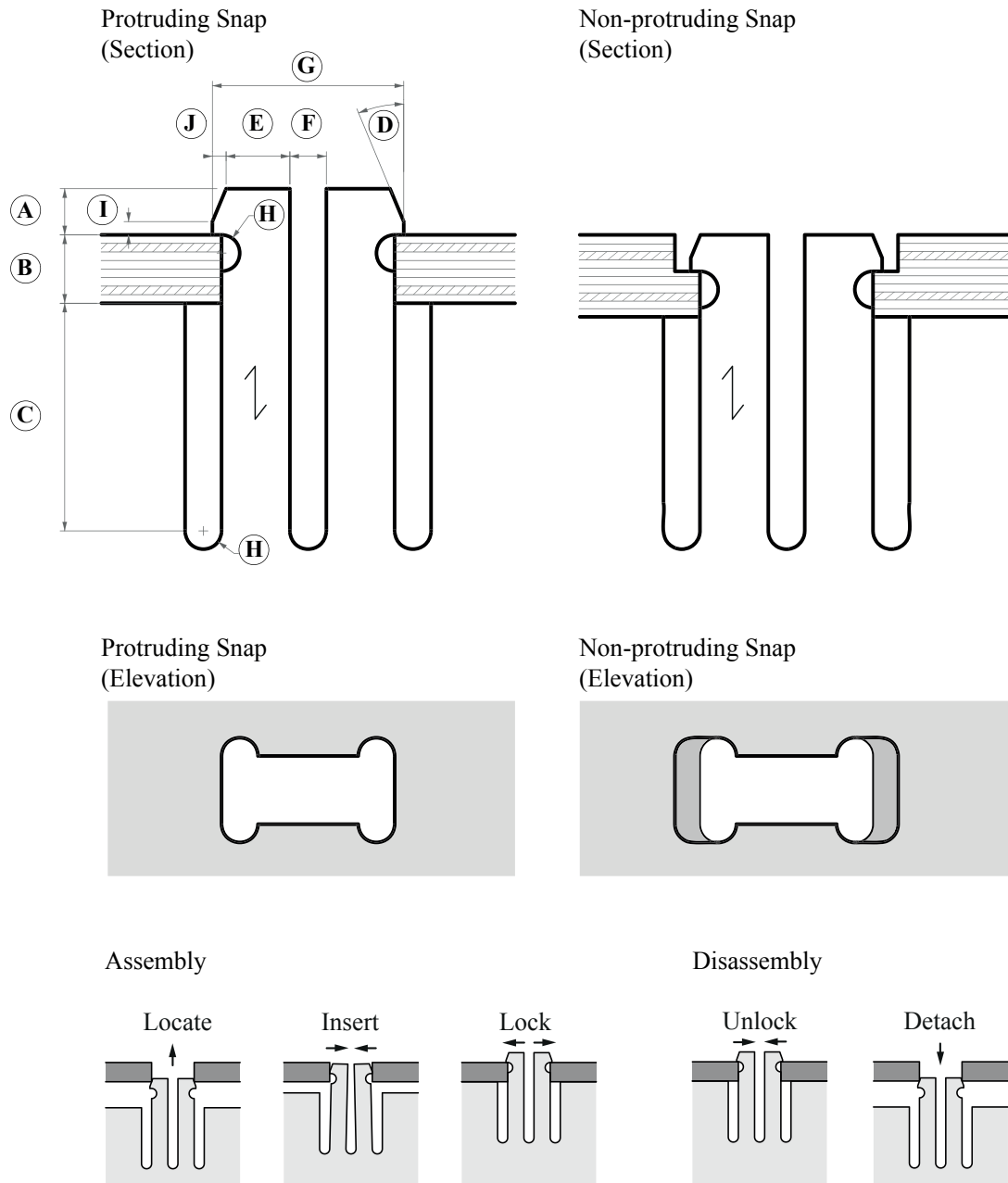


Figure 5.4 – CNC fabricated Snap-fit Joint for LVL Panels - Protrusion (A), panel thickness (B), cantilever length (C), insertion angle (D), cantilever height (E), cantilever spacing (F), mating cutout (G), fillet radius (H), lateral pressure zone (I), undercut (J). Top right shows a version of the joint without hook protrusion. Bottom shows a schematic time-lapse assembly and disassembly.

forces. Generally, we consider the snap-fit-joint as a special type of tab-and-slot-joint, with an integrated retention feature. This combination of integrated joints allows us to achieve a

mechanical behavior equivalent to a screwed joint. The specific shear-resistance of such a joint combination depends on the individual length and overall amount of the tabs. We have first tested this behavior on a simple box girder prototype (Figure 5.5).

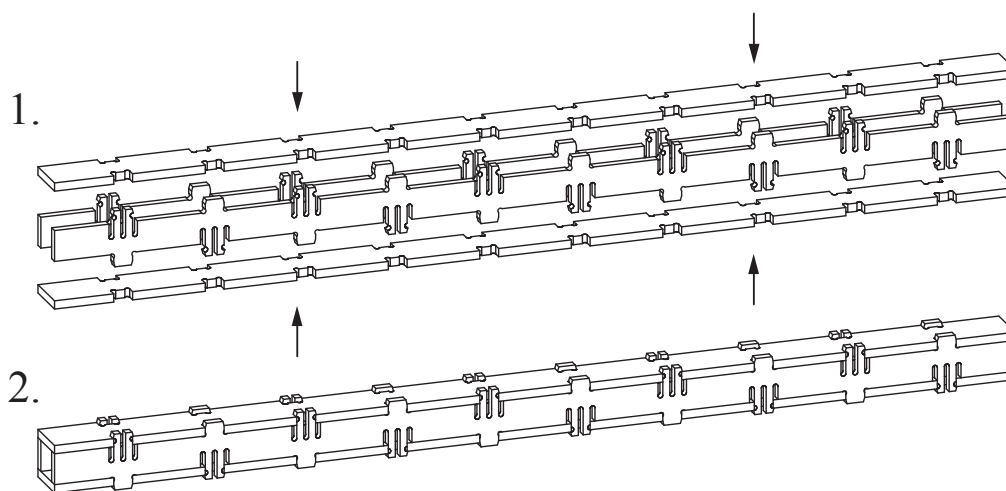


Figure 5.5 – Box Girder Specimen for the Mechanical Analysis of Combined Snap-fit and Tab-and-slot Joints - A combination of the snap-fit joint with shear-resistant tab-and-slot joints allows for a mechanical behaviour equivalent to a screwed joint.

### 5.4 Fabrication and Assembly

The geometry of the joint is parameterized in a *Rhino3D* Python script. The geometry of the snap-fit joint is automatically generated based on the panel thickness and the before mentioned calculations. The *G-Code* for a *CNC* milling machine is also generated automatically at the same step.

The assembly of a snap-fit jointed beam is carried out by clipping the two webs to the bottom panel and finally connecting the top panel. This is done very quickly and no fixation is needed to get the precise geometry. The time of cutting is gained back with the simplicity of assembly of the beam. Moreover, the beam can be assembled and disassembled at any time. This means that the panels could be transported flat and then put together only when needed. The transportation volume for a beam with equivalent static height is greatly reduced.

### 5.5 Mechanical Performance

In order to evaluate the mechanical behavior of the *Snap-fit joints*, a set of three beams have been tested with a three point flexural test, loaded at mid-span. The results were validated with a Finite Element numerical model (Figure 5.6). The performance of the snap-fit beam is then compared to a beam with screwed connection. Finally, an optimized snap-fit beam is

proposed with the conclusion of the analysis.

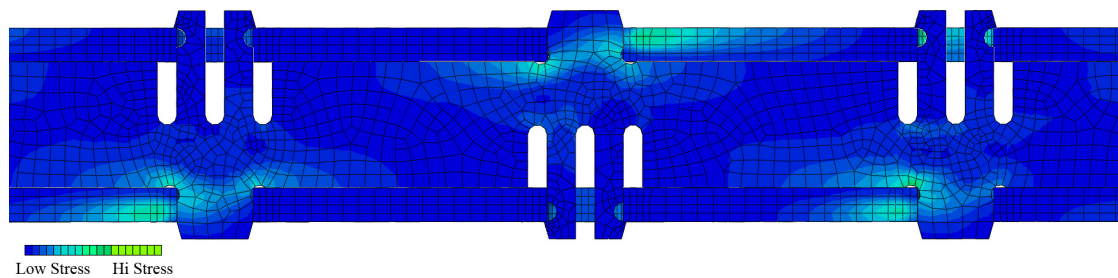


Figure 5.6 – FEM Simulation of a 3-point Flexural Test with the Box Girder Specimen Geometry - The image shows compression on the tab-and-slot joints on side of the specimen. The FEM results were subsequently compared with a series of physical load tests.

## 5.6 Physical Load Tests

The snap-fit beam specimens have been built with spruce Kerto-Q panels with a nominal thickness of 21 mm. The panels consist of seven laminated layers (| – ||| – |), five of them in the main grain direction and two in the perpendicular direction (Technical Research Centre of Finland 2009). Kerto-Q has the advantage of being very dimensionally stable to humidity changes with good structural characteristics. The beam spans 2210.5mm for a total length of the beam of 2431.6mm. The size was constraint by the maximal dimension of the *CNC* milling machine 2.5m. The displacements were both measured with Linear Variable Differential Transformer (LVDT) sensors on the top flange and with the stereo correlation technique on the bottom flange.

## 5.7 Numerical Model

Using the Finite Element Software Abaqus, the snap-fit joint beam was numerically simulated. The following material values were taken from the national technical approval certificate (VTT) of the panel manufacturer (see table 5.2).

The Kerto-Q material was modeled as perfectly linear elastic. Linear brick 8-nodes elements with reduced integration (C3D8R) were used for the mesh. Attention was paid to refine the mesh at the contact zones. The contact is modeled with the general contact function of Abaqus. Its interaction property has two features: a tangential behavior defined by a friction coefficient  $\mu = 0.4$  (Technical Research Centre of Finland, 2009) and a normal behavior defined as ‘hard contact’. Contact constraints are for both enforced with the penalty method. Separation after contact is allowed.



Variables	Values from VTT for KertoQ 21 mm
Density	$\rho_{mean} = 510 \text{ kg/m}^3$
$E_1$	$E_{0,mean} = 10000 \text{ N/mm}^2$
$E_2$	$E_{90,edge} = 2400 \text{ N/mm}^2$
$E_3$	$E_{90,flat} = 130 \text{ N/mm}^2$
$\nu_{12}$	0.09 [-]
$\nu_{13}$	0.85 [-]
$\nu_{23}$	0.68 [-]
$G_{12}$	$G_{0,edge,mean} = 600 \text{ N/mm}^2$
$G_{13}$	$G_{0,flat,mean} = 60 \text{ N/mm}^2$
$G_{23}$	$G_{90,flat,mean} = 22 \text{ N/mm}^2$

Table 5.2 – Variables and Values from VTT for KertoQ 21 mm

## 5.8 Results

This section presents the results of the experimental tests and the numerical model. The results of the test are consistent with the numerical results. A final deflection at mid-span of 35mm was reached for the failure load of 6.000N. The failure occurred in the panel. The numerical model gives a deflection of 32mm for the same load. As we can see from the results in Abaqus (Figure 5.6), the snap-fit hook is not participating to the shear connection. Its stiffness is much lower than the tab connection as it was designed to be easily bent for the joining operation.

## 5.9 Optimization of the Snap-fit Connection for the Beam

Looking at the result of the first snap-fit beam, the design of the beam could be improved or optimized by changing the hook geometry and the number of hooks. In the case of the beam, the snap-fit does not need to take any traction forces when the beam is loaded. The snap-fit is only necessary to keep the pieces together during construction. This means that the hooks do not need to be designed for high traction forces but should only be able to retain the four panels from going apart. The snap-fit cantilever can then be slender designed to make it more flexible, which would reduce the risk of fiber crushing during insertion. Moreover, as the hook is not participating in the resistance of the shear connection, fewer snap-fits are needed and could be replaced by more tap joints to improve the shear capacity of the shear connection. Furthermore, it is not necessary to have the hook pointing in two directions. As it can be seen on the deformed shape of the beam in Figure 4, the hooks pointing in the direction opposite of the shear stresses are losing contact as soon as the beam deforms and are then unnecessary. Less snap-fit hook will considerably reduce the cutting time with the CNC and improve the competitiveness of the technique over the glued or screwed connection. Finally, in order to have flat surfaces, the height of hooks and taps can be trimmed to the panel surface. The analysis of the optimized beam gives a deflection of 25mm at mid-span for the same load of 6.000N.

## 5.10 Comparison with Screwed Connections

Metal fasteners such as screws allow for a fast and convenient assembly of wood components on site. Unlike adhesives, constant climatic conditions are not required for their assembly. However, for the edgewise jointing of structural wood panels with screws with a shaft diameter  $d$ , a lateral distance must be respected. For the Kerto Panels, the minimum distance is defined as  $5*d$ , while the minimum screw shaft diameter  $d$  is 6mm [DIB11]. From this, we obtain a minimum lateral distance of 30mm and a minimum panel thickness of 60mm. Following these regulations, screwed edgewise joints cannot be used on thin *LVL* panels. Furthermore, large amounts of fasteners are necessary for load-bearing joints and additional locator features are necessary to improve precision and ease of assembly. The combination of integrated connectors presented in this paper supports loads not with additional fasteners, but with the parametric geometry of the joints, which can automatically be optimized depending on the specific material characteristics and actual, local load-bearing requirements. Elements can be transported to the construction site flat-packed and put together on site. This reduces the necessary transportation volume. Moreover, they can be quickly put together or disassembled if needed. Finally, the snap-fit connection is a mono-material connection, including advantages such as aesthetics, ease-of recycling or a homogenous thermal conductivity of the parts, which can reduce condensation and decay [Gra86].

## 5.11 Applications and Features

**5-axis Fabrication of non-orthogonal joints** As one of the most important features, 5-axis cutting allows us to fabricate the snap-fit joint not only at  $90^\circ$ , but also for a fabrication-constrained range of non-orthogonal joints (Figure 6). Such angular joints can be used for the design of structurally efficient timber folded-plates.

### 5.11.1 Double-layer Structures

As mentioned in our comparison with screwed joints, the combination of *Snap-fit joints* and *tab-and-slot-joints* allows for the edgewise jointing of thin *LVL* panels (for example Kerto-Q 21, 27, 32 mm). We can therefore, instead of a single layer of thick panels, design double layer structures, where we achieve a large static height at a low self-weight and take advantage of the compressive and tensile strength of the panels at the top and bottom (Figure 5.8). Another advantage of such double-layer structures is the prefab-integration of insulation materials, which are protected from mechanical damage inside the components during transportation.

A particular structural advantage of the snap-fit and tab-and-slot joints on such double layer assemblies is the possibility to establish a direct edgewise connection between all four layers of a fold (Figure 5.9). With longer snap-fit connectors, the interior panels of a fold can first cross through each other like a mortise-and-tenon joint, and then snap into the exterior layers above. The interior panels now double-lock the exterior panels in place, and the two additional

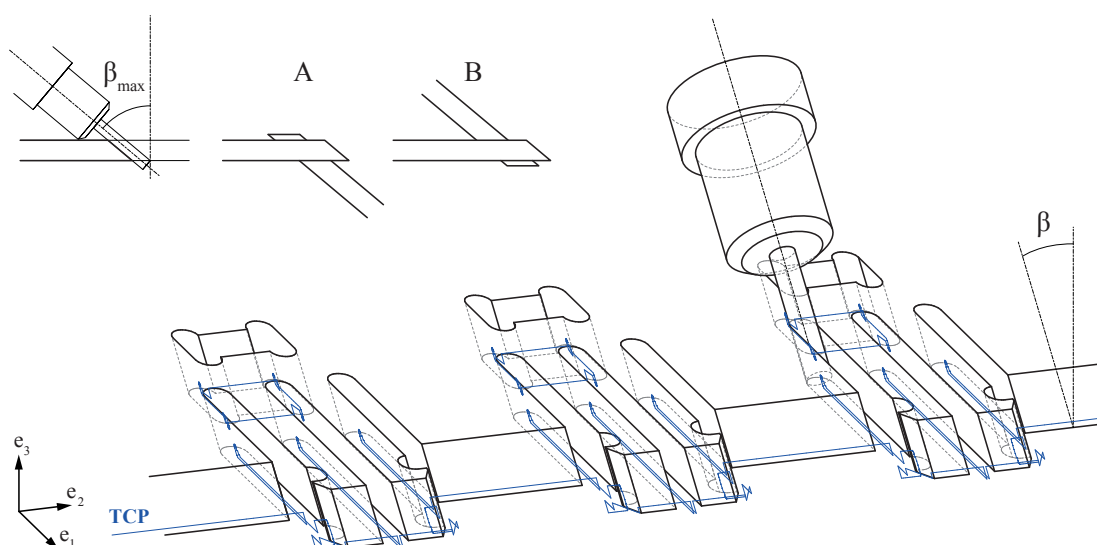


Figure 5.7 – Side-cutting Fabrication of a Non-orthogonal Snap-fit Joint with a 5-axis *CNC* Router - The illustration at the top left shows the main fabrication constraint of the side-cutting technique, which is the maximum tool inclination  $\beta_{max}$ . It is determined by the geometry of the tool and the tool holder. From this angle, we obtain the most obtuse (A) and the most acute angle (B) for the non-orthogonal snap-fit joint. The blue line (TCP) shows the tool center point path, generated with our RhinoPython script. Note the automatic height compensation for inclined faces.

line-joints per edge improve the overall stiffness and rigidity of the connection.

In an assembly with multiple components, additional elements can be added to a naked edge where both the exterior and the interior layer are fitted with either male or female connectors (Figure 5.10) and (Figure 5.11). This assembly constraint results from the fact that panels with *Snap-fit joints* must be inserted along a vector that lies on the plane of the male part of the connection.

Finally, this assembly technique can also be applied to folded plate shells corrugated in two directions, allowing for the design of doubly-curved and free-form shell structures [TB09], [Fal10]. In such structures, multiple edges must be jointed simultaneously, which has, depending on the chosen assembly technique (Figure 5.10a) or (Figure 5.10b), certain implications on the geometry of the folded plate shell (Figure 5.12). This prototype also demonstrates a possible combination of the *Snap-fit joints* with dovetail joints on the line-joint between the exterior panels of a fold. While performing similarly to the tab-and-slot joints, the dovetails do not require a protrusion on the panel with female connectors.

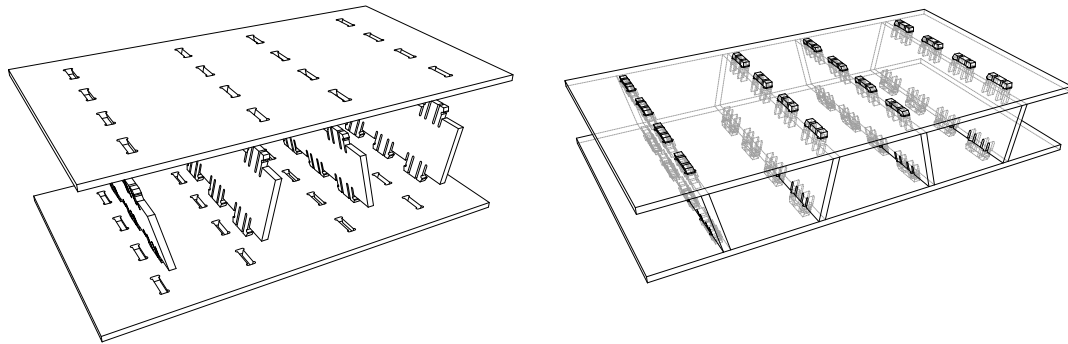


Figure 5.8 – Sandwich Element with Inclined Vertical Connectors - The snap-fit joint allows for a simple, precise and quick assembly of non-orthogonal connections. There is no difference between the fabrication and assembly of a  $90^\circ$  joint and a  $110^\circ$  joint. This can be exploited for the assembly of corrugated sandwich components.

## 5.12 Conclusions and Outlook

This first study on a snap-fit connection for structural wood panels clearly shows the potential of its application. Numerical parameterized geometry and *CNC* cutting technology enable the production of the joint. Few restrictions on the design need to be taken into account due to the wood's material properties. The behavior of the first application on a box-beam was satisfactory but showed that improvements of the connection are still possible. Finally, the construct-ability of more complex joint geometries was shown on the last part, taking advantage of the ability to join thin panels, which was used for the jointing of double-layer prototypes. The possibility of disassembling the parts at any time and transporting them unassembled opens a wide range of future applications such as temporary or modular structures.

## 5.13 Acknowledgements

We would like to thank Andrea Stitic and Stéphane Roche for the discussions and the conduction of the three-point flexural tests on the box beam specimen, as well as Jouni Hakkarainen and the Metsa Group for the supply of information and materials.

## Chapter 5. Snap-fit joints - CNC fabricated, Integrated Mechanical Attachment for Structural Timber Panels



Cassette

Shear block

Direct

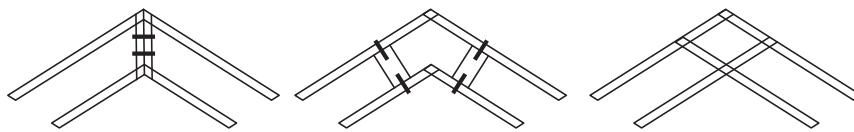


Figure 5.9 – Prototype for a Snap-fit Jointed, Double-layered Corner (90° and 120° fold) - built from 17mm plywood, 75mm spacing. Note the double-snap-fit- element, which has a hook for the first layer and another hook for the second layer. The snap-fit joint in the middle is used as a spacer element. This technique can be used for structural improvement as well as for the fitting of (flocked) insulation materials.

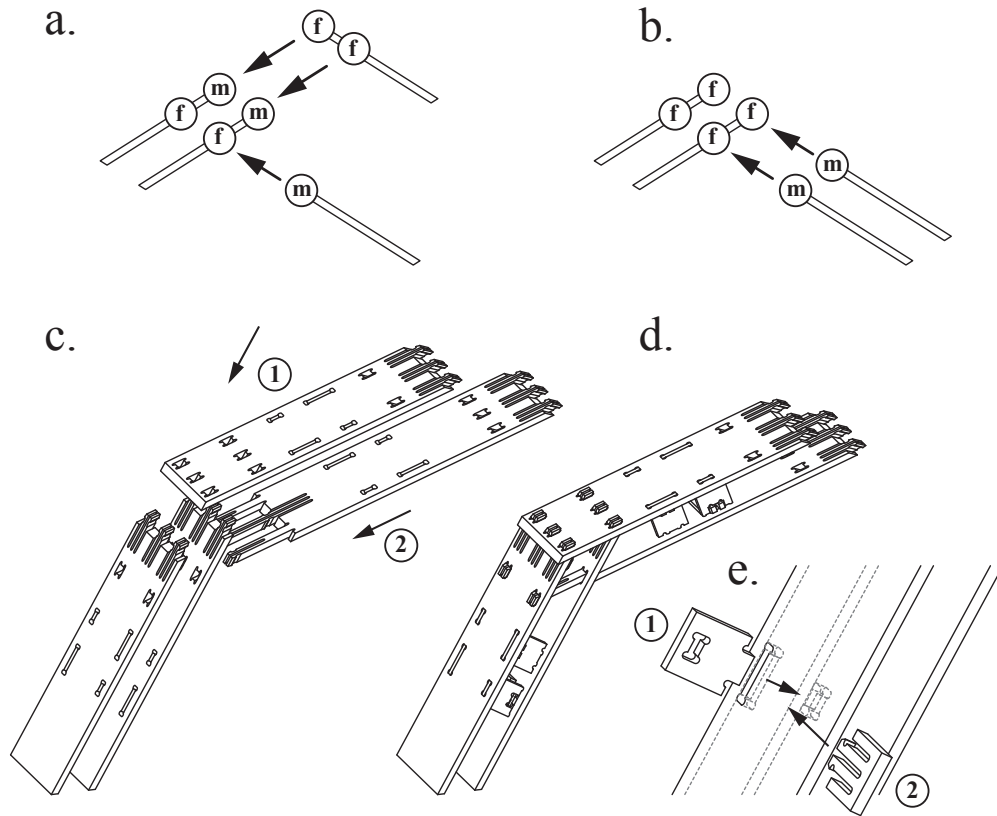


Figure 5.10 – Assembly of Multiple Double-layer Components in one Direction - (a) and (b) show two possible male (m) / female (f) connector configurations and the resulting insertion directions of the panels. (a) requires spacer elements only on one interior panel, while (b) requires spacers on both interior panels. (c) and (d) show this method applied to an arch prototype. (e) shows additional snap-fitted shear block elements for this 1-directionally-folded structure.

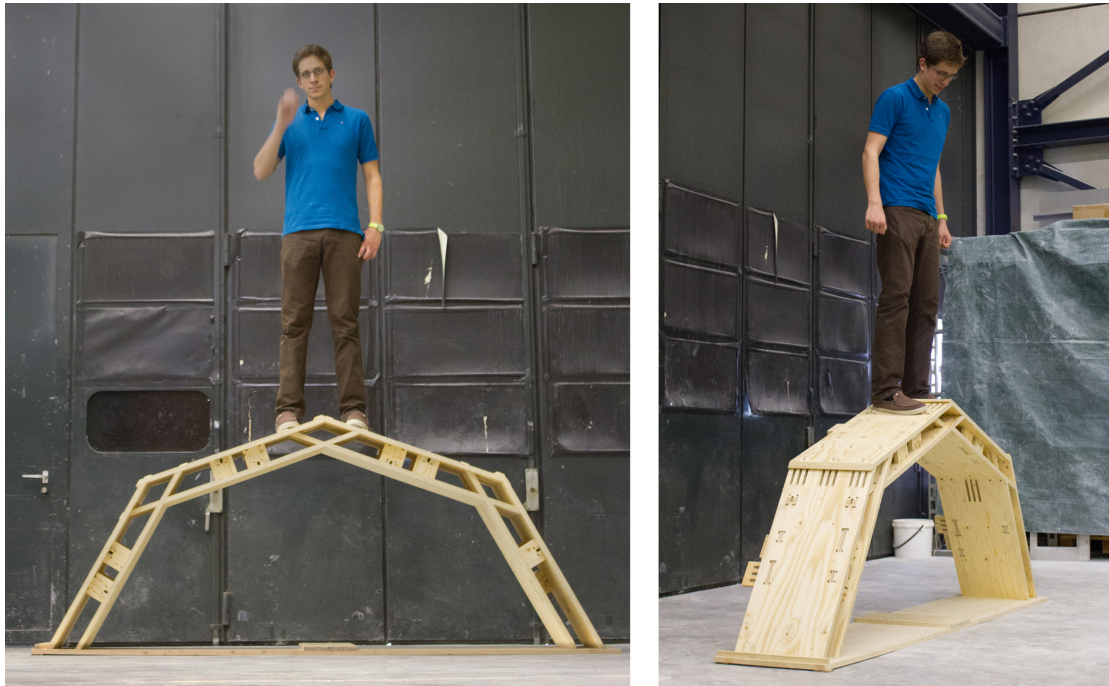


Figure 5.11 – Physical Prototype of the 1-directionally-folded Double-layer Arch. - The prototype was built from Kerto-Q 21mm panels and spans over 2.5m.

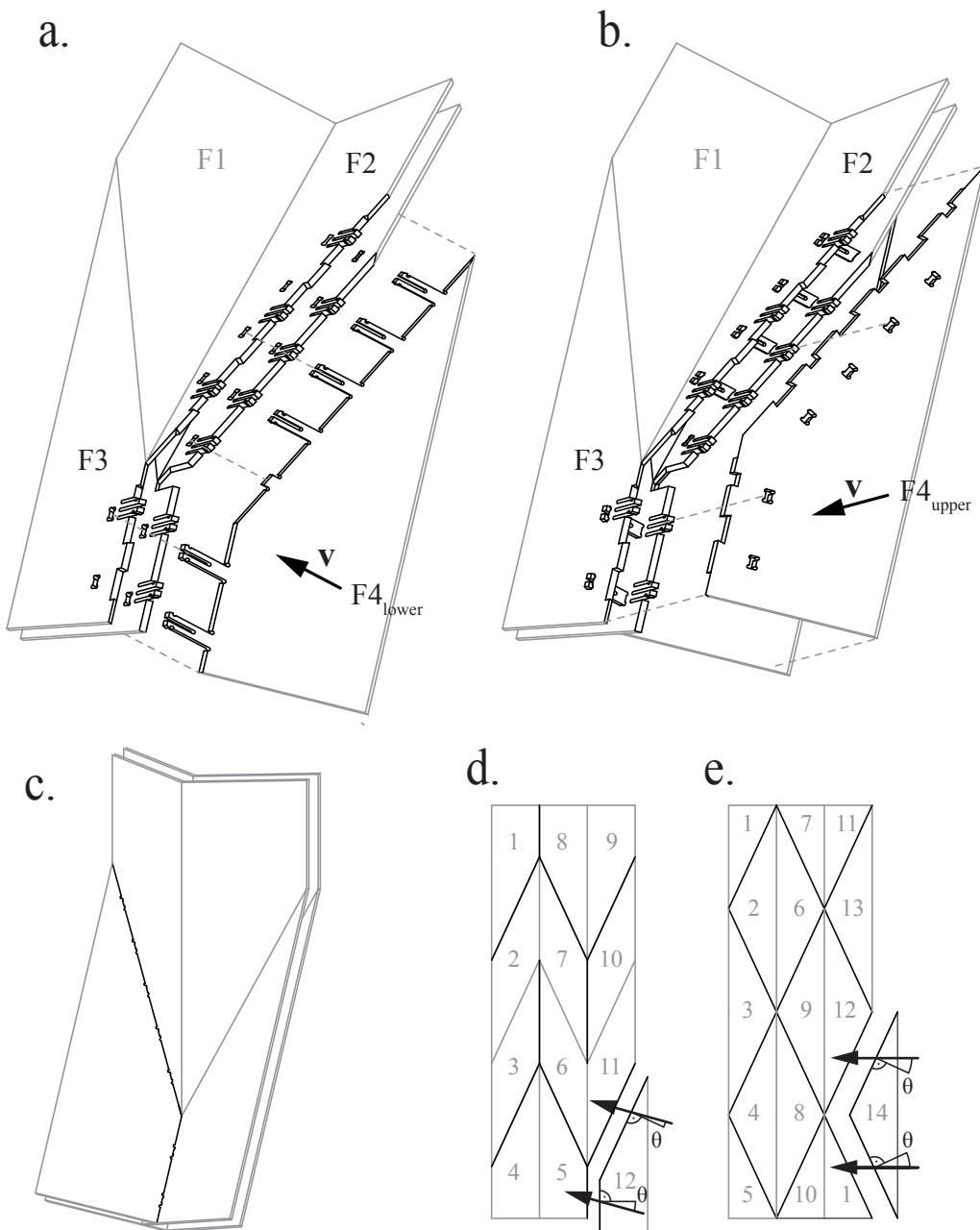


Figure 5.12 – Assembly of a Double-layer Folded Plate Shell - (a.) Two edges of one panel ( $F4_{lower}$ ) simultaneously connect panels on two layers ( $F2_{lower} / F2_{upper}$ ) and ( $F3_{lower} / F3_{upper}$ ) via their four edges. The direction may be chosen within the plane of ( $F4$ ). (b) shows the insertion of the upper panel ( $F4_{upper}$ ) with female connectors. Here, the line of insertion must lie on all planes the panel will be attached to ( $F2$  and  $F3$ ). For only two edges, a solution will always be found at the intersection line of the two planes. This constraint does not apply to the technique shown in (Figure 5.10b). (c) shows the interior view of the double layer assembly. Joints will only be visible on the mountain folds. The drawings (d) and (e) show two possible fold patterns which are corrugated in two directions and their order of assembly. The illustrated Herringbone (d) and diamond patterns (e) require only a small deviation ( $\theta$ ) of the *Snap-fit joints* insertion direction from a line perpendicular to the edge to be joined.



### Additions and Remarks<sup>83</sup>

The publication in this chapter introduced the basic concept of a snap-fit joint, as well as its adaptation to cross-laminated timber panels and the related manufacturing methods. Furthermore, it introduced specific applications for timber folded plate structures, ranging from a box girder which served for the analysis of the joints behavior under loads, to the completely integral jointing of double-layered timber folded plates, folded in one and in two directions. The latter was only introduced briefly in the applications section 5.11, on page 127. The following sections will provide additional information.

### Integral Double-layer Connection

The integral double-layer connection presented in this chapter is taking advantage of the limited range of dihedral angles  $\varphi = 90^\circ \pm 40^\circ$  in the timber folded plate applications, which result both from structural considerations and fabrication constraints. The fundamental concept of the double-layer joint is the intersection of the interior plates with one another, followed by their direct connection with the exterior plates. This type of connection will *not* work for in-plane connections, or for assemblies with very obtuse dihedral angles<sup>84</sup>. It can not be used for the joints within flat or low-curvature surfaces.

In section 5.11 the principle was introduced briefly and a comparison with alternative connections was provided in figure 5.9. Additional information on the benefits of this connection is shown in Figure 5.13. First, it introduces another common solution (5.13a), where additional transversal, angular elements are used to connect the plates. However, unlike the other options in this figure, this version does not take advantage of integral edge-to-edge connections on the plate for the assembly of plates at different dihedral angles within a folded plate. Custom-shaped connector elements may be required for each edge. The diagram below illustrates another shortcoming: The four empty circles represent the four plates which are connected in this joint. The lines illustrate that these plates are not connected with each other directly, but through the additional connector element. (hatched circle).

In figure 5.13b, box-shaped components have been assembled with integral joints, but the connection between the boxes is established with mechanical fasteners. The diagram below shows that again, the four plates that come together in this detail are not connected directly. Instead, the connection between the neighboring upper or lower plates is established through two additional components. Figure 5.13c shows a similar configuration, where integral joints have been combined with shear-block elements. There is a direct connection between the

---

<sup>83</sup>This additional section was not included in the original publication.

<sup>84</sup>an example for a shell built from discrete timber plates with obtuse angles is presented by [ICD14]

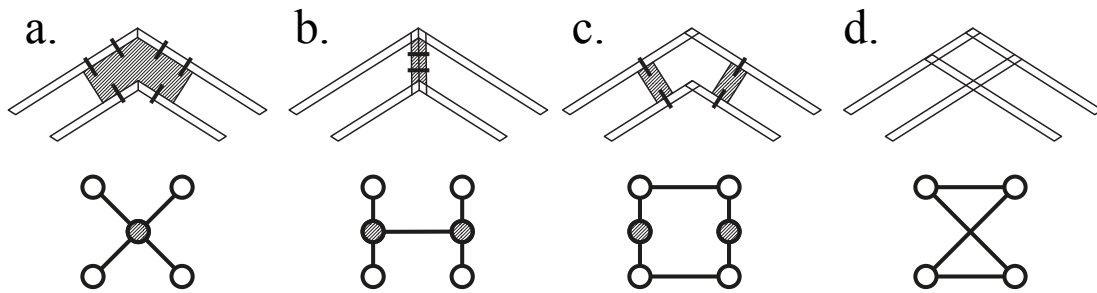


Figure 5.13 – Comparison of Double-layer Angular Edge Joints for LVL panels

upper and lower layers, but the left exterior plate connects to the right interior layer through two other components.

Finally, the intersecting configuration 5.13d connects all four plates directly. At the same time, the joint geometry fixes the spacing between the plates and provides a certain shear-block through the rotational stiffness of the individual joints. It must however be noted that the comparison in figure 5.13 is comparing the joint geometry and connectivity. Despite certain obvious advantages of the integral version in 5.13d, a mechanical analysis of these double-layer joints has not been performed yet.

#### 4-step Integral Assembly of Double-layered, Bidirectionally Folded Structures

Using the Nejiri-Arigata-inspired joining technique that was demonstrated in chapter 4, an assembly vector can be chosen within in a 3-dimensional rotation window. This is essential for the simultaneous assembly of multiple joints.

However, this 3-dimensional rotation is not possible for certain steps in the assembly of a double-layered folded plate structure, when the direct 4-point connection technique is used. Figure 5.14 shows the four steps that are required for such an assembly. The first two steps 5.14a and 5.14b show the joining of a single segment (with two parallel joints) in a double-layered folded plate, and have already been demonstrated in the figures 5.10 and 5.11. The second two steps 5.14c and 5.14d show the same two situations, but now for the simultaneous connection of two segments. In these two steps, a common assembly vector  $\vec{v}$  must be found for the 4 joints that must be connected simultaneously. As mentioned before, in the previous chapter a common vector was found within the intersection of the two 3D rotation windows, based on the possibility for out-of-plane assembly directions, and enabled through the Nejiri Arigata inspired joint geometry.

This technique however will not work when a joint intersects a first layer, before it connects to the second layer. This is the case in the steps 5.14b and 5.14c. For these two steps, the assembly vector *must* lie on the plane of the part which is being inserted. For the other two steps, 5.14a and 5.14d, an out-of-plane vector could be chosen. However this would not ideal for the assembly of the snap-fit joints, because the geometry used in this chapter is based

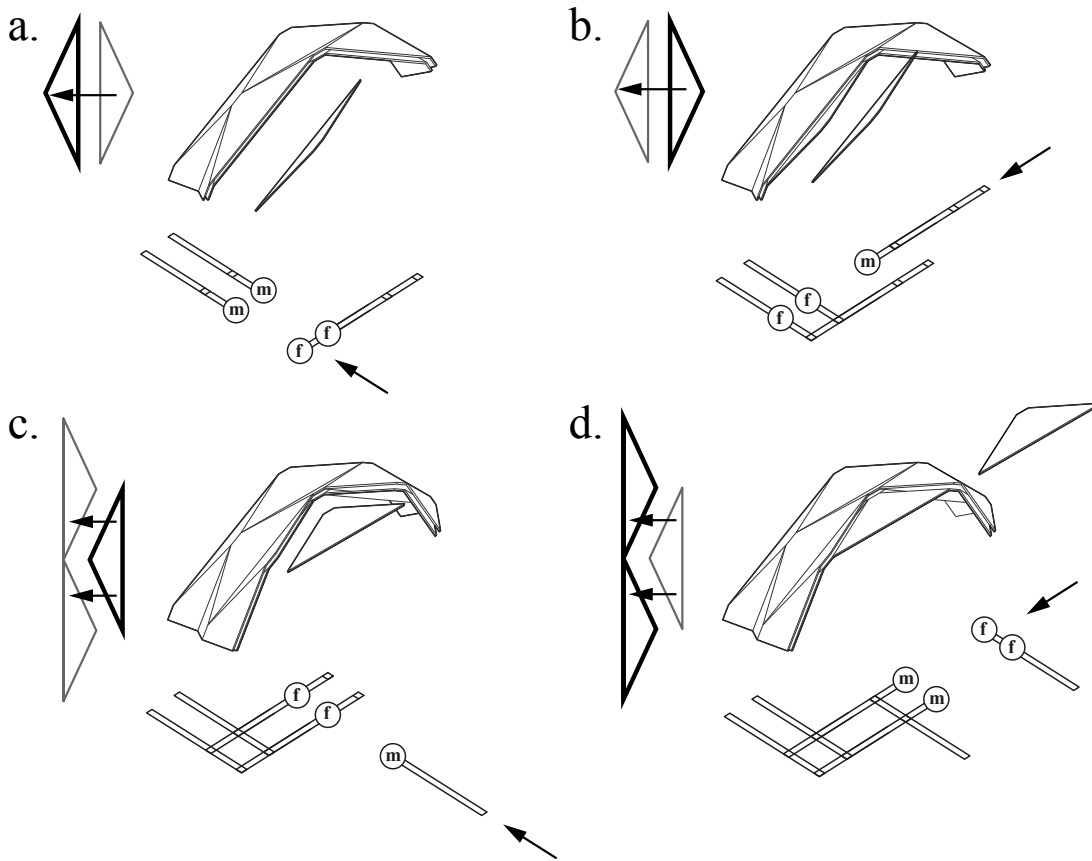


Figure 5.14 – 4-step Integral Assembly of Double-layered Timber Folded Plates. *m* indicates male connectors such as snaps, *f* indicates female connectors such as latches.

on self-activation, where the deflection of the joints is generated from the force with which the component is being inserted.<sup>85</sup> This force is expected along the cantilever of the snap-fit joints. However, the double-layered folded plate prototypes in this chapter demonstrate that 3D (out-of-plane) vector-spaces are not necessarily required for all joints, depending on the folded plate geometry.

- **Single-Edge Inverse, Single-Edge Regular** - Figure 5.14a/b - For these two steps, a rotation of the joint is not necessary at all. An Assembly vector perpendicular to the edge can be used, but the snap-fit joints must be assembled along a vector that lies on the plane of the part with the male connectors (snaps). For step 5.14a, the assembly vector must lie not on the plane of the part which is being inserted, but on the plane of its two counterparts (Inverse Assembly). Step 5.14b shows the regular single-edge assembly.
- **Dual-Edge Regular** - Figure 5.14c - In this step, a rotation of the joints is required because two non-parallel edges must be jointed simultaneously. However in this case

<sup>85</sup>an alternative method for the activation of the snaps is shown in the last section of this chapter

the snap-fit joints are on the part which is being inserted, therefore they lie on a common plane. The joints on both edges can be rotated on this common plane, within a range of  $\pm 15^\circ$ <sup>86</sup> from their regular shape, where the cantilever is perpendicular to the edge. This way, a 2D range of possible assembly directions can be defined for both edges. The intersection between these two 2D ranges shows all possible vectors for this assembly step.

- **Dual Edge Inverse** - Figure 5.14d - Finally, the fourth step in the double-layered assembly is the most restrictive case. It is very similar to the last step: Again, the plate which is being inserted needs to connect to non-parallel edges simultaneously, but this time the snap-fit joints are not on the plate which is being inserted, but on the four counterparts. In consequence, the assembly vector for this step must lie on both of the non-parallel planes of the two counterparts. The only possible vector in this case is presented by the intersection of these planes. However the same rules apply for the rotation of the snap-fit joints: The maximum on-plane rotation of  $\pm 15^\circ$  defines a 2D range of possible assembly vectors for both planes. The parts can be jointed if the intersection line between the two planes lies within the two 2D ranges.

An important consequence is that in the *Dual Edge Inverse* step, multiple edges can only be jointed if there is a common vector on *all* of the planes of the counterparts. For two (double-layered) counterparts, there will always be a common vector found at their intersection line. For three or more counterparts a solution is typically impossible. In a regular antiprismatic folded plate, or in the Miura-Ori based Folded Plate designed by Buri [BW06], only two edges must be jointed simultaneously at a time<sup>87</sup>. However a double-layered construction requires an *offset* of the folded plate. In both cases the offset geometry will require the simultaneous assembly of three edges. In Figure 5.15, these short additional edges are not jointed. Possible solutions for the jointing of these edges, if required, include the Nejiri-Arigata-inspired technique from the previous chapter, or alternatively snap-fit joints with an out-of-plane assembly direction.

### Antiprismatic Double-Layer, Bidirectionally Folded Prototype

In figure 5.12, a detailed isometric drawing of the double-layered, bidirectionally-folded geometry was provided, based on the *Miura-Ori* folding pattern. The drawing illustrates both the *Dual-Edge Regular* (5.12a) and the *Dual-Edge Inverse* (5.12b) steps.

The alternative *Antiprismatic* folding pattern was also indicated in figure 5.15e. Based on the advantages of the antiprismatic geometry which were described in the additions of chapter 4, a fully detailed version was also developed for this version. Figure 5.15 shows an isometric

---

<sup>86</sup>  $\pm 15^\circ$  has been chosen as a moderate rotation, which does not distort the geometry of the joints very much. Larger rotations may be possible, especially when the snap-fit joint is not being activated through the insertion force.

<sup>87</sup> see both assembly sequences on the figures 5.12d and 5.12e

drawing of this prototype, once again illustrating the *Dual-Edge Regular* (5.15a) and the *Dual-Edge Inverse* (5.15b) steps.

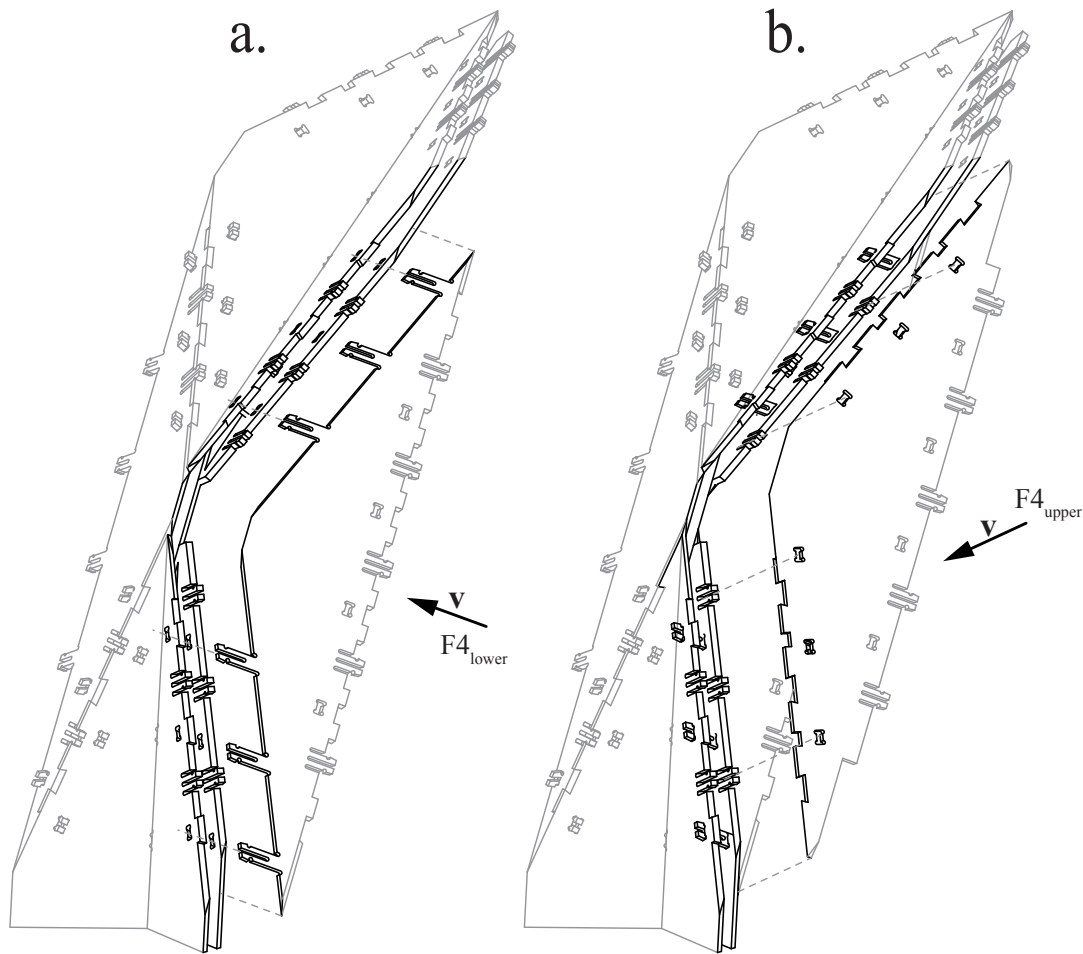


Figure 5.15 – Antiprismatic Double-Layer Bidirectionally-folded Prototype

The drawing shows that, depending on the panel thickness and the spacing between the plates, the latches and snaps must be positioned in an alternating manner. In 5.15a, the snaps of the counterparts are always positioned in between the snaps of the part which is being inserted. Another detail is shown in 5.15b: The snap fit joints on the exterior layer have been combined with dovetail joints. This is an alternative to the protrusion of the panel, which was illustrated in the first prototypes (Figures 5.9, 5.10 and 5.11). The short unconnected edges are visible in the middle of both steps.

A computer-generated visualization of this prototype is shown in figure 5.16. This image shows that in such a configuration, the snap-fit joints would only be visible on the transversal interior edges. The visual appearance could be improved through a replacement of the snaps on these particular edges with dovetail joints.

Figure 5.17 shows a cross-section through the same prototype. This cross-section shows how

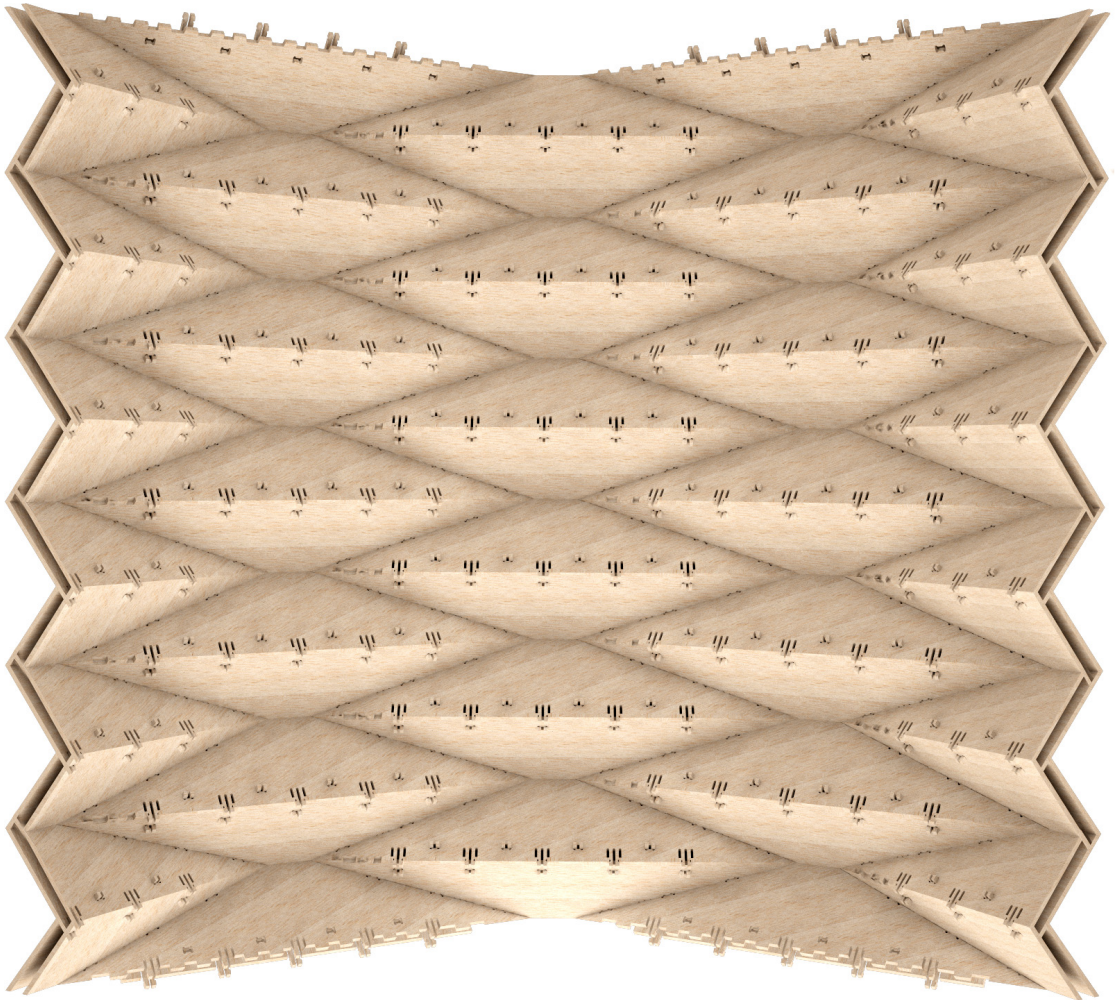


Figure 5.16 – Antiprismatic Double-Layer Bidirectionally-folded Prototype - Interior View

the two layers are interconnected, entirely without additional connectors, but only through the geometry of the components themselves. This particular cross-section shows that the intersecting connections have been applied to both the long transversal edges, and to the shorter diagonal edges of the structure.

### Application to Doubly-curved Shells

A doubly-curved folded plate shell and its advantages were presented and discussed in chapter 4. It was demonstrated that the previously developed algorithms could be used to automatically process geometrical variations of components. The small incremental variation of the geometry of each component lead to the double curvature in the overall geometry of the folded plate shell. The exact same technique can be applied to the double-layer prototype in figure 5.15 and 5.17. However, this requires a complete algorithmic implementation of the plate and joint geometry and its dependencies.





Figure 5.17 – Antiprismatic Double-Layer Bidirectionally-folded Prototype - Cross-section

### Preactivation

During the assembly of the 1-directionally-folded arch physical prototype, it was observed that the simultaneous assembly of multiple snap-fit joints becomes increasingly difficult. This is because the mating forces of each individual snap are adding up to an increasingly high force that is needed for the insertion of the parts. This is particularly problematic with double-layered structures, where always at least two edges must be jointed simultaneously.

One possible solution for this problem lies in the joints parameter setting. While the friction of the snaps can hardly be influenced, parameters such as the insertion angle  $\alpha$  or the cantilever cross-section can be changed to allow for a lower deflection force and an easier insertion of the parts. However, these changes will bring other problems, such as a longer protrusion of the snaps, or a lower pull-out resistance.

An alternative solution, which requires no compromise in the performance of the joints, is an external activation of the snaps (Figure 5.18): While in regular cantilever snaps, the deflection force is generated through a transformation of the insertion force due to the joint geometry, it is also possible to apply an external force (for example with pliers) and to temporarily block the cantilevers. This technique requires additional pins on top of the snaps, and an additional custom shaped jig<sup>88</sup>. This jig must be designed in a way that its geometry 1. lets the two cantilevers deflect and 2. fits through the regular latch of the snaps. For an added convenience of assembly, the shape of the jig has been designed with an additional locator feature, which allows for fast and simple connection of the parts.

In the design of the geometry of both the pins on top of the snaps, and the additional jigs, the

---

<sup>88</sup>Note that this is only possible with the mirrored double-snaps which have been used throughout this chapter

forces induced by the deflection of the cantilevers must be considered. The shapes must be designed in a way that remains within the limitations of the material properties.

With this pre-activation technique, one snap can be activated at a time, which allows even for large amounts of snaps per edge or the simultaneous assembly of multiple edges. It also solves general problems with plastic deformations and fracture around the hook of the snaps: During a regular, self-activated deflection, high compressive forces and friction may cause damage to the hook geometry, which is crucial for the joints retention function. In a self-activated joint, this problem can only be addressed through a compromise between the deflection force, the hook's undercut length and the insertion angle  $\alpha$ . The pre-activation method presents an interesting alternative to this technique.

Finally, although additional tools and jigs are needed for the pre-activated snaps, it must still be considered an integral mechanical attachment technique. The joint works entirely with mechanical forces and the additional jigs can be removed after the joints engagement.

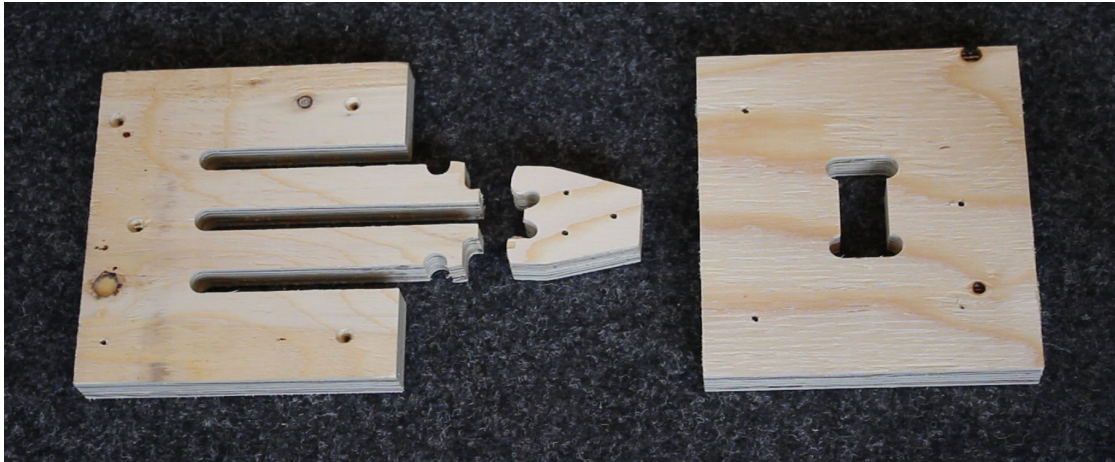


Figure 5.18 – Pre-Activation of Snap-fit Joints - Additional Jigs can be used to pre-deflect the cantilever on the snap-fit joints.



## **Bibliography**

- [Bon05] Paul Bonenberger. *The First Snap-Fit Handbook - Creating and Managing Attachments for Plastics Parts*. Carl Hanser Verlag, 2005.
- [Bur10] Hani Buri. *Origami - Folded Plate Structures*. PhD thesis, EPFL, Lausanne, 2010. EPFL Doctoral Thesis No. 4714.
- [BW06] Hani Buri and Yves Weinand. BSP Visionen - Faltwerkstrukturen aus BSP-Elementen. In *Grazer Holzbau-Fachtage*, 2006.
- [Com07] BASF The Chemical Company. Snap-fit design manual. BASF Corporation, Engineering Plastics, Florham Park, New Jersey, 2007.
- [DIB11] DIBt. *Allgemeine bauaufsichtliche Zulassung Kerto-Q Z-9.1-100, Paragraph 4.2 and Attachment No 7, Table 5*. Deutsches Institut für Bautechnik, 2011.
- [Fal10] Andreas Falk. Form exploration of folded plate timber structures based on performance criteria. In *Taller, Longer, Lighter: meeting growing demand with limited resources : IABSE-IASS Symposium 2011. London*. Hemming Group Ltd., 2011, 2010.
- [fTA13] European Organisation for Technical Approvals. Eta-07/0029 kerto ripa elements - wood based composite slab element for structural purposes, 2013.
- [Gra86] Wolfram Graubner. *Holzverbindungen, Gegenüberstellung von Holzverbindungen Holz in Holz und mit Metallteilen*. Deutsche Verlags-Anstalt Stuttgart, 1986.
- [Hah09] Benjamin Hahn. Analyse und beschreibung eines räumlichen tragwerks aus massivholzplatten. Master's thesis, EPFL, Lausanne, 2009. Master Thesis.
- [ICD14] ICD/ITKE. Laga exhibition hall, 2014. <http://icd.uni-stuttgart.de/?p=11173>.
- [LLC00] Bayer MaterialScience LLC. Snap-fit joints for plastics - a design guide. Bayer Polycarbonates Business Unit, Pittsburgh, Pennsylvania, 2000.
- [lMea13] Riccardo la Magna et al. From nature to fabrication: Biomimetic design principles for the production of complex spatial structures. *International Journal of Spatial Structures*, Vol. 28 No. 1:27–39, 2013.
- [Lus95] Anthony Luscher. *An Investigation Into the Performance of Cantilever Hook-type Integral Attachment Features*. PhD thesis, Department of Mechanical Engineering, Rensselaer Polytechnic Institute, Troy, NY, 1995.
- [Mes06] Robert W. Messler. *Integral Mechanical Attachment: A Resurgence of the Oldest Method of Joining*. Butterworth Heinemann, 2006.
- [oCC14] Intergovernmental Panel on Climate Change. Ipcc, accessed june 30, 2014. <http://www.ipcc.ch/index.htm>.

- [RNW14] Christopher Robeller, SeyedSina Nabaei, and Yves Weinand. Design and fabrication of robot-manufactured joints for a curved-folded thin-shell structure made from clt. In Wes McGee and Monica Ponce de Leon, editors, *Robotic Fabrication in Architecture, Art and Design 2014*, pages 67–81. Springer International Publishing, 2014.
- [TB09] Martin Trautz and Peter Von Buelow. The application of folded plate principles on spatial structures with regular, irregular and free-form geometries. In *IASS - Evolution and Trends in Design, Analysis and Construction of Shell and Spatial Structures, Valencia*, 2009.



## **Conclusion and Further Work**

### **Part III**



## 6 Conclusion

In his discovery of folded plates as a structural principle, Hermann Craemer emphasized the seamlessness, the perfectly continuous and rigid joints between the plates that could be achieved with in-situ cast concrete, as inherent to the concept of folded plate structures.<sup>89</sup>

Later, changes in the labour market, the industrialization and new materials have led to the construction of prefabricated folded plates, which had to break with the concept of seamlessness, in favor of other benefits. On site, such prefabricated, discrete plates or modules must be connected with joints, which introduce weak points in these surface-active structures. The rigidity and stiffness of these joints is essential for the overall structure.

In addition to these structural challenges, the precision, rapidity and ease-of-assembly of a folded surface structure from separate plates depends on the joining technique. This has a particular relevance, when large amounts of smaller modules need to be assembled, which was the case in previous prefabricated constructions with fiber-reinforced plastics in the 1960s, and with engineered wood panels, beginning in the 2000s.

With automated fabrication technology readily available at the timber manufacturing companies, the construction of advanced designs, such as doubly-curved folded surface structures, which obtain their structurally beneficial double curvature<sup>90</sup> through incremental changes in the geometry of the individual plates was already proposed in previous studies.

However, prototypes were only realized as singly-curved folded surfaces, consisting of geometrically identical components and fabricated with machine-tool-technology, using templates and guides for the cutting and assembly of geometrically identical components.<sup>91</sup>

Instead, this thesis investigated the use of *integral mechanical attachment* techniques, which integrate guides for the assembly as locator features, and elements for the attachment as connector features, entirely through geometrical features in the form of the plates.

---

<sup>89</sup> see page 23

<sup>90</sup> see page 87

<sup>91</sup> see page 30

### Investigations

The first investigation demonstrated that the geometry of the joints can improve the rigidity and stiffness of edgewise joints for timber folded plate structures. The 1DOF multiple-tab-and-slot-joints were applied to CLT panels for the first time, combined with additional adhesive bonding. This type of joint allowed for a load-bearing edgewise joint between the plates, which is normally not possible, because glued joints cannot resist forces normal to the interface. The dovetail-type multiple-tab-and-slot-joints however did not only increase the contact surfaces between the parts, but they also allowed to transform traction and bending forces into shear and compression along the side faces of the joints, which can be well supported by the adhesive bonding. This was demonstrated through a curved-folded thin-shell prototype structure, which spanned over a length of 13.5 meters, with a shell thickness of only 77mm.

The second investigation showed the application of the joints without additional connectors, such as adhesive bonding, which allows for the flat-packed transport and the on-site assembly of parts. Instead, the blocking of the insertion direction of the joints was achieved through the mutual blocking of multiple parts with different insertion directions. Furthermore, the construction of a bidirectionally folded surface structure presented a major challenge, because multiple non-parallel edges of the components had to be assembled simultaneously. When using 1DOF joints, the assembly directions of all simultaneously connected joints must be parallel.

Inspiration for a solution to this problem was found in traditional Japanese joinery, where *Nejiri Arigata* Joints demonstrated the assembly of 1DOF edgewise joints for plates not along a vector that lies within one of the two plates, but along the external bisector of the dihedral angle. This was made possible through the cross-section profile of the joints, in which multiple pins are used jointly to block all but one relative translation between the parts.<sup>92</sup> While the *Nejiri Arigata* Joints only used this technique for an assembly along the exterior bisector of the plates, this thesis shows how the technique can be used for a range of insertion directions, which are found within a 3-dimensional rotation window, which can be calculated for every edge of a folded plate structure, based on its dihedral angle and fabrication-constrained parameters.

The possibility to now rotate the assembly direction of 1DOF edgewise joints, allowed for the simultaneous assembly of multiple non-parallel edges. The 3-dimensional assembly vector-spaces visualize all possible directions for individual joints. A boolean intersection of these rotation windows shows if a set of edges can be jointed simultaneously and provides a common set of possible rotations for their assembly. These concepts were implemented in an algorithmic tool, through the API of a CAD software. The tool was then used for the construction of a first bidirectionally folded and doubly-curved folded surface prototype, built from LVL panels.<sup>93</sup>

---

<sup>92</sup>see page 99

<sup>93</sup>see page 91

---

While the investigations in the chapters 3 and 4 were utilizing integral mechanical attachment techniques from the category of rigid interlocks, the investigation in chapter 5 introduced another category, so-called *elastic interlocks*, which are commonly used in other industry sectors. These techniques are based not only on geometry parameters, but also on material parameters, including the elasticity modulus, the maximal strain and the friction coefficient. These elastic interlocks present an addition to the mutual interlocking of parts, which will firmly connect individual parts, which can be used to reduce and replace guides and additional connectors during the assembly of larger structures, which are not completely assembled yet. Such snap-fit joints can retain elements and resist bending moments, but not shear forces along the edges, which makes them an ideal addition to the rigid interlocks, which can resist the shear forces, but not retain elements along their direction of insertion.

It was demonstrated how the combination of these joint features allows for the fully integral jointing of *double-layered* corner joints in timber folded plate structures. Through an intersection of the interior layers through each other, enabled by double-length connectors, a direct connection between all four layers in such connections can be established. This is made possible through a special assembly sequence, where the layers interlock with one another.<sup>94</sup> Finally this concept was combined with the findings from chapter 4. The technique for the assembly of bidirectionally-folded surface structures, through the simultaneous assembly of multiple edges, was adapted for double-layered constructions, which results in additional fabrications and assembly constraints. A four-step procedure for such assemblies was described.

### **An Integral Approach**

The individual technical challenges, such as the automatic fabrication of the joints, the integral jointing of bidirectionally-folded, doubly-curved and finally double-layered constructions have been consolidated step by step into a coherent system, assembled entirely through Integral Mechanical Attachment. This consolidation was made possible through the successive integration of the findings into algorithms, which allowed to develop complex procedures in incremental steps.

One of the greatest benefits of prefabrication is the efficient use of centralized, advanced technology for the production of parts, especially in combination with engineered wood panels, which can be machined easily and precisely into various shapes. Considering the readily available technology in timber construction companies, such as 5-axis CNC routers, and in architectural design, such as CAD API's and Visual Programming, the automatic fabrication of integrated joints appears self-evident.

The constraint-shaped rotation window for the assembly of the joints (Figure ??) illustrates the design principle of integrally jointed structure systems, in which the connections are not addressed at the end of the design process. Instead, the joints introduce an additional set

---

<sup>94</sup> see page 136



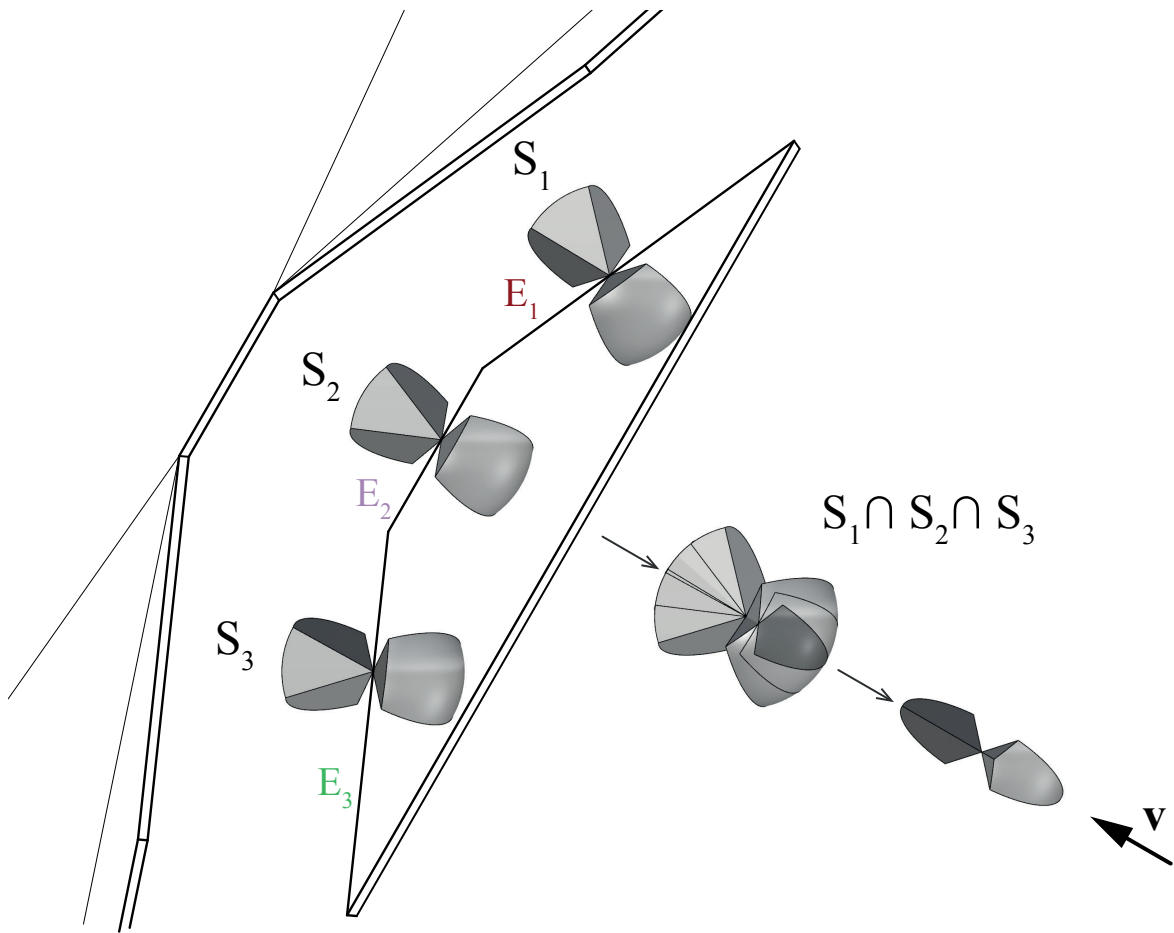


Figure 6.1 – Constraint-shaped range of possible rotations for the assembly vector

of constraints in the initial design of a structure. Together with the material properties, they are located at the beginning of the design process, followed by architectural and structural considerations.

In the age of machine-tool technology, mass-production constrained architectural designs to the construction with large numbers of identical elements. Information-tool-technology however allows for the efficient fabrication of mass-*customized* parts, enabled by digital geometry processing. This combination puts instrumental geometry at the disposal of architects, as a powerful tool for the integration of functions into the form of objects and structure systems.

## 7 Further Work

The investigations in this thesis demonstrated new joint geometries, fabrication- and assembly techniques, which were verified with physical prototypes. These prototypes were primarily used for the verification of the assembly and fabrication procedures. The load-bearing behavior of the connections was also discussed for all prototypes, including schematic drawings, finite element models and physical loading of prototypes. These experiments have provided some first, valuable information about the behavior of the proposed integral joints.

However, further work is necessary to fully understand the structural performance of these joints. Specific investigations are necessary to study the connections resistance to in-plane and out-of-plane forces, and bending moments. In these investigations, the influence of various parameters, most notably the joints Euler angle rotations  $\theta_1$ ,  $\theta_2$  and  $\theta_3$ , the length of the individual tabs and slots, and different types of stress reduction notches, must be analyzed. This research must show in how far exactly the integral mechanical attachment techniques can reduce or replace mechanical fasteners in timber folded plate structures. Finally, a simplified numerical method must be established that allows for the structural dimensioning of the joints, through the modification of the before mentioned parameters. This method is essential in order to take advantage of such parametric joints, which cannot be dimensioned as easily as mechanical fasteners.

Some of this work has already been initiated and conducted in parallel to the investigations in this thesis. A new doctoral research project has been initiated in 2012 at the Timber Construction Laboratory IBOIS for these investigations. The work of the civil engineer Stephane Roche is focused on the general mechanical behavior of integral multiple-tab-and-slot joints.

In terms of materials, multiple types of cross-laminated engineered wood panels have been used for the experiments and prototype constructions in this thesis. A focus was put on panels which are suitable for larger-scale structural applications, including the necessary certifications. Laminated veneer lumber panels (LVL) were used in the chapters 4 and 5. These panels have proven to be particularly suitable for the fabrication of integral joints, which is largely due to their high homogeneity. The material is dense and defects such as knots or

holes are rare and appear only in one of the 3mm thick layers at a time. This has proven to be more difficult with Cross-laminated timber (CLT), which were used in chapter 3. Chipping in general and knots in the boards have proven to be more problematic for the sharp exterior corners of the dovetail joints. The stress-reduction notches in the CLT panels have caused similar problems. A finger-joint geometry is yet to be tested on such panels. Here, all cuts for the flanks of the fingers could be parallel to the stress cuts in the CLT, to reduce chipping and breaking of corners.

Beech LVL panels are also yet to be tested with the integral 1DOF-joints presented in this thesis. 3DOF multiple-tab-and-slot joints combined with mechanical fasteners have already been applied successfully to the LaGa shell structure by the Institute for Computational Design in Stuttgart (see page 20). Apart from their sustainability, through the use of local resources, these panels provide a high density and mechanical strength.

Similar to the previously mentioned parameter studies for the joints themselves, parameter studies are yet to be carried out for the antiprismatic, bidirectionally-folded surface structures introduced in the chapters 4 and 5. In this thesis, the geometry parameters have been optimized for the fabrication and assembly of the shells, as well as some basic structural considerations. However, after the first proof-of-concept for the construction principle, provided by this work, the influence of various parameters on the mechanical performance of these structure systems must be studied. (see additions of chapter 4) These include the dihedral angles  $\varphi$  together with the system angle  $\gamma$ , the length of the modules, and the angles between neighboring edges  $\lambda$  (see page 110), while also considering and respecting the assembly and fabrication constraints provided by this thesis. A new doctoral research project has been initiated in 2014 at the Timber Construction Laboratory IBOIS for these investigations. The work of the civil engineer Andrea Stitic is focused on the analysis of folding form possibilities for timber folded plate structures.

The double-layer, bidirectionally-folded surface structure illustrated in chapter 5 has been presented as a virtual prototype, which demonstrates the assembly. As mentioned in the additions of chapter 5, a physical prototype is yet to be built to verify this method. An important tool for the construction of this prototype has been introduced with the pre-activation of the snap-fit joints (see page 140), which is crucial for the simultaneous assembly of large amounts of snap-fit connectors.

Also, the construction of a doubly-curved version (see page 139), analog to the one presented in chapter 4 is yet to be built, which requires the consolidation of the presented techniques into algorithmic tools. This necessary for the processing of the resulting, geometrically different parts.

## Appendices **Part**



## A Joint Parameter Interactions

it was explained in chapter 4 (see figure 4.12, page 84), that the 3-dimensional rotation window, which represents all possible assembly directions for a given edge  $E$ , is defined through three cardan rotations  $\theta_1$ ,  $\theta_2$  and  $\theta_3$ . The maximum values of these individual parameters are influenced by one another. For example,  $\theta_3$  was set to  $15^\circ$ , following the recommendations by Simek and Sebera, for all prototypes in this thesis. A higher value for the parameters  $\theta_3$  will decrease the range for  $\theta_2$ , while a smaller value for  $\theta_3$  will increase the range for  $\theta_2$ .

The reason for this behaviour is the limitation of the tool inclination during the joint fabrication process, to a maximum value of  $\beta_{max}$ . Let us assume we cut a dovetail joint where the dihedral angle  $\varphi$  between the plates is  $90^\circ$ . In this case, an inclination of the dovetail side faces at  $\theta_3 = 15^\circ$ , will result in a maximum tool inclination of  $\beta = 15^\circ$  during the fabrication.<sup>95</sup>  $\beta$  is only influenced by  $\theta_3$  in this case.

However, if we increase or decrease the joints dihedral angle  $\varphi$  by  $20^\circ$ , to become  $70^\circ$  or  $110^\circ$ , the maximum tool inclination  $\beta$  will be  $20^\circ$ . The dominant factor is now  $\theta_2$ . In both cases, an increase of  $\theta_3$  will reduce the targets possible side rotation  $\theta_{2,max}$  and vice versa, for a given  $\beta_{max}$ .

$\theta_1$ , the out-of-plane rotation of the assembly vector, about the joints edge, also has an effect on the two other rotations. The magnitude with which  $\theta_3$  will reduce the range for  $\theta_2$  is the highest when  $\theta_1 = 0^\circ$  or  $\theta_1 = \theta_{1,max}$ , and the lowest for the exterior bisector of the dihedral angle ( $\frac{\theta_{1,max}}{2}$ ). In the bisector case,  $\theta_3$  will be split: half of it will affect the tool inclination on part A, the other half of it will affect the tool inclination on part B. For the case where  $\theta_1 = 0^\circ$  or  $\theta_1 = \theta_{1,max}$ ,  $\theta_3$  will fully affect only one of the two parts, resulting in a higher maximal tool inclination for the fabrication of this joint.

Following up on the work presented in this thesis Geoffrey Mattoni analyzed the interrelations of these parameters in his masters thesis. [Mat14] The following figures are taken from his

---

<sup>95</sup>this example does not include miter-jointed segments (see additions of chapter 4, page 110) Joints with miter-segments will always result in a minimum tool inclination  $\beta_{min} = \frac{\varphi}{2}$ .

## Appendix A. Joint Parameter Interactions

analysis which was carried out in in Maple.

Figure A.1 illustrates the previously described interrelations: The white range, which shows the range for the possible insertion directions, is the largest for  $\frac{\theta_{1,max}}{2}$  (middle of the graphs). Figure A.2 shows the 3-dimensional range accordingly.

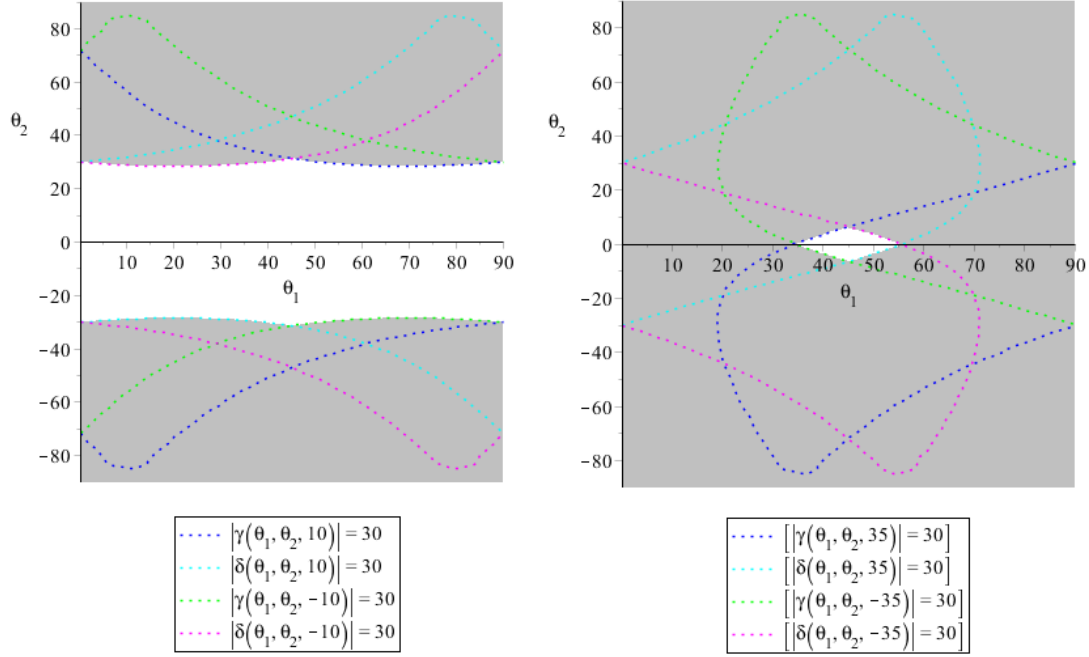


Figure A.1 – Graphics for suitable insertion vectors, for a 90° dihedral angle, and a 30° constrained tool, for two  $\theta_3$ . In grey, the area of unworkable insertion vector. Figure taken from [Mat14]

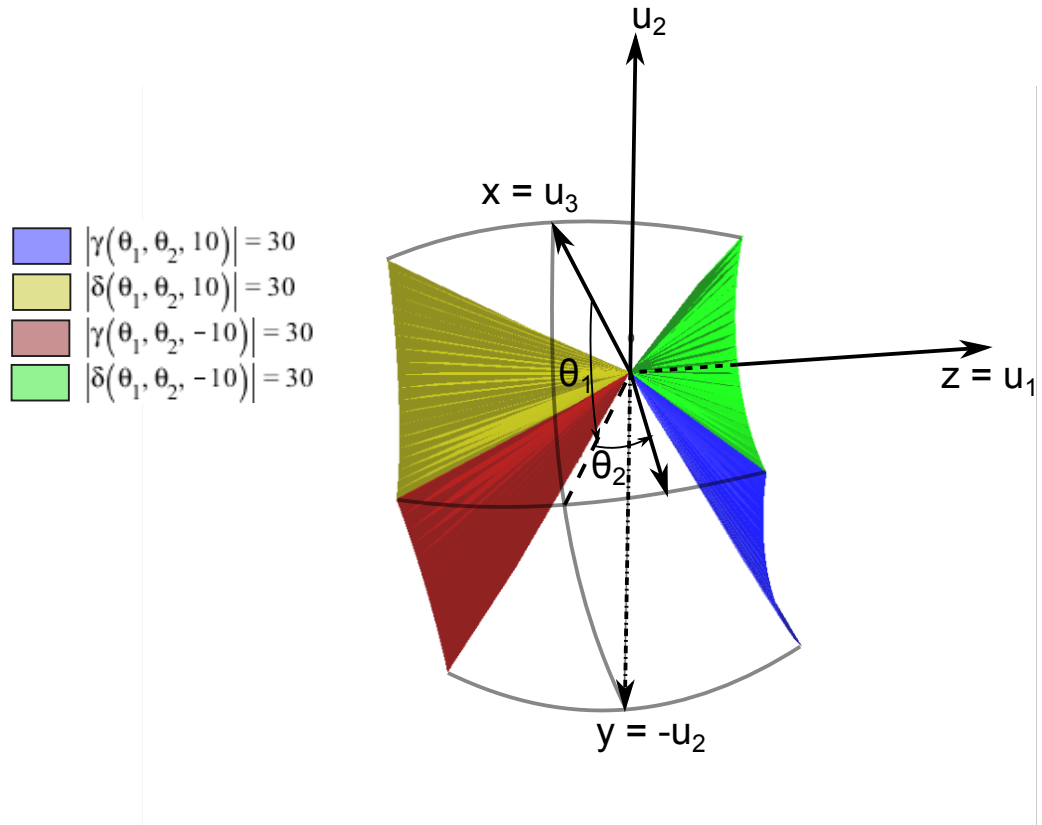


Figure A.2 – Limits for the insertion vector, drawn with the spherical frame, for  $\theta_3 = 10^\circ$ ,  $\beta_{max} = 30^\circ$  and  $\varphi = 90^\circ$ . Figure taken from [Mat14]





## B Integral Joints for UHPFRC Formwork

An alternative application for the integral joining techniques presented in this thesis, was investigated in the construction of formwork for thin-shell folded surface structures built from concrete. Generally, the construction of formwork for curved shells is costly and time-consuming. Large additional sub-structures may be necessary to create the surfaces of singly- or doubly-curved moulds, such as a series of transversal contour ribs or plates.

The algorithmic tools<sup>96</sup> developed in this thesis allow for the rapid, precise and efficient fabrication and assembly of bidirectionally folded surface structures, built from cross-laminated timber panels. Furthermore, it was demonstrated how double-layered structures can be built, considering certain geometry constraints for the surface offset.

It was therefore investigated, if such double-layered assemblies can be used for formwork applications. Experiments were carried out with the previously discussed tools for the geometry and fabrication of the timber structures, without modifications. Ultra High Performance Fiber Reinforced Concrete (UHPFRC) was used for the construction of prototypes. For the moulds, 15mm / 11-layer surface-coated<sup>97</sup> birch plywood panels for concrete formwork were used.

### UHPFRC Folded Arch Prototype

An UHPFRC folded surface prototype was designed, based on the geometry of the plywood prototype presented in figure 4.13<sup>98</sup>. This singly-curved arch, with a span of 1.65m, transversal dihedral angles  $\varphi_{trans} = 120^\circ$  and diagonal dihedral angles  $\varphi_{diag} = 113.5^\circ$  served as the inner part of the mould. A second layer for the formwork was generated with a continuous offset of 35mm (48 plate components in total). Like in the previous prototypes, regular dovetail joints were used for the transversal folds, and the Neijri-Arigata inspired technique with rotated insertion vectors was used for all other folds. The parts were fabricated using the same Makam7s 5-axis CNC Router.

---

<sup>96</sup>the Grasshopper component (see page 111) was used for the joint processing

<sup>97</sup>Metsäwood "Form" panels, with a phenolic film hot-pressed onto the panel surface

<sup>98</sup>see page 85



Figure B.1 – Formwork for the UHPFRC folded surface prototype, assembled from 48 dovetail-jointed components. Fabricated from 15mm birch plywood panels for formwork applications.

For the assembly (see figure B.1a), one additional self-tapping screw was applied to the middle-pin of each joint. Thin adhesive tape was applied to the exterior side of the joints on the inner layer of the mould, and the interior side of the joints on the outer layer of the mould. This was necessary for the tightness of the mould, in order to close the small tangential notches, and to cover the uncoated side-faces of the plates at the joints.

The UHPFRC was cast into the mould through one side, which was left open for this purpose. After a curing period of 3 days, the mould could be removed easily (see figure B.1b). The surfaces of the UHPFRC prototype were of high quality (see figure B.2).

### Collaboration

The UHPFRC folded surface prototype was fabricated in collaboration with Paul Mayencourt, Research Assistant at the Laboratory for Timber Construction EPFL IBOIS, and Christoph Loraux, PhD Assistant at the Structural Maintenance and Safety Laboratory EPFL MCS.

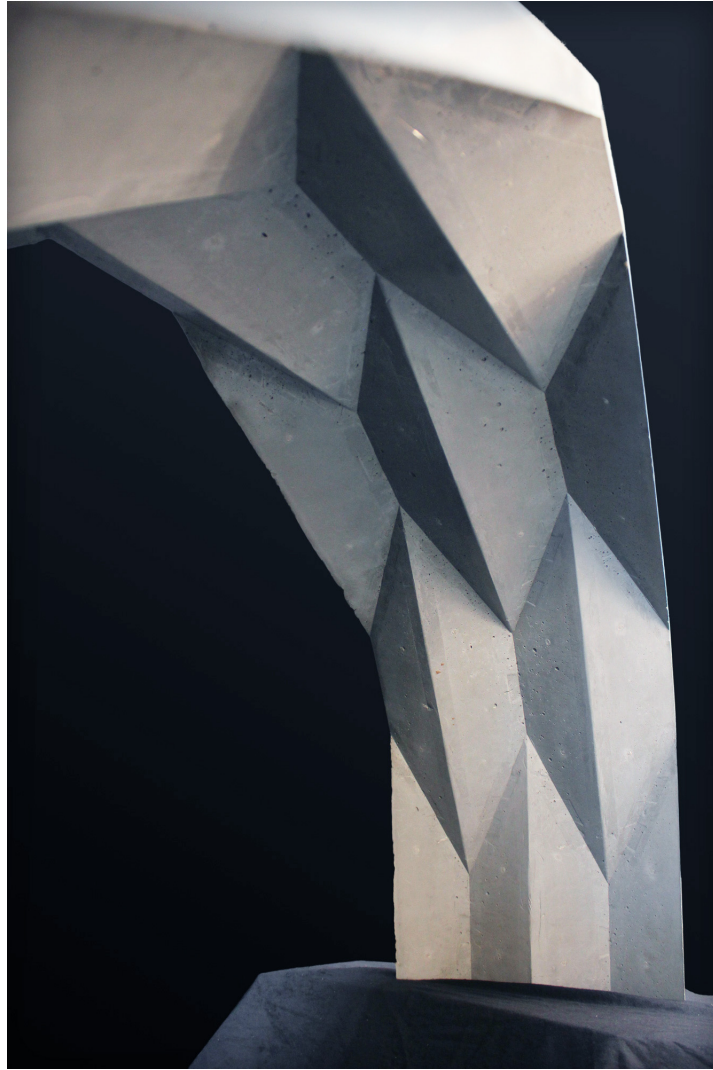


Figure B.2 – Interior View of the UHPFRC folded surface prototype



# List of Figures

<b>I</b>	<b>Introduction and State-of-the-Art</b>	<b>1</b>
<b>1</b>	<b>Introduction</b>	<b>5</b>
1.1	Integral Mechanical Attachment . . . . .	6
<b>2</b>	<b>State-of-the-Art</b>	<b>7</b>
2.1	Hand-crafted Dovetail Joint . . . . .	9
2.2	Integral Plate Joints fabricated with Machine-tool-technology . . . . .	11
2.3	Cam-and-bolt corner-joint for furniture made from particle boards . . . . .	12
2.4	Numerically Controlled Joinery Machines . . . . .	13
2.5	Swissbau Pavilion, Experimental Prototype Structure presented at the Swissbau Exhibition in Basel, 2005 . . . . .	16
2.6	Integral Multiple-Tab-and-Slot Joint Prototypes, 2010 . . . . .	18
2.7	First Applications of Integral, 2-plane, 3DOF, Multiple-Tab-and-Slot Joints . . .	19
2.8	Landesgarteschau Exhibition Hall 2014 . . . . .	21
2.9	Threefold Load-bearing Action of a Folded Plate . . . . .	22
2.10	Origins of Folded Plate Structures . . . . .	23
2.11	Folded Plate Church in Hoensbroek, Netherlands, 1964. Built from precast concrete components, with a span of 25 m. . . . .	25
2.12	Antiprismatic Folded Plates . . . . .	27
2.13	Gluelam Folded Plate structure for the Music Rehearsal Hall in Thannhausen, 2002	29
2.14	Timber Folded Plate Barrel Vault . . . . .	30
2.15	Timber Folded Plate Barrel Vault Details . . . . .	30
2.16	Temporary Chapel St. Loup . . . . .	32
<b>II</b>	<b>Investigations</b>	<b>41</b>
<b>3</b>	<b>Robot-Manufactured Joints for a Curved-Folded Thin-Shell Structure Made from CLT</b>	<b>43</b>

## List of Figures

---

3.1	Curved-folded Paper Model - Design proposal for a thin-shell structure built from curved timber panels . . . . .	44
3.2	Residual Stresses in elastically bent panels . . . . .	45
3.3	Curved-folded Timber Shell Prototype . . . . .	47
3.4	Curved-folding Geometry . . . . .	48
3.5	Algorithmic Joint Geometry Generation . . . . .	50
3.6	1DOF Joint Geometry Toolpath Schematic . . . . .	51
3.7	1DOF Joint Geometry Toolpath Details . . . . .	51
3.8	Joint fabrication (tool path plot). Left planar finger-joint type connection (connections CV-CX), Right prismatic dovetail-type joint (connections W-CV) . . .	52
3.9	Preliminary structural analysis results under the self-weight load case. Top Von-Mises stress distribution. Bottom total deformation . . . . .	53
3.10	Concave and convex mold for the lamination and formatting of the curved panels at scale 1:5 . . . . .	54
3.11	Planar finger-type joints . . . . .	54
3.12	Von-Mises stress distribution for Dovetail-type connections $CV_1 - W_1$ and $CV_2 - W_2$ on the full-scale prototype. Results are generated from a full three dimensional finite element simulation . . . . .	55
3.13	Von-Mises stress distribution for detailed model . . . . .	56
3.14	Side-cutting with the robot router . . . . .	57
3.15	Sawblade-cutting with the robot router . . . . .	58
3.16	Assembly of the roof panels . . . . .	59
3.17	Schematic Drawing of the Connector Elements made from Cross-laminated LVL Panels . . . . .	60
3.18	Assembly of the Dovetail-type Connectors . . . . .	61
3.19	Robot-fabricated Dovetail Joints on a Curved CLT Panel . . . . .	62
3.20	Exhibition of the Completed Pavilion in Mendrisio, September 2013 . . . . .	63
3.21	IBOIS Curved CLT Pavilion 2013 - Adhesive bonding interfaces and distribution of forces . . . . .	65
3.22	Detailed Finite Elements Analysis of the Contact Surfaces on the Dovetail Joints . . . . .	66
3.23	Connection $W_1 - CV_1$ Before the Removal of the Temporary Curved CLT Pavilion . . . . .	67
3.24	Joint Deformation During Elastic Bending . . . . .	70
<b>4</b>	<b>Interlocking Folded Plate - Integrated Mechanical Attachment for Structural Wood Panels</b>	<b>73</b>
4.1	Concept of Mutual Blocking of Components . . . . .	75
4.2	Antiprismatic Folded Plate Shell . . . . .	76
4.3	Structural Principle of an Antiprismatic Folded Plate . . . . .	76
4.4	Antiprismatic Folded Plate Shells - Built Structures . . . . .	77
4.5	Antiprismatic Folded Plate with 1DOF joints? . . . . .	77
4.6	Interlocking folded plate prototype . . . . .	80
4.7	Joint geometry . . . . .	80

4.8	Distribution of traction and compression in a folded plate shell . . . . .	81
4.9	1DOF joint force distribution . . . . .	82
4.10	Fabrication constraints . . . . .	82
4.11	Simultaneous assembly of non-parallel edges . . . . .	83
4.12	Insertion direction rotation . . . . .	84
4.13	Folded-plate arch prototype . . . . .	85
4.14	Flexural behaviour of the arch prototype . . . . .	86
4.15	Doubly-curved folded-plate geometry . . . . .	87
4.16	Connectivity graph of the folded plate shell prototype . . . . .	88
4.17	Folded plate shell schematic assembly . . . . .	90
4.18	Completed folded-plate shell prototype . . . . .	91
4.19	Load-displacement curve of the doubly-curved shell prototype . . . . .	91
4.20	Doubly-curved Prototype, Folded in 2 Directions - Interior View 1 . . . . .	92
4.21	Doubly-curved Prototype, Folded in 2 Directions - Interior View 2 . . . . .	93
4.22	Antiprismatic Folded Plate Geometry . . . . .	94
4.23	Comparison of an Antiprismatic and Miura-Ori Cylindrical Shell . . . . .	95
4.24	Edge-to-edge connectivity of Antiprismatic Folded Plates . . . . .	97
4.25	Nejiri Arigata Joint Geometry . . . . .	98
4.26	Quadrilateral Pin Cross-section Shapes for Tab-and-Slot Joints . . . . .	99
4.27	2D Rotation of Assembly Vector . . . . .	100
4.28	Simultaneous Assembly . . . . .	100
4.29	Interrelation of joint parameters . . . . .	101
4.30	Common Assembly Rotation Window . . . . .	103
4.31	Algorithmic Generation of the Joint Geometry and the Machine Code . . . . .	104
4.32	Joint Fabrication . . . . .	105
4.33	Assembly of a line of G-Code for a standard horizontal cut point . . . . .	108
4.34	Miter-jointed Transition Segments . . . . .	111
<b>5</b>	<b>Snap-fit joints - CNC fabricated, Integrated Mechanical Attachment for Structural Timber Panels</b>	<b>115</b>
5.1	Variations of Elastic Cantilever Locks for Plastics . . . . .	117
5.2	Basic Cantilever Hook Nomenclature . . . . .	120
5.3	Retention Force Diagram . . . . .	121
5.4	CNC fabricated Snap-fit Joint for LVL Panels . . . . .	123
5.5	Box Girder Specimen with Combined Snap-fit and Tab-and-slot Joints . . . . .	124
5.6	FEM Simulation of a 3-point Flexural Test with the Box Girder Specimen Geometry	125
5.7	Side-cutting Fabrication of a Non-orthogonal Snap-fit Joint with a 5-axis CNC Router . . . . .	128
5.8	Sandwich Element with Inclined Vertical Connectors . . . . .	129
5.9	Prototype for a Snap-fit Jointed, Double-layered Corner . . . . .	130
5.10	Assembly of Multiple Double-layer Components in one Direction . . . . .	131
5.11	Physical Prototype of the 1-directionally-folded Double-layer Arch . . . . .	132



## List of Figures

---

5.12 Assembly of a Double-layer Folded Plate Shell . . . . .	133
5.13 Comparison of Double-layer Angular Edge Joints . . . . .	135
5.14 4-step Integral Assembly of Double-layered Timber Folded Plates . . . . .	136
5.15 Antiprismatic Double-Layer Bidirectionally-folded Prototype . . . . .	138
5.16 Antiprismatic Double-Layer Bidirectionally-folded Prototype - Interior View . .	139
5.17 Antiprismatic Double-Layer Bidirectionally-folded Prototype - Cross-section .	140
5.18 Pre-Activation of Snap-fit Joints . . . . .	141
 <b>III Conclusion and Further Work</b>	 <b>144</b>
 <b>6 Conclusion</b>	 <b>147</b>
6.1 Constraint-shaped range of possible rotations for the assembly vector . . . . .	150
 <b>7 Further Work</b>	 <b>151</b>
 <b>Appendices</b>	 <b>153</b>
 <b>A Joint Parameter Interactions</b>	 <b>155</b>
A.1 Graphics for suitable insertion vectors . . . . .	156
A.2 Limits for the insertion vector . . . . .	157
 <b>B Integral Joints for UHPFRC formwork</b>	 <b>159</b>
B.1 Formwork for the UHPFRC folded surface prototype . . . . .	160
B.2 Interior View of the UHPFRC folded surface prototype . . . . .	161

## List of Tables

2.1	Taxonomy of joining techniques by the forces used [Mes06] . . . . .	7
2.2	Taxonomy of fabrication techniques for folded plates . . . . .	25
2.3	Increasing the Role of Integral Mechanical Attachment . . . . .	35
2.4	Increasing the Complexity of Assembly . . . . .	35
5.1	Taxonomy of Integral Mechanical Attachment techniques [Mes06, p.15] . . . .	116
5.2	Variables and Values from VTT for KertoQ 21 mm . . . . .	126



# Christopher Robeller

Avenue de la Poste 27  
1020 Renens, Switzerland

Date of Birth: 25/03/1981, Bobingen  
Nationality: German  
Marital Status: Single

## Education

2011 - 2015	Doctoral Student Swiss Federal Institute of Technology Lausanne EPFL
06/2008	Professional Diploma in Architecture with Distinction London Metropolitan University

## Work Experience

2011 - 2015	Research Assistant Laboratory for Timber Construction IBOIS Swiss Federal Institute of Technology Lausanne EPFL
2008 - 2010	Research Associate Institute for Computational Design ICD University of Stuttgart
2002 - 2004	Architectural Assistant Architekturbüro Messerschmid, Stuttgart